Immunofluorescence Localization of Polyketide Synthases in the Medicinal Plant *Hypericum perforatum*

Von der Fakultät für Lebenswissenschaften

der Technischen Universität Carolo-Wilhelmina

zu Braunschweig

zur Erlangung des Grades einer

Doktorin der Naturwissenschaften

(Dr. rer. nat.)

genehmigte

D i s s e r t a t i o n

von Asma K. Belkheir

aus Benghazi / Libyen

1. Referent: Professor Dr. Ludger Beerhues
2. Referent: Privatdozent Dr. Robert Hänsch
eingereicht am: 12.01.2009
mündliche Prüfung (Disputation) am: 26.02.2009
Druckjahr 2009

Vorveröffentlichungen der Dissertation

Teilergebnisse aus dieser Arbeit wurden mit Genehmigung der Fakulät für Lebenswissenschaften, vertreten durch den Mentor der Arbeit, in folgenden Beiträgen vorab veröffentlicht:

Tagungsbeiträge

Belkheir, A., Beerhues, L., Immunochemical Studies of Polyketide Synthases from *Hypericum perforatum*. (Poster). Botanikertagung 2007, Hamburg, 3 - 7 September, 2007

Belkheir, A., Hänsch, R., and Beerhues, L., Immunofluorescence Localization of Polyketide Synthases in the Medicinal Plant *Hypericum perforatum* (Presentation). 6th Kurt Mothes Workshop Secondary Metabolism, Jena / Beutenberg Campus, 18-19 September, 2008

To my Parents,

and those whose contributions were most generous

Acknowledgment

I refer my special gratitude to Professor Dr. L. Beerhues for providing the interesting theme and facilities to pursue my Ph.D. study at the Institut für Pharmazeutische Biologie. His valuable supervision, guidance, enthusiasm and especially great patience have facilitated the completion of this dissertation.

I am deeply thankful to PD Dr. R. Hänsch, member of the Institute of Plant Biology, TU Braunschweig, for his interest in this work and for taking over the co-referee, and also for his valuable guidance on Laser Scanning Microscopic analyses and providing the Cryostate Microtome.

My great appreciation is given to Prof. Dr. B. Liu for patient guidance, constructive discussion, and valuable ideas during my work.

I would like to express my thanks to the staff of the Institute of Pharmaceutical Technology, TU Braunschweig, especially to Dr. S. Reichl and L. Albrecht for providing the microtome.

My grateful thanks to all staff members of the Institute of Pharmaceutical Biology, TU Braunschweig, for their kind help in their own specialities.

My special thanks to my former and current colleagues and co-workers of Pharmaceutical Biology for the pleasant working atmosphere and companionship during laboratory works.

I acknowledge Libyen government for financial support to extend my gratitude.

Finally, I would like to express my deepest thanks and profound gratitude to my family in Libyen which provided me with continuous moral support during my stay in Germany. My special thanks to my brother *Mustafa Belkheir* whose contributions were most generous during the course of this study.

Contents

List of Figures

List of Figures

List of Schemes

List of Tables

Abbreviations

AIDS	Acquired immunodeficiency syndrome
APS	Ammonium persulfate
Approx.	Approximate
BPS	Benzophenone synthase
BSA	Bovine Serum Albumin
sec	Second
cm	Centimetre
CHS	Chalcone synthase
CNA	Central nervous system
cDNA	Complementary deoxyribo nucleic acid
dm	Decimetre
°C	Degree Celsius (centigrade)
DTT	Dithiothreitol
DOC	Deoxycholate
E. coli	*Escherichia coli*
Na_2EDTA	Ethylenediaminetetraacetic acid- disodium salt dehydrate
ε	Extinction coefficient
FPLC	Fast Protein Liquid Chromatography
FITC	Fluorescein isothiocyanat
6x His	Hexa histidine tag
HPLC	High performance liquid chromatography
h	Hour
5-HT	5-hydroxytryptamine
H. androsaemum	*Hypericum androsaemum*
H. calycinum	*Hypericum calycinum*
H. perforatum	*Hypericum perforatum*
IF	Immunofluorescence
IgG	Immunoglobulin G
pI	Isoelectric point
IPTG	Isopropyl- 1 - thio- *β* - *D*- galactopyranoside

kDa	Kilo Dalton
LSM	Laser scanning microscopy
L	Liter
LB	Luria Bertani
GST	Glutathione-S-transferase
GST-BPS	Glutathione-S-transferase- fusion benzophenone synthase
GST-CHS	Glutathione-S-transferase- fusion chalcone synthase
g	Gram
µl	Microliter
µm	Micrometre
mA	Milliampere
mbar	Millibar
ml	Milliliter
mg	Milligram
mm	Millimetre
mM	Millimolar
M	Molar
Mr	Molecular mass
MS	Murashige Skoog
MW	Molecular weight
MWCO	Molecular weight cutoff
Nm	Nanometer
Ni-NTA	Nickel-nitrilotriacetic acid
OD	Optical density
ORF	Open reading frame
O.N.	Over night
PMSF	Phenylmethane sulphonyl fluride
PKSs	Polyketide synthases
PKSs III	Type III polyketide synthases
PCR	Polymerase chain reaction
PVDF	Polyvinylidendifluoride
PBS	Phosphate bufferd saline
R_t	Retention time

rpm	Revolutions per minute
SDS	Sodium dodecyl sulphate
SDS-PAGE	SDS-Polyacrylamide Gel Electrophoresis
TEMED	*N,N,N',N'*- tetramethylethylene – diamine
TCA	Trichloroacetic acide
TBS	Tris bufferd saline
TBS- T	Tris bufferd saline with 0.1 % Tween 20
U	Unit
V	Volt
v/v %	Volume per volume percentage
w/v %	Weight per volume percentage

1 Introduction

1.1 *Hypericum perforatum* (St. John's wort)

1.1.1 Introduction

St. John's wort is an important medicinal plant of the genus *Hypericum*, which includes 450 species worldwide. *Hypericum perforatum* belongs to the family Clusiaceae (formerly Hypericaceae or Guttiferae). The plant was used from the ancient Greeks time through the Middle Ages to ward off evil and protect against disease (Fig. 1-1).

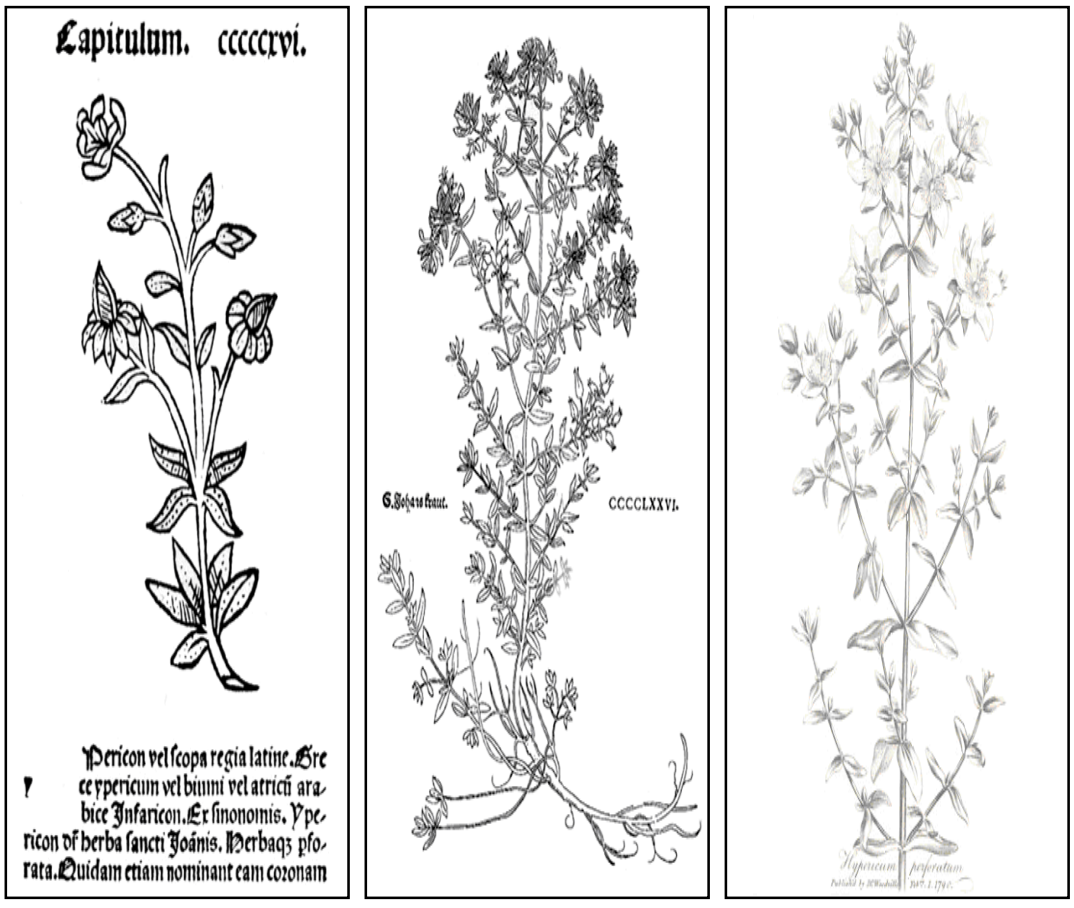

(a) **(b)** **(c)**

Fig. 1- 1: *Hypericum perforatum:* (a) from: Ortus sanitatis, 1511; Original in Civia Biblioteca Bergamo. (b) from: „New Kreüterbuch" of Leonhart Fuchs, 1543. (c) from: Woodville's Medical Botany, 3rd edition, 1832, originally published in 1790-1793. Courtesy of Hunt Institute for Botanical Documentation, Carnegie Mellon University, Pittsburgh, PA.

1 Introduction

The common name of the plant is St. John's wort. This name apparently relates to numerous explanations, one relates to the fact that the flowers bloom around St. John's Day (June 24). Another is that the red pigments, which are exuded when the buds and flowers are squeezed, were associated with the blood of St. John the Baptist. Yet another refers to an ancient English tradition of throwing the flower into a bonfire on the eve of St. John's Day. The botanical name of the plant is *Hypericum perforatum.* The genus name *Hypericum* is derived from two Greek words, *hypo* and *eikon*, which translate into "*over*" and "*icon*" as in "over an apparition" alluding to its use in ancient times for protecting against demonic possession and its ability to defend "evil spirits". The species name *perforatum* is based on the perforated appearance of the leaves (Fig.1-2) due to their translucent leaf glands, which can be observed when held up to light (Upton, 1997).

Fig. 1- 2: *Hypericum perforatum* showing spotted glands in leaves.

St. John's wort is an herbaceous perennial plant that is native and broadly distributed in Europe and West Asia (Fig. 1-3). It has also been introduced into the Americas and grows wild in many meadows, where it has become naturalized (Barnes et al., 2001).

Fig. 1- 3: *Hypericum perforatum*: (left) wild, (right) cultivated.

1.1.2 Botanical Description

Hypericum perforatum is a perennial herb, erect, much branched, especially distally, 1.0-10.0 dm from a taproot (Fig. 1- 4; Stueber, 2003). The morphological characteristics of *H. perforatum* are described in Table 1-1, which is compiled from Upton (1997) and Robson (2003).

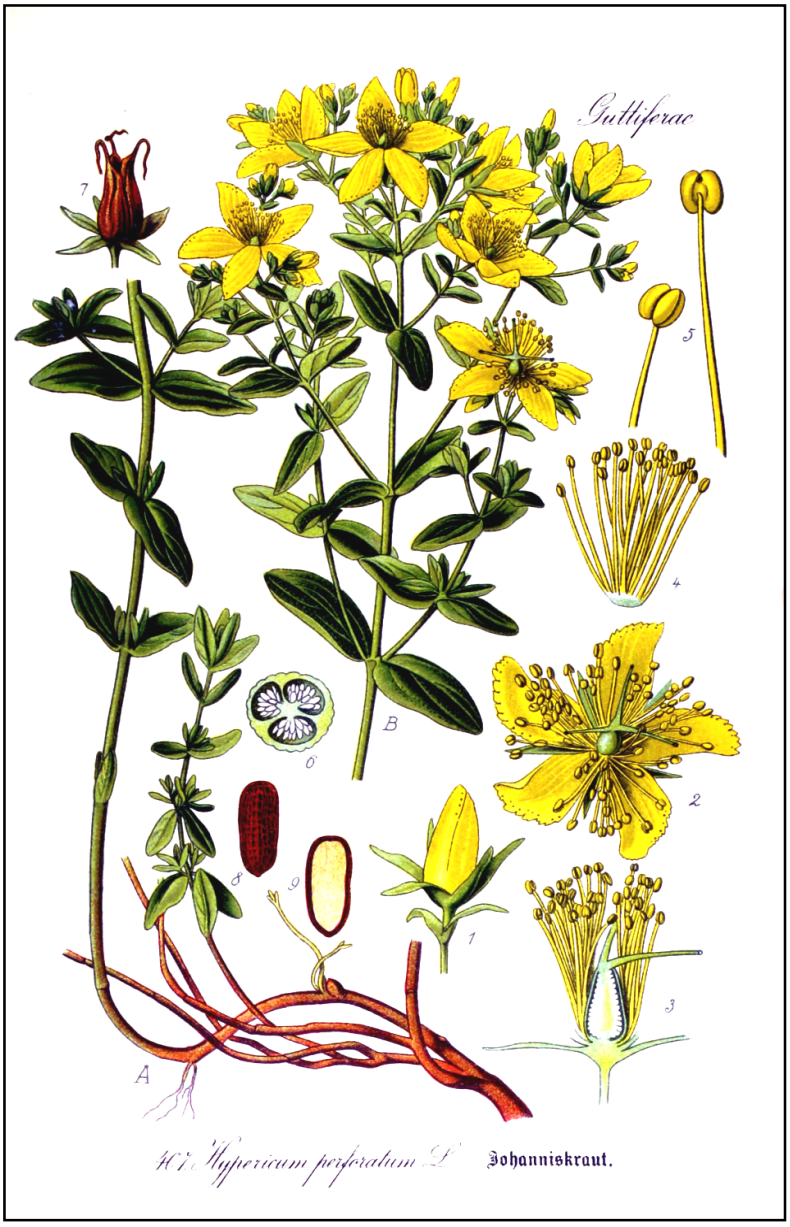

Fig. 1- 4: *Hypericum perforatum*, from: Flora of Germany, Austria and Switzerland (1888).

Table 1- 1: Morphological characteristics of *H. perforatum*:

Morphological Characteristics of *Hypericum perforatum*		
Organ	**Characteristics**	
Flower	Flowers bear five golden yellow petals with black dots (glands) and five green sepals, 15-35 mm in diameter.	
Stem	Internodes 2-lined, glabrous, with black glands on the raised lines.	
Leaves	1.5-4.0 cm long, egg-shaped to elongated, very short petiolate, marked with translucent black dots.	
Inflorescence	Large rounded or flat-topped, compound cymes with 25-100 flowers each.	
Roots	The taproot may reach depths of 4 to 5 feet. Lateral roots grow 2 to 3 inches beneath the soil surface but may reach depths of 3 feet.	

Fig. 1- 5: *H. perforatum.*

1.1.3 Chemical Constituents

H. perforatum contains numerous biologically active constituents. Most researches consider its effects to be due to a variety of constituents rather than any single component. Key constituents of *H. perforatum* can be divided into several classes, which are compiled from several sources (Kitanov and Blinova, 1987; Upton, 1997; Barnes *et al*., 2001; McCutcheon, 2000; Bisset, 2001; Greeson *et al.*, 2001; Hölzl and Petersen, 2003) and are presented below.

- **Naphthodianthrones**

This group includes the compounds *hypericin, pseudohypericin, protohypericin* and *protopseudohypericin* (Fig.1-6). They are present at about 0.1-0.15% of fresh material. Hypericin is found in glands, which are present in all aboveground parts of plants. The group also includes derivatives occurring in lower concentrations, such as *isohypericin, demethylpseudohypericin, hypericodehydrodianthrone, pseudohyperico-dehydrodianthrone and cyclopseudohypericin.* Not all these compounds are present naturally in the plant, they might be produced during harvest and storage.

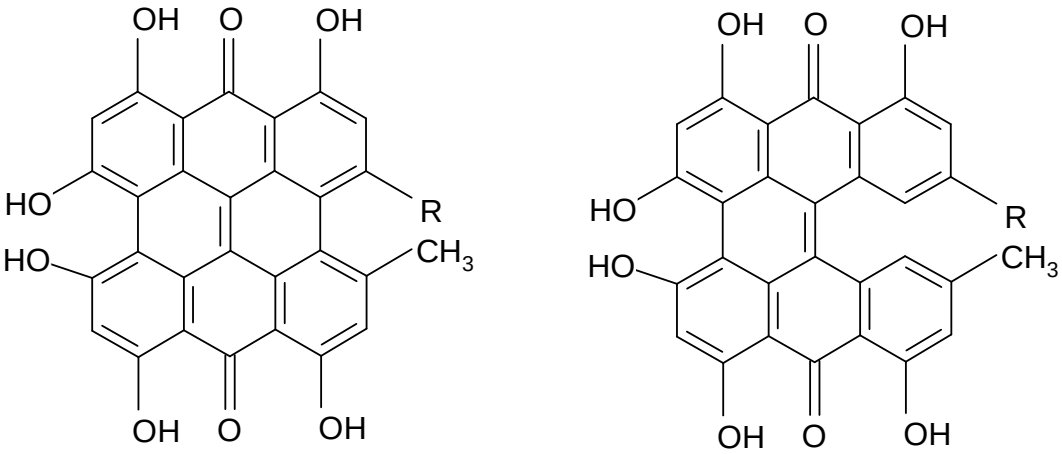

$R=CH_3$	hypericin	$R=CH_3$	protohypericin
$R=CH_2OH$	pseudohypericin	$R=CH_2OH$	protopseudohypericin

Fig. 1- 6: Structural formulae of naphthodianthrones from *Hypericum perforatum.*

- **Prenylated phloroglucinols**

Prenylated phloroglucinols, namely *hyperforin* (2.0-4.5%) and *adhyperforin* (0.2-1.9%) (Fig.1-7), are found in all aboveground parts of the plant.

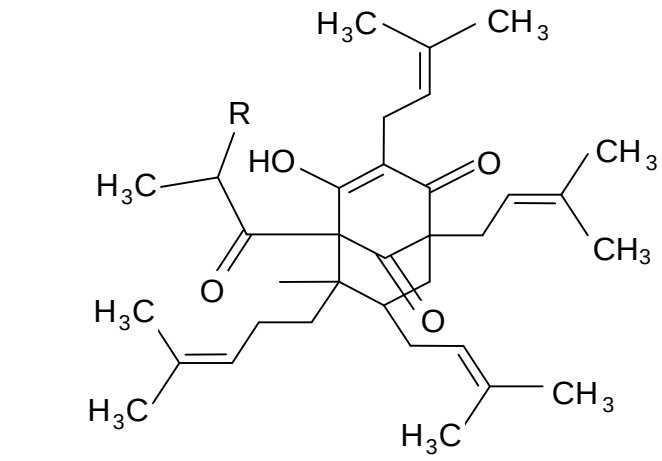

R=CH_3 hyperforin R=CH_2CH_3 adhyperforin

Fig. 1- 7: Structural formulae of prenylated phloroglucinols from *Hypericum perforatum*.

- **Flavonoids and biflavonoids**

Numerous flavonoid compounds including *flavonoid aglyca* and *flavonoid glycosides* (2-4%) (Fig. 1-8) as well as biflavonoid compounds including *I3,II8-biapigenin* (0.1-0.5%) and *amentoflavone* (*I3',II8-biapigenin)* (0.01-0.05%) (Fig.1-9) are found in the upper portion of the plant.

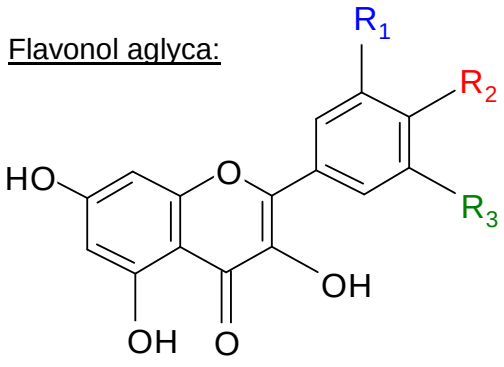

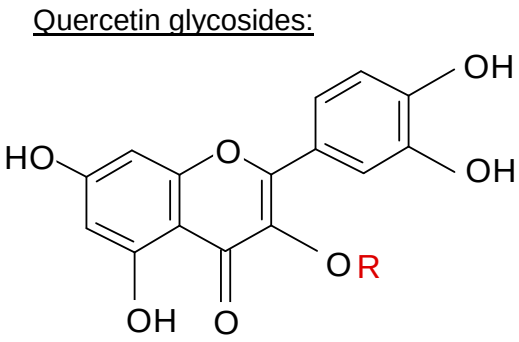

Name:	R_1	R_2	R_3
Quercetin	H	OH	OH
Kaempferol	H	OH	H
Myricetin	OH	OH	OH

Name:	R
Quercitrin	*α*-1-rhamnosyl
Isoquercitrin	*β*-D-glucosyl
Hyperoside	*β*-D-galactosyl
Rutin	*β*-rutinosyl

Fig. 1- 8: Structural formulae of flavonoids from *Hypericum perforatum*.

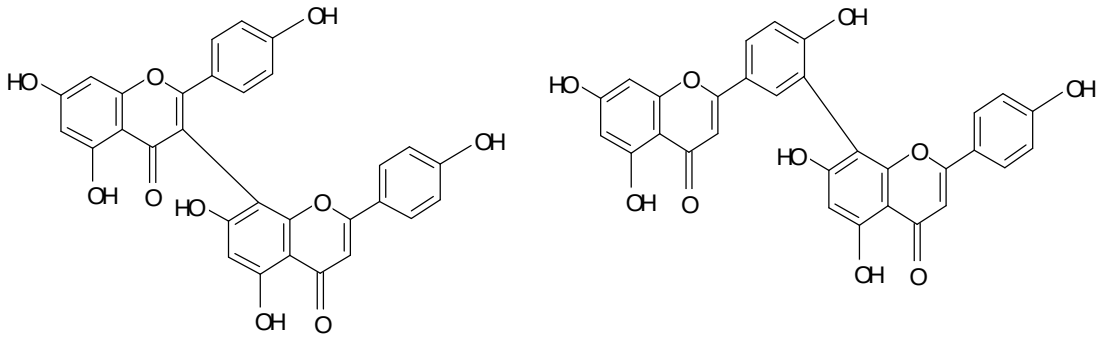

Fig. 1- 9: Structural formulae of biflavonoids from *Hypericum perforatum*.

- **Xanthones**

Xanthones include *1,3,6,7-tetrahydroxyxanthone (norathyriol)* at a concentration of 0.4 mg/100g dry herb and *mangiferin, isomangiferin* and *kielcorin*, a *xanthonolignoid* (Fig.1-10) . Xanthone compounds are found in root and shoot.

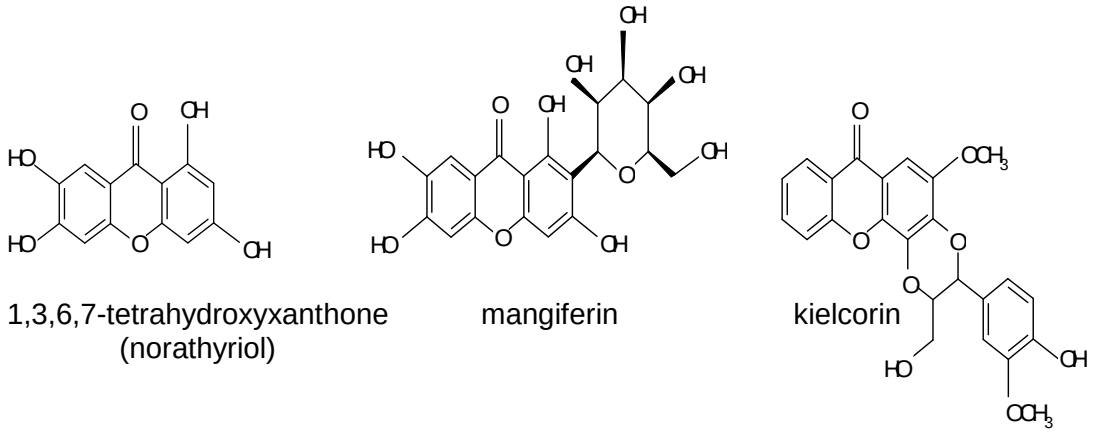

Fig. 1- 10: Structural formulae of xanthones from *Hypericum perforatum*.

- **Other Constituents**

⇒ Tannins and proanthocyanidins (8-9%).

⇒ Phenolic acids and other phenolic compounds, such as caffeic, chlorogenic, *p*-coumaric, ferulic, *p*-hydroxybenzoic, and vanillic acids.

⇒ Coumarins (scopoletin and umbelliferone).

⇒ Terpenes and *n*-alkanes/ *n*-alkanols (0.05-0.9%).

⇒ Other water-soluble components, such as organic acids, peptides, polysaccharides.

1.1.4 Uses, Pharmacological Activity and Clinical Properties

H. perforatum is a well-known traditional medicinal plant distributed throughout the world. It has been used medicinally for at least 2000 years, but the studies of its bioactive constituents and pharmacological activities still continue. However, various studies support a number of its traditional uses. Over the centuries it has been used for the treatments of cold, chest congestion, menstrual cramps, headaches, diarrhea, fever, snake bite, asthma, tuberculosis, skin problems, wounds, bruises, burns, and infections. Currently, *H. perforatum* is mainly used for the treatment of mild to moderate depression (Zobayed *et al*., 2005). *H. perforatum* is commercially available in tablet, capsule, oil, spray, tea, and tincture form (Fig.1-11). In Germany, it is widely used for the treatment of depression and is prescribed approximately 20 times more often than fluoxetine, one of the most highly prescribed antidepressants in the United States. In the USA, it is increasingly used as an over-the-counter remedy by a significant portion of the lay population for the treatment of depression (Greeson *et al.*, 2001).

Fig. 1- 11: Dosage forms of*H. perforatum*.

1.1.4.1 Pharmacological Activities of *H. perforatum* Extract

Commercially, two different types of *H. perforatum* preparations are available; *aqueous-alcoholic extracts* and *oil extracts.* They differ in both their constituents and the indications for their use (McCutcheon, 2000).

The pharmacological activities of the two different types of *H. perforatum* extracts compiled from several sources (Upton, 1997; Barnes *et al.*, 2001; Greeson *et al.*, 2001; McCutcheon, 2000) are presented in Table 1-2.

Table 1- 2: Pharmacological activities of *H. perforatum* extracts:

Extract Type	Pharmacological activity	Study
Aqueous-alcoholic extract	ð *Internally:* • Treatment of mild to moderate depression and seasonal affective disorder. Use for severe depression is under study. • It influences the level of certain CNS neurotransmitters**.** • It has been used for neurological disorders including anxiety, restlessness, irritability, nervous tension, restless sleep, migraine headache, pain, and spasms due to nerve injury**.** • It has been used for ague, rheumatism, gout and enuresis due to nervous anxiety or nerve irritation. • It has been used as an antidiarrheal and diuretic agent. • It has anti-HIV activity and several benefits in the treatment of AIDS. ð *Topically:* • It has been used for bites, bruises, wounds and swellings. • It has been used as a wash or gargle for oral pain.	F Clinical studies, animal and *in-vitro* studies. F *In- vitro* studies. F Animal and *in-vitro* studies. F Traditional Medicine. F Traditional Medicine. F *In vitro* studies. F Clinical studies and animal studies. F Traditional Medicine.
Oil extract	ð *Internally:* • Anti-inflammatory for dyspeptic complaints, gastric disorders, and mouth and throat pain. • Strong anti-bacterial activity. • Analgesic activity. • Significantly more effective than placebo in depression and anxiety. ð *Topically:* • Treatment of wounds and burns.	F Animal and *in-vitro* studies. F *In- vitro* studies. F Animal studies. F One clinical study. F Traditional Medicine.

The major bioactive constituents of the aqueous-alcoholic extract that have pharmacological activity are *phloroglucinols (hyperforin)* and *flavonoids.* In addition, lesser amounts of *hypericins* and *xanthones* and traces of *proanthocyanidins* are found. The major bioactive constituents of the oil extract are *phloroglucinols, flavonoids* and essential oil. It does not contain *hypericins* but rather *lipophilic hypericin derivatives,* which impart the characteristic red color (McCutcheon, 2000).

1.1.4.2 Pharmacological Activity of Isolated Constituents from *H. perforatum*

H. perforatum contains several classes of bioactive detectable compounds. The constituents of *H. perforatum* and their activities, compiled from several sources (Upton, 1997; Greeson *et al.*, 2001; Hölzl and Petersen, 2003 and Hobbs, 1998) are summarized in Table 1-3.

Table 1- 3: Pharmacological activities of isolated constituents of *H. perforatum*:

Constituent	Pharmacological activity
Hypericin	Antiviral (*in-vitro*), anti-depressant (MAO inhibitor), anti-cancer (*in-vitro*), photodynamic, used in AIDS research.
Hyperforin	Anti-depressant, antibacterial (multidrug-resistant *Staphylococcus aureus*), neurotransmitter reuptake inhibitor, anticarcinogenic (induction of apoptosis).
Flavonoids and biflavonoids	Antiinflammatory, antiulcerogenic, sedative, tumor inhibition, in vitro MAO inhibiting activity.
Xanthones	Anti-depressant (exhibit selective MAO_A inhibition), antimicrobial, antiviral, diuretic, cardiotonic.
Tannins and Proanthocyanidins	Antioxidant, antimicrobial, antiviral, vasorelaxant, styptic.
GABA	Neurotransmitter that may have sedative effects
Essential oil (terpenes)	Calming, sedating, anti-inflammatory, antiseptic, antispasmodic, anti-asthma, headaches, anti-fungal.

1.1.4.3 Mode of the Antidepressant Action of *H. perforatum*

The exact mechanism of action for the antidepressant effect of *H. perforatum* is not yet fully understood although remarkable progress has been made in recent years. The major bioactive compound responsible for the antidepressant activity is hyperforin. Previously, in vitro studies had suggested that the primary mode of action is inhibition of monoamine oxidase A (MAO A) by hypericin, however, later studies failed to confirm this. Recent results of biochemical and pharmacological studies indicated that hyperforin inhibits the synaptosomal re-uptake of brain neurotransmitters (serotonin "5-HT", noradrenaline, dopamine, glutamate and GABA) into the presynaptic nerve terminal. By blocking the neurotransmitter re-uptake, hyperforin leads to increased concentrations of neurotransmitters in the synaptic cleft (Fig. 1-12) (Capasso *et al.*, 2003; Heinrich, 2004). Interestingly, hyperforin does not directly interact with the neurotransmitter transporter but increases the intracellular sodium concentration, thereby affecting the efficiency of the symporters (Müller, 2003). This novel mechanism also explains why hyperforin is a broad-band neurotransmitter re-uptake inhibitor.

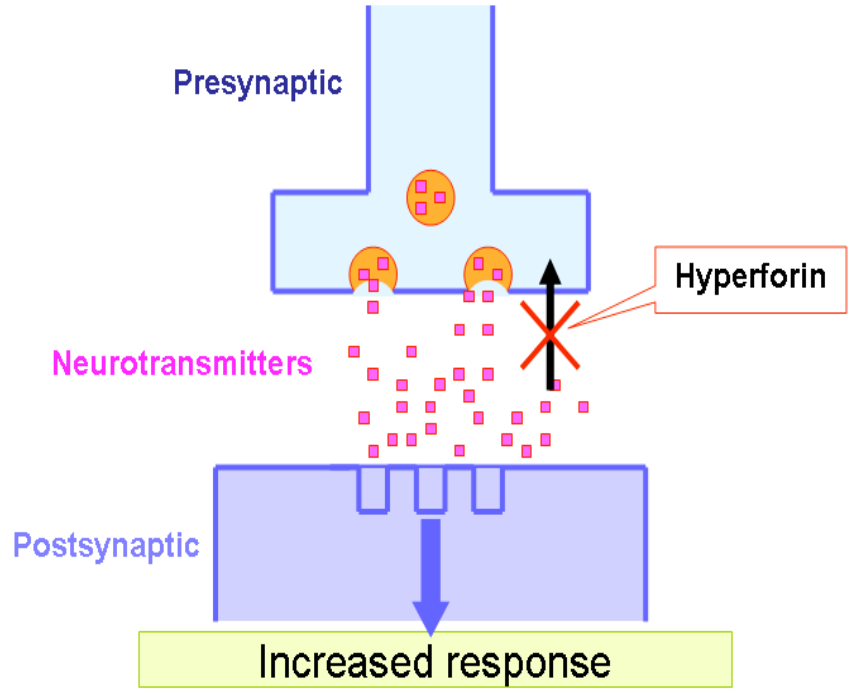

Fig. 1- 12: Mode of the antidepressant action of *Hypericum perforatum* (Capasso *et al.*, 2003)

1.2 Polyketides Biosynthesis in *Hypericum perforatum*

1.2.1 The Plant type III Polyketide Synthases (PKSs III)

The type III PKSs catalyse the formation of structurally diverse polyketides. Type III polyketides are one of the most important families of natural products that exhibit a wide variety of bioactivities. Polyketides have served as antibiotics, anticancer drugs, antifungal agents, immunosuppressants, and insecticides. The biosynthetic pathways of all polyketides share a common principle: they are synthesized by sequential reactions catalysed by different enzyme activities called polyketide synthases (PKSs) (Tsai, 2004). At least three architecturally different types of PKSs have been discovered. Type I and type II PKSs consist of many subunits and active sites. On the other hand, type III PKSs are structurally simple, homodimeric iterative PKSs (Fig.1-13) (monomer Mr ≈ 42-45 kDa) with two independent active sites which catalyze a series of decarboxylation, condensation and cyclization reactions to generate polyketides of different lengths. The type III PKSs catalyze repeated chain elongation between a CoA-linked starter unit (usually an aromatic CoA) and acetyl units (derived from malonyl-CoA). Following chain extension, the linear polyketide intermediate is cyclized in the same active site cavity (Tsai, 2004; Jez *et al.*, 2001).

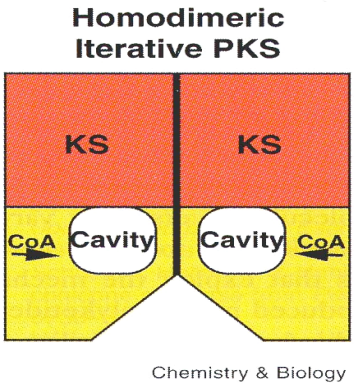

Fig. 1- 13: Proposed model of active site cavities in homodimeric iteractive PKSs. KS = ketosynthase; CoA = coenzyme A

1.2.2 Biosynthesis of Active Aromatic Polyketide Derivatives by Type III PKSs in *H. perforatum*

All biologically active detectable constituents of the medicinal plant *H. perforatum* originate from the polyketide metabolism. Three type III polyketide synthases (PKSs) involved are benzophenone synthase (BPS), chalcone synthase (CHS) and isobutyrophenone synthase (BUS). They catalyze the formation of enzyme-bound polyketide intermediates by using the same extender molecule but different starter substrates. The intermediates then undergo regio-specific cyclization reactions via Claisen condensation, yielding hydroxylated aromatic polyketide secondary metabolites. The biosynthesis of benzophenone derivatives, such as sampsoniones and xanthones, is catalyzed by BPS which stepwise condenses one unit of benzoyl-CoA as a starter with three molecules of malonyl-CoA as extender units to give a linear tetraketide (Scheme 1-1,a). This intermediate is cyclized by intramolecular Claisen condensation into phlorbenzophenone (Liu *et al.*, 2003). Phlorbenzophenone is the precursor of more complex polyprenylated benzophenone derivatives, such as guttiferone F and sampsonione A, which exhibit interesting pharmacological activities. Besides polyprenylation, phlobenzophenone can undergo intramolecular cyclization to give xanthones, which are precursors of psorospermin and rubraxanthone (Fig.1-14).

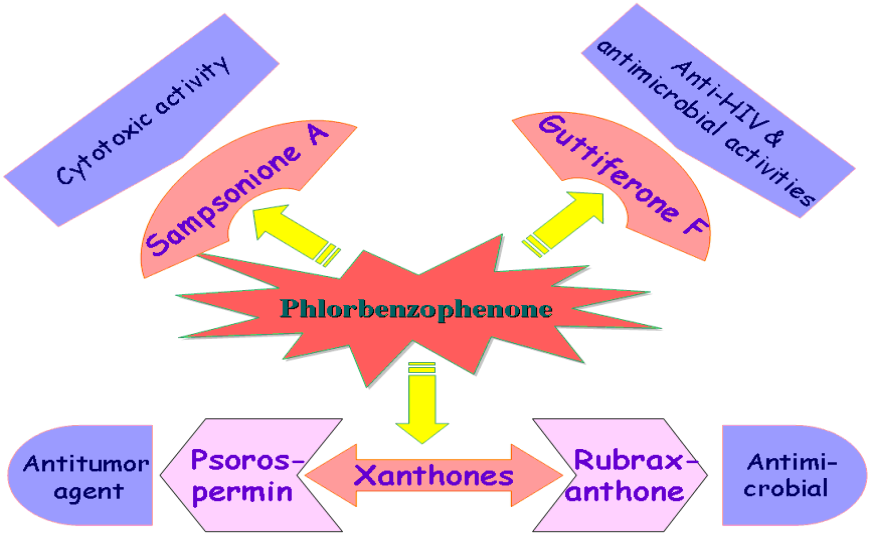

Fig. 1- 14: Pharmacological activities of benzophenone derivatives in *Clusiaceae species*.

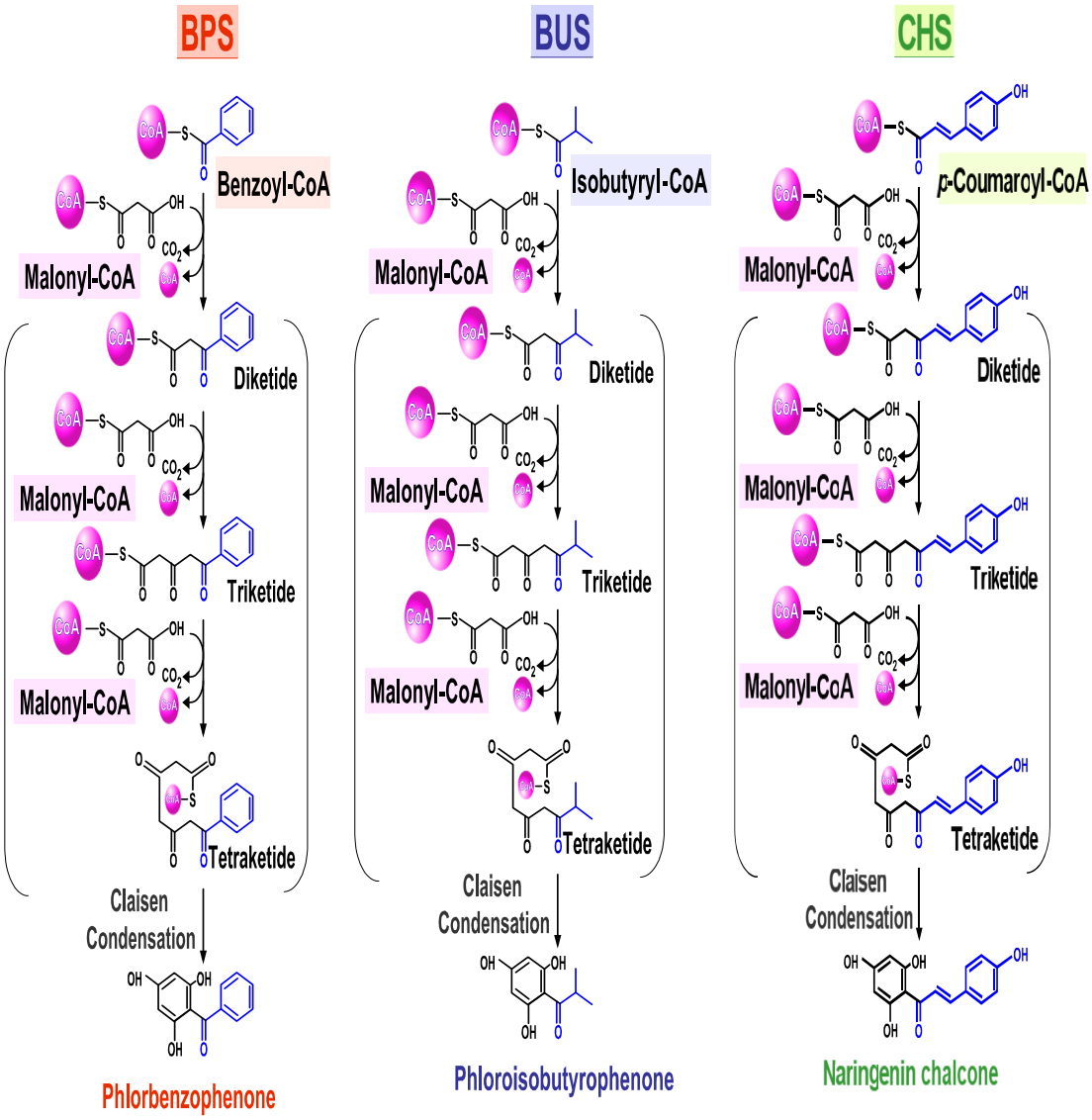

Scheme 1-1: Proposed reaction mechanisms underlying the biosynthesis of hydroxylated aromatic polyketide secondary metabolites by three type III polyketide synthases in *H. perforatum*.
a: Conversion of benzoyl-CoA and three malonyl-CoAs to phlorbenzophenone by BPS.
b: Conversion of isobutyryl-CoA and three malonyl-CoAs to phlorisobutyrophenone by BUS.
c: Conversion of *p*-coumaroyl-CoA and three malonyl-CoAs to naringenin chalcone by CHS.

Biosynthesis of chalcones is catalyzed by CHS, which involves the sequential condensation of the starter unit *p*-coumaroyl-CoA with three molecules of malonyl-CoA as extender units (Scheme 1-1, c). The resulting tetraketide intermediate is cyclised by intramolecular Claisen condensation into a hydroxylated aromatic ring system (naringenin chalcone) (Liu *et al.*, 2003). Naringenin chalcone is then converted by downstream enzymes into flavonoids and biflavonoids which serve multiple functions in plants (Fig.1-15).

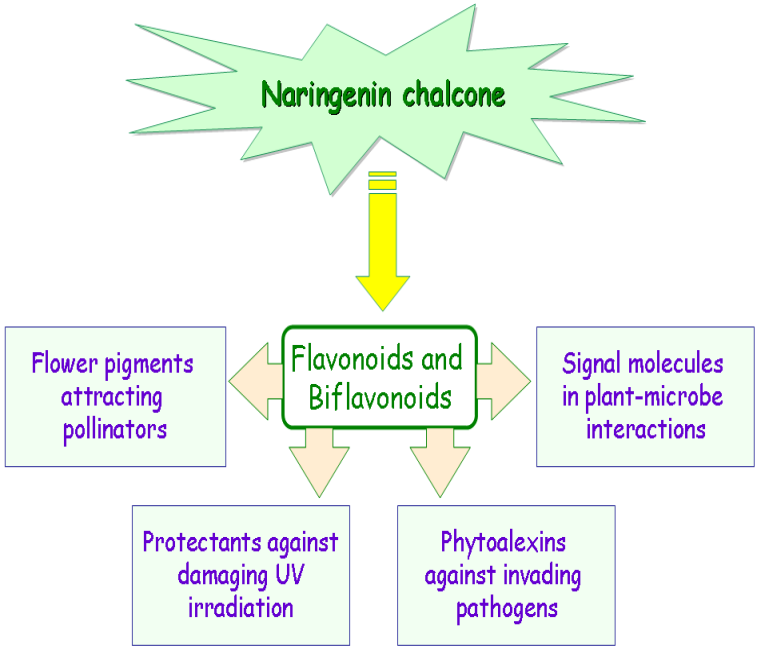

Fig.1- 15: Functions of flavonoids and biflavonoids in plants.

Like naringenin chalcone and phlorbenzophenone, phlorisobutyrophenone is formed under catalysis of BUS which stepwise condenses one unit of isobutyryl-CoA with three molecules of malonyl-CoA to give a linear tetraketide (Scheme 1-1, b). This intermediate is cyclized by intramolecular Claisen condensation to yield phlorisobutyrophenone as the hydroxylated aromatic ring system (Beerhues, 2006). Phlorisobutyrophenone is the precursor of hyperforin which is the major biologically active constituent of *H. perforatum* (Fig. 1-16).

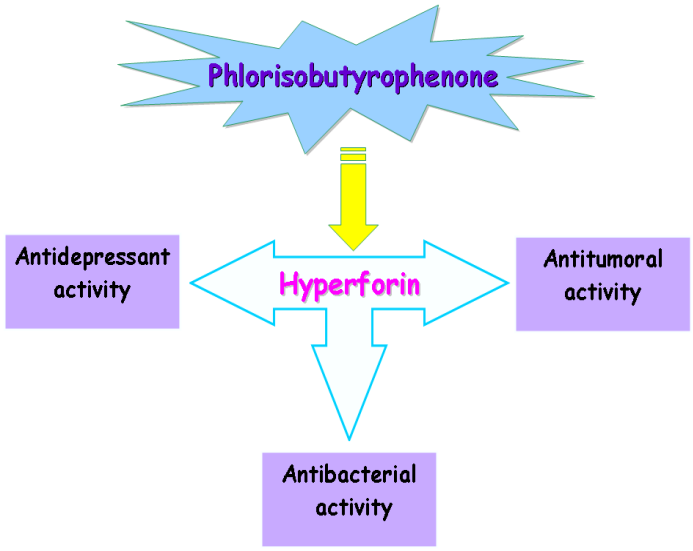

Fig.1- 16: Pharmacological activities of phlorisobutryrophenone derivatives in *H. perforatum*.

The biosynthesis pathways of the major classes of polyketide secondary metabolites found in *in-vitro* cultures and in differentiated plants of *H. perforatum* and *H. androsaemum* (Beerhues, 2006; Dias, 2003) are summarized in Scheme 1-2.

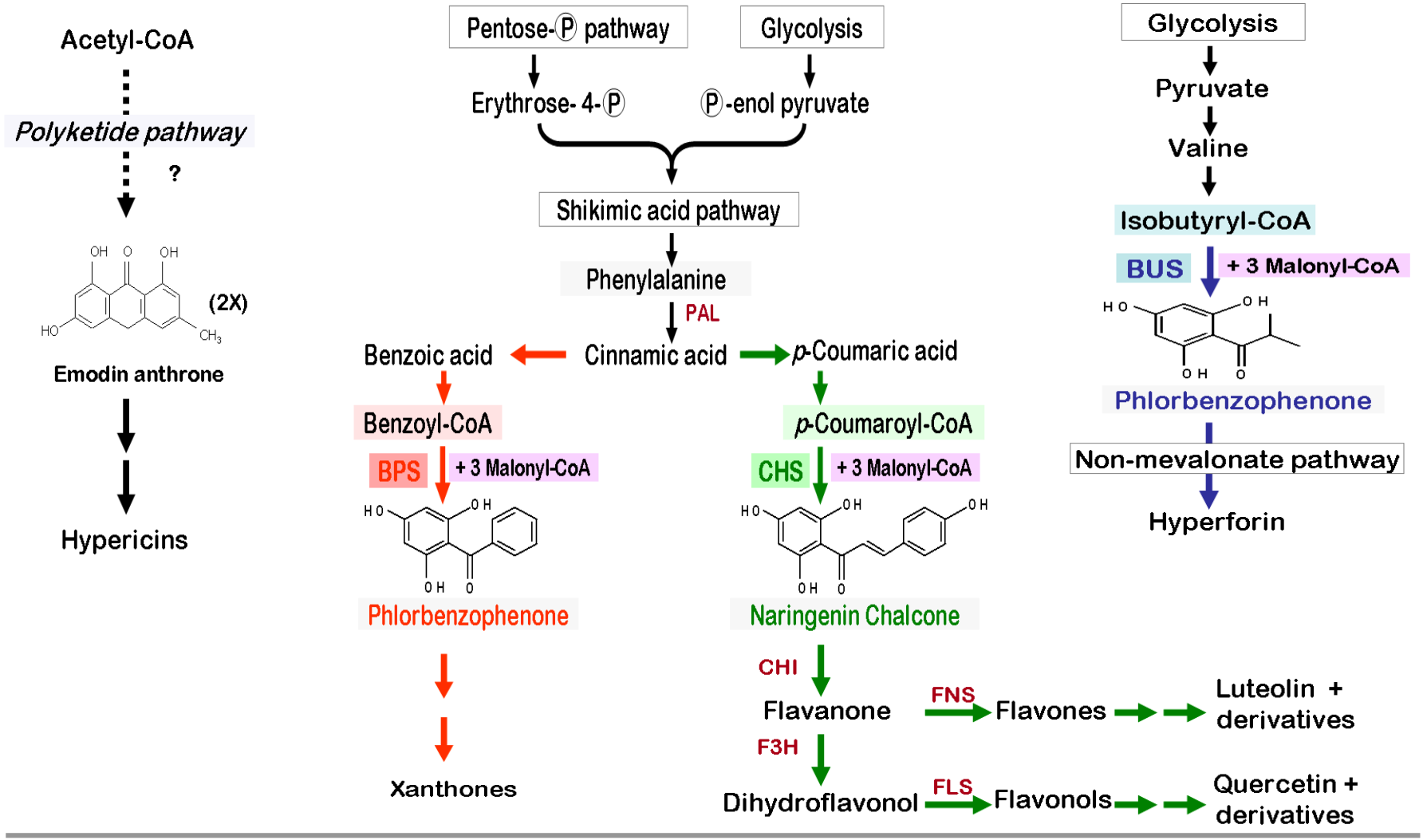

Scheme 1- 2: The biosynthetic pathways of the major classes of polyketide secondary metabolites found in *in-vitro* cultures and intact plants of *H. perforatum and H. androsaemum*. *CHI*, chalcone isomerase; *F3H*, flavone 3-hydroxylase; *FLS*, flavonol synthase; *FNS*, flavone synthase; *PAL*; phenylalanine ammonia-lyase.

1.2.3 Distribution of Polyketide Secondary Metabolites in Different Plant Parts and Developmental Stages

The concentration of secondary metabolites in *Hypericum*-derived drugs is not only related to genetic and environmental conditions, but also to numerous factors such as harvesting and handling practices, drying process and plant parts used (Upton, 1997; Seidler-Łożykowska, 2003). Generally, accumulation of secondary metabolites is a defense mechanism of plants against invading pathogens, e.g. bacteria and fungi, and mechanical damage from herbivores (Zobayed *et al.*, 2005).

- **Hypericin**

Hypericin is located in small glandular structures. These glands are present in all above-parts (flowers, capsules, leaves, stems), but not in roots. According to a study done by Berghöfer (1987) the concentration of hypericin in buds of *H. perforatum* is 0.36-0.44 % of dry mass, followed by 0.19 % in flowers, 0.12 % in capsules, 0.08 % in leaves, and traces in stems (Hölzl and Petersen, 2003 and literature cited therein). Hypericin was not detectable in roots.

- **Hyperforin**

According to Berghöfer and Hölzl (1986), hyperforin was detected in buds, flowers, and capsules (Hölzl and Petersen, 2003). Maisenbacher and Kovar (1992) detected that 4.4% of hyperforin was present in ripe fruits. In addition, their study showed that the hyperforin level increased during the ontogenetic development from flowers to ripe fruits. Similarly, Tekel'ova et al. (2000) found a gradual increase in the hyperforin level from buds to unripe fruits. Márttonfi and Repčák (1994) demonstrated that hyperforin was present in pistils and that the largest amount was located in capsules (Seidler-Łożykowska, 2003).

- **Flavonoids and biflavonoids**

There are several studies that detected flavonoids and biflavonoids in *H. perforatum.* The largest amount of flavonoids was found at the beginning of blooming, i.e. yellow buds, and decreased as the plant bloomed and then over-bloomed (Seidler-Łożykowska, 2003). Bomme (1997) demonstrated a maximum amount of flavonoids in leaves at the beginning of the blossom stage. Furthermore, Kattnig and his coworkers (1997) observed that the largest amount of monoflavonoids was detected before flowering, while biflavonoids reached their highest level in the blossom and then decreased when over-bloomed. In addition, their study indicated that the rate of monoflavonoids to biflavonoids in the whole plant was 1: 0.03 and in flowers 1: 0.15 (Seidler-Łożykowska, 2003).

- **Xanthones**

Xanthones were detected in trace amounts in the plant. They accumulate sporadically throughout the growing period, however, the accumulation of xanthones was influenced greatly after elicitation. Xanthones described for *H. perforatum* belong to the tetraoxygenated type, such as norathyriol (1.1.3, Fig.1-10). Kitanov and Nedialkov (1998) found that *H. perforatum* plants do not accumulate xanthones in significant amounts in the aerial parts, with the exception of mangiferin. However, in the presence of a pathogen, the production of xanthones is strongly influenced due to the defence function against infection. The accumulation of xanthones in *H. perforatum* cultures was strongly induced by *Colletotrichum gloeosporioides*, especially when primed with salicylic acid and methyl jasmonate. The results confirmed that these compounds act as defence metabolites in intact *H. perforatum* plants and in *in-vitro* plants (Conceição et al., 2006).

Accumulation of polyketide secondary metabolites in wild plants and in one-year-old *in-vitro* cultures of *H. perforatum* was described by Dias *et al.* (2001) and Dias, 2003) as follows:

- Flavonoids are accumulated in the aerial parts of *in vivo* plants; however, *in-vitro* cultures of *H. perforatum* were almost devoid of flavonoids and these compounds were not detectable in calli.
- Biflavonoids were only detected in the wild plants in small amounts.
- Xanthones were found in the extracts of shoot cultures and in calli. However, they were not detected in the aerial parts of wild plants.
- Hyperforin was detected in wild plants and in *in-vitro* shoots.

Distribution of polyketide secondary metabolites in various organs of *H. perforatum*, as summarized in the literature (Upton, 1997; Łożykowska, 2003; Hölzl and Petersen, 2003), is listed in Table 1-4.

Table 1- 4: Relative distribution of constituents in organs of *H. perforatum*:

Plant organ	Hypericin	Hyperforin	Flavonoids	Biflavonoids	Xanthones
Flowers and buds	Medium amount (+)	High amount (++)	High amount (++)	Medium amount (+)	Traces (-)
Capsules	Low amount (±)	High amount (++)	Traces (-)	Traces (-)	?
Leaves	Low amount (±)	Medium amount (+)	High amount (++)	Not detectable	Traces (-)
Stems	Traces (-)	Medium amount (+)	High amount (++)	Not detectable	Traces (-)
Roots	Not detectable	Not detectable	?	?	Medium amount (+)

1.3 Overview of the Project

The aim of this work was to localize by indirect immunofluorescence the two polyketide synthases, BPS and CHS, in various organs of the medicinal plant *H. perforatum*. So far, little is known about the tissue-specific distribution of these enzymes in *Hypericum* species.

The main experimental steps of this project are summarized in Fig. 1-17.

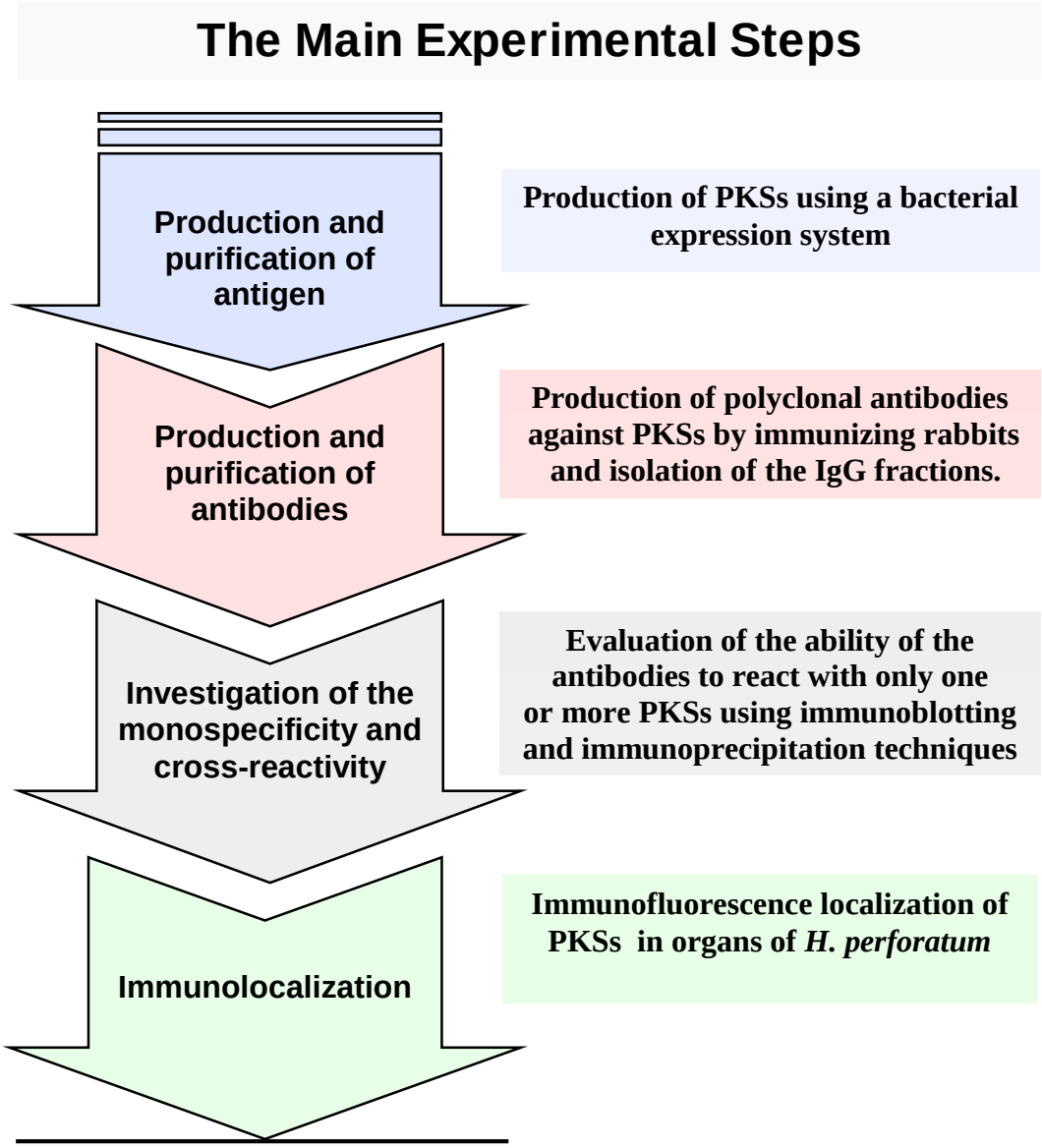

Fig.1- 17: Overview of the studies performed in this work.

2 Methods and Materials

2.1 Chemicals

2.1.1 General Chemicals

Reagents	Supplier
Acetic acid	Roth
Ammonium chloride	Roth
L(+)-Ascorbic acid sodium salt	Roth
Calcium chloride	Fluka
Citric acid	Roth
Dithiothreitol (DTT)	Diagnostic Chemicals Limited
Ethyl acetate	Fisher Scientific
Ethylenediamine tetraacetic acid disodium salt dehydrate (Na_2EDTA)	Roth
Formaldehyde 37% free from water	Merck
L-Glutathione reduced	Roth
Glycerol	Roth
Glycine	Roth
Hydrochloric acid	Roth
Imidazol	Roth
Methanol (HPLC)	Fisher Scientific
Phenylmethane sulphonyl fluoride(PMSF)	Roth
Ortho-phosphoric acid	Roth
Polyclar® AT	Serva

Reagents	Supplier
Polyethyleneglycol 8000	Roth
Potassium dihydrogen phosphate	Roth
Potassium chloride	Roth
Potassium hydroxide	Fluka
Sodium acetate	Roth
Sodium azide	Serva
Sodium carbonate	Roth
Sodium chloride	Roth
Sodium deoxycholic acid	Aldrich
Sodium dihydrogen phosphate- monohydrate	Merck
Sodium dodecyl sulphate(SDS)	Roth
Sodium phosphate dihydrate	Merck
Sodium thiosulphate	Fluka
Sucrose	Roth
Trichloroacetic acid	Fluka
Tris	Roth

2.1.2 Special Chemicals

2.1.2.1 Protein Assay

Reagents	Supplier
Bovine Serum Albumin (BSA)	Roth
Coomassie® brilliant Blue G250	Serva
Ortho-phosphoric acid-85%	Roth

2.1.2.2 Protein Gel Electrophoresis

2.1.2.2.1 SDS Polyacrylamide Gel Electrophoresis (SDS-PAGE)

Reagents	Supplier
Acrylamide/bisacrylamide 30%	Bio-Rad
Ammonium persulfate (APS)	Bio-Rad
Bromophenol blue	Aldrich
β-Mercaptoethanol	Fluka
Sodium dodecyl sulphate (SDS)	Roth
PageRuler™ Protein Ladder,10 kDa to 200 kDa	Fermentas
Unstained Protein Molecular Weight Marker, 14.4 kDa to 116 kDa	Fermentas
N,N,N',N'-Tetramethylethylene-diamine (TEMED)	Bio-Rad

2.1.2.2.2 Native Polyacrylamide Gel Electrophoresis (Native PAGE)

a. Acidic Native Gel

Reagents	Supplier
Acetic acid	Roth
Acrylamide/bisacrylamide 30%	Bio-Rad
β-Alanine	Fluka
APS	Bio-Rad
Methyl Green	Fluka
TEMED	Bio-Rad

b. Basic Native Gel

Reagents	Supplier
Acrylamide/bisacrylamide 30%	Bio-Rad
APS	Bio-Rad
Bromophenol blue	Aldrich
TEMED	Bio-Rad

2.1.2.2.3 Electrophoresis Blotting Gel

Reagents	Supplier
Milk powder	Roth
Tween® 20	Fluka

2.1.2.2.4 Staining Techniques

2.1.2.2.4.1 Staining of Electrophoresis Gels

a. Coomassie Blue Stain

Reagents	Supplier
Coomassie® brilliant Blue R 250	Serva
Coomassie® brilliant Blue G250	Serva

b. Silver Stain

Reagents	Supplier
Silver nitrate	Roth

c. E-Zinc™ Reversible Stain Kit

Reagents	Supplier
E-Zinc stain	Pierce
E-Zinc Developer	Pierce
E-Zinc Eraser	Pierce

2.1.2.2.4.2 Staining of the Blot Membrane

Indian-Ink-Stain

Reagents	Supplier
Fount India-Tinte	Pelikan

2.1.2.3 Enzyme Assays

2.1.2.3.1 BPS Assay

Reagents	Supplier
Benzoyl-CoA	Sigma
Malonyl-CoA	Sigma
2,4,6 Trihydroxybenzophenone	ICN Biomedical Inc.

2.1.2.3.2 CHS Assay

Reagents	Supplier
p-Coumaroyl-CoA	Synthesized (Dr. B. Liu "our group")
Cinnamoyl-CoA	Synthesized (M. Gaid "our group")
Malonyl-CoA	Sigma
Naringenin (4´,5,7 -Trihydroxy-flavanone)	Sigma

2.1.2.4 Elicitor Reagents

Reagents	Supplier
Methyl jasmonate	Serva
Salicylic acid	Sigma

2.1.2.5 Nutrient Media

Medium	Constituents	Notes
Luria - Bertani (LB) medium: It was used for growing bacteria (*E. coli*) at 37°C.	1% Pepton (Roth), 0.5% Yeast extract (Roth), 1% Sodium chloride (Roth).	F All constituents were dissolved in Milli-Q water up to one liter. F pH was adjusted to 7.5 with NaOH F The medium was sterilized by autoclaving.
LB agar plates: They were used as solid medium for growing bacteria (*E. coli*) at 37°C.	1.5 % agar (Roth), 150 µg / ml ampicillin (Roth), 60 µg /ml chloramphenicol (Fluka).	F The antibiotic solutions were added to the agar plate or into the liquid medium just before use.
Murashige Skoog (MS) medium (Murashige and Skoog, 1962): It was used as artificial medium for growing tissue cultures.	1. Microelements: (1 L) 6.2 mg H_3BO_3 (Roth), 16.9 mg $MnSO_4 \cdot H_2O$ (Fluka), 10.6 mg $ZnSO_4 \cdot 7 H_2O$ (Merck), 0.83 mg KI (Sigma), 0.25 mg $Na_2MoO_4 \cdot 2 H_2O$ (Merck), 0.025 mg $CuSO_4 \cdot 5 H_2O$ (Merck), 0.025 mg $CoCl_2 \cdot 6 H_2O$ (Merck), 37.2 mg $Na_2EDTA \cdot 2 H_2O$ (Roth), 27.5 mg $FeSO_4 \cdot 7 H_2O$ (Merck).	F Twenty-fold stock solutions were prepared for micro-elements, vitamins and macroelements. They were diluted 20 times to give the final concentrations. F Deionized water was added to nearly one liter and the pH was adjusted to 5.8 with 5 N NaOH. The final volume of the medium was adjusted to one liter.

Medium	Constituents	Notes
Murashige Skoog (MS) medium:	2. Vitamins: (1 L) 0.5 mg Nicotinic acid (Merck), 0.5 mg Pyridoxin-HCl (Merck), 0.1 mg Thiamin HCl (Serva), 2.0 mg Glycin (Roth), 0.1 mg Myo-Inositol (Sigma). 3. Macroelements: (1 L) 1.65 g NH_4NO_3 (Merck), 1.9 g KNO_3 (Fluka), 0.44 g $CaCl_2 \cdot 2\ H_2O$ (Merck), 0.37 g $MgSO_4 \cdot 7\ H_2O$ (Merck), 0.17 g KH_2PO_4 (Merck). 3. Carbohydrates: (1 L) 20 g Sucrose (Serva), 8 g Agar-agar (ROTH).	F The medium was autoclaved for sterilization. F Glucose (Merck) at a concentration of 1.6 % may be added instead of sucrose as a carbon source.

2.1.2.6 Immunoassay

2.1.2.6.1 Immunoblotting Materials

	Materials	Supplier
Blotting materials:	• PVDF blotting membrane (Immobilon-P)	Millipore
	• Blotting filter paper	Schleicher & Schuell
Primary antibody:	• Anti-BPS IgG • Preimmune-BPS IgG • Anti-CHS IgG • Preimmune-CHS IgG	see 2.11.9.1 and 2.11.9.2.
Secondary antibody:	• Peroxidase-conjugated AffinPure Goat Anti-Rabbit IgG (H+L)	Dianova
Blotting Detection materials:	• ECL™ Western Blotting Detection Reagents	Amersham Biosciences

2.1.2.6.2 Immunohistochemistry

	Materials	Supplier
Embedding materials:	• Cryo-embedding compound	Plano
	• Technovit®7100 kit	Heraeus-Kulzer
	• Technovit®3040 kit	Heraeus-Kulzer
Blocking material:	• BSA	Roth
	• Fish gelatin	Sigma
Secondary antibody:	• Alexa Fluor® 488 goat anti-rabbit IgG (H+L)	Molecular Probes (Invitrogen)
Detection materials:	• Diagnostic slides, Teflon®	Roth
	• Microscope slides	Roth
	• Poly-laysin coated slides	Roth
	• Poly-laysin solution	Sigma
	• Citifluor Glycerol / PBS solution	Agar scientific
	• Cover slides	Roth

2.2 Preparation of Bidistilled Water

The aqueous solutions, buffers, and media were prepared using Milli-Q water from a Milli-Q Water Purification System (Millipore). The water used for FPLC and HPLC gradients was prepared using GFL-2104 double water stiller (MultiLAB) and arium® 611 (Sartorius).

2.3 Solutions

Name	Preparation
100 mg / ml ampicillin solution:	ð Dissolve 1 g of ampicillin (sodium salt, Roth) in a total of 10 ml of distilled water. Filter-sterilize the solution and store at -20°C
30 mg / ml chloramphenicol solution:	ð Dissolve 0.3 g of chloramphenicol (Fluke) in a total of 10 ml of absolute ethanol, store at -20°C.
0.5 M IPTG solution:	ð Dissolve 1.2 g of IPTG (Roth) in 10 ml of distilled water. Filter-sterilize the solution and store at -20°C.
1U / µl factor Xa solution:	ð Dissolve 400 U factor Xa (Amersham Biosciences) in 400 µl cold distilled water, freeze in 80 µl aliquots at -80°C.
10% SDS solution**:**	ð Dissolve 10 g SDS (Roth) in 60 ml distilled water and add distilled water to a final volume of 100 ml.
10% Ammonium persulfate (APS) solution:	ð Dissolve 100 mg APS (Bio-Rad) in 1 ml of distilled water. Make the APS solution freshly or get it from a -80°C freezer.

Name	Preparation
Coomassie blue Staining solution:	ð Dissolve 0.2 g Coomassie®brilliant Blue R 250 and 0.05 g Coomassie®brilliant Blue G 250 in 42.5 ml ethanol, 5 ml methanol, 10 ml acetic acid and 42.5 ml distilled water; stir overnight; filtrate before use; store in a dark bottle.
Destaining solution for Coomassie blue Stain:	
1. Fast destaining :	ð Mix 50 % (v/v) methanol and 10 % (v/v) acetic acid with distilled water.
2. Slow destaining:	ð Mix 10 % (v/v) methanol and 10 % (v/v) acetic acid with distilled water.
Silver staining solutions:	
1. Fixing solution:	ð Mix 30 % (v/v) ethanol and 10 % (v/v) acetic acid with distilled water.
2. Sensitizing solution:	ð Dissolve 0.2 % (w/v) sodium thiosulphate and 0.5 M sodium acetate in 30 % (v/v) ethanol and distilled water.
3. Silver solution:	ð Dissolve 0.2 % (w/v) silver nitrate and 0.01 % (v/v) formaldehyde in distilled water.
4. Developing solution:	ð Dissolve 6 % (w/v) sodium carbonate (water-free) and 0.02 % (v/v) formaldehyde in distilled water.
5. Stop solution:	ð Dissolve 1.5 % (w/v) Na_2EDTA in distilled water.

Name	Preparation
Bradford-dye solution (for protein assay):	ð Dissolve 100 mg Coomassie®-brilliant Blue G- 250 in 50 ml ethanol (60 %), add 100 ml *ortho*-phosphoric acid (85 %) and complete the volume to 1 L with distilled water, store at 4°C and filter before use.
DOC solution:	ð Dissolve 0.1 % (w/v) sodium deoxycholic acid and 0.02 % sodium azide in distilled water.
TCA solution:	ð Dissolve 55 % (w/v) trichloroacetic acid in distilled water.
India-Ink-solution:	ð Mix 1 ml acetic acid and 0.1 ml Fount India Ink with 100 ml PBS buffer containing 0.1 % (v/v) Tween-20.
Milk-Blocking solution:	ð Dissolve 5 % (w/v) milk powder in TBS-T buffer.
Fixative solution (for immuno-histochemical assay):	ð Dissolve 2 g *p*-formaldehyde (ROTH) in 45 ml distilled water. 10 N NaOH is added subsequently under heating until the solution becomes clear. After cooling, the pH is adjusted to 7.5. The volume is filled up to 50 ml with water, then to 100 ml with 0.1 M phosphate buffer, pH 7.2. Finally, 0.1 ml Triton X-100 (Sigma) and 0.1 ml glutaraldehyde (ROTH) are added. The solution is stored at 4˚C in the dark.

Name	Preparation
BSA-Blocking solution:	ð Dissolve 10 % (w/v) BSA (ROTH) and 0.1 % (v/v) fish gelatin (Sigma) in 1x PBS buffer, pH 7.2.

2.4 Buffers

	Name	Preparation
Buffer for Lysis of Cells by Sonification:	Resuspending buffer:	ð 0.1 M KH_2PO_4, pH 7.2.
Buffers for Affinity Purification of GST-Fusion Proteins:	1. Binding buffer (PBS buffer):	ð 140 mM NaCl, 2.7 mM KCl, 10 mM Na_2HPO_4, 1.8 mM KH_2PO_4, pH 7.3.
	2. Elution buffer	ð 50 mM Tris-HCl, 10 mM reduced glutathione, pH 8.0.
	3. Factor Xa cleavage buffer:	ð 50 mM Tris-HCl, 150 mM NaCl, 1 mM CaCl, pH 7.2.
Buffers for Affinity Purification of 6xHis-tagged Fusion proteins:	1. Lysis buffer:	ð 50 mM Na_2HPO_4, 300 mM NaCl, pH 8.0.
	2. Washing buffer:	ð 20 mM Imidazol, 50 mM Na_2HPO_4, 300 mM NaCl, pH 8.0.
	3. Elution buffer:	ð 250 mM Imidazol, 50 mM Na_2HPO_4, 300 mM NaCl, pH 8.0.

	Name	Preparation
Buffers for Extraction of protein from plant tissues:	1. PBS buffer containing polyclar®AT:	ð PBS buffer, pH 7.3, 5% (w/v) Polyclar® AT (Serva), 2.5% (w/v) sodium ascorbate (ROTH).
	2. 0.1 M potassium phosphate buffer:	ð 0.1 M potassium phosphate buffer, pH 7.5, containing 10 mM DTT.
	3. 50 mM Tris-HCl buffer containing protease inhibitor:	ð 50 mM Tris-HCl, pH 7.4, containing 10 mM DTT, 0.5 mM sucrose, 1 mM PMSF.
Buffers for SDS-PAGE:	1. Electrode buffer:	ð 0.025 M Tris, 0.192 M glycine, 0.1 % (w/v) SDS, pH 8.3.
	2. Stock sample buffer:	ð 2 ml 0.5 M Tris-HCl pH 6.8, 0.2 g SDS, 5 ml glycerol, 0.5 ml β-mercaptoethanol, 0.1 ml bromophenol blue (1% in ethanol), 2.4 ml distilled water.
Buffers for acidic Native Gel:	1. Electrode buffer:	ð 0.35 M β-alanine, 0.14 M acetic acid, pH 4.3.
	2. Stock sample buffer:	ð 1.45 ml glycerol 50%, 0.5 ml 0.25 M acetate-KOH pH 6.8, traces of methyl green.

	Name	Preparation
Buffers for basic Native Gel:	1. Electrode buffer:	ð 0.05 M Tris, 0.38 M glycine, pH 8.9.
	2. Stock sample buffer:	ð 5 ml glycerol, 2.13 ml 0.5 M Tris-HCl pH 6.8, 2.7 ml distilled water, traces of bromophenol blue.
Buffer for Affinity Purification of Rabbit IgGs:	1. Binding buffer:	ð 20 M sodium phosphate, pH 7.0
	2. Elution buffer:	ð 0.1 M citric acid, pH 3.6.
Buffers for Immunoblotting:	1. Tris-buffered saline(10x TBS):	ð Dissolve 8 g NaCl, 3 g Tris-base and 0.2 g KCl in 100 ml distilled water, pH 8.0.
	2. 1x TBS –T:	ð Mix 10 ml 10x TBS with 100 ml distilled water containing 0.1% (v/v) Tween-20
	3. 10x Blot buffer:	ð Dissolve 5.8 g Tris-base, 2.9 g glycine and 0.37 g SDS in 100 ml distilled water.
	4. 1x Blot buffer:	ð Mix 10 ml 10x Blot buffer and 20 ml methanol with 100 ml distilled water.
Buffer for fixative solution:	0.1 M Phosphate buffer:	ð Dissolve 1.09 g Na_2HPO_4 and 0.32 g NaH_2PO_4 in 100 ml distilled water, pH 7.4.

2.5 Plant material

Studies were performed with *Hypericum perforatum* plants.

- Intact fresh plants were harvested from the medicinal plant garden of the Institute of Pharmaceutical Biology, Technical University Braunschweig, Germany.
- *In vitro* plants were grown on solid Murashige Skoog (MS) medium containing 2% sucrose as carbon source without any phytohormones under controlled condition at 25˚C and 16 h light / 8 h dark cycle. The medium was refreshed at four-week-intervals. The seeds of *H. perforatum* were sterilized as described in (2.11.14).

2.6 Bacterial strains

The following *E. coli* strains were used:

- *E.coli BL21- Codon- plus (DE3) - RIL* (Stratagene) transformed with the recombinant vector *pGEX* containing the desired heterologous gene.
- *E.coli BL21- Codon- plus (DE3) - RIL* (Stratagene) transformed with the recombinant vector *pRSET B* (Biolab) containing the desired heterologous gene.

2.7 Autoradiography Materials

Material	Supplier
X-Ray Film, X-Omat (Kodak)	Sigma
X-Ray Film Developer and Fixer (Kodak)	Sigma

2.8 Chromatography and Protein Fractionation Materials

Materials	Supplier
GSTrap FF, 1ml Column	Amersham Biosciences
Glutathione agarose	Invitrogen
Ni-NTA Agarose	QIAGEN
HiPrep 16/60 Sephacryl S-200 HR	Amersham Biosciences
HiTrap Protein A HP, 1 ml Column	Amersham Biosciences
Disposable PD-10 Desalting Columns	Amersham Biosciences
Microsep™ Cenrifugal Devices (10 K, blue)	Pall Life Sciences
Microsep™ Cenrifugal Devices (50 K, green)	Pall Life Sciences
Vivaspain Centrifugal Cocentrators (10 K, blue)	Viva science Sartorius group
Hyperclone C_{18} 3 µm column (3.20 mm x 150 mm)	Phenomenex
Hyperclone C_{18} 5 µm column (4.60 mm x 150 mm)	Phenomenex

2.9 Disposable Plastic Ware

Commonly used disposable plastic ware was purchased in standard grade from the following companies: Sarstedt, Renner, Biozym, Diagnostic GmbH.

2.10 Molecular Biological Methods

2.10.1 Expression of PKSs in *E. coli* Cells as Tagged Fusion Proteins

PKSs (BPS and CHS) were previously cloned from cell cultures of *Hypericum androsaemum* (Liu *et al.*, 2003). The recombinant proteins included either a protein or a small peptide tag (GST / 6x His tag). Expression vectors were constructed for the heterologous production of the proteins in *E. coli.*

a. GST-fusion proteins

The PKSs were over-expressed in *E. coli* as glutathione-S-transferase (GST) fusion proteins. The amplified *open-reading frames (ORFs)* were ligated into an expression vector derived from the *pGEX* vector series. Recombinant plasmids were introduced into *E. coli BL21-Codon Plus (DE3)-RIL* (Stratagene) for over-expression.

b. 6xHis-tagged proteins

The general protocols for expression were done as previously, but the cloning materials were different. PKSs were over-expressed in *E. coli* as hexa-histidine-tag (6xHis) fusion proteins. The amplified *open-reading frames (ORFs)* were ligated into an expression vector derived from the *pRSET B* vector series. Recombinant plasmids were introduced into *E. coli BL21-Codon Plus (DE3)-RIL* (Stratagene) for over-expression.

2.10.2 Growth of Cells and Induction of Expression

a. GST-fusion proteins

E.coli BL21(DE3) containing the desired gene was picked from frozen culture by scratching the sterile loop across the entire agar surface of the agar plate containing 150 µg/ml ampicillin and 60 µg/ml chloramphenicol without tearing into it. The plate

was incubated upside down in an incubator at 37°C over-night. A single recombinant *E. coli* colony was inoculated into 10 ml of LB medium containing 100 µg/ml of ampicillin and 30 µg /ml chloramphenicol. Inoculated LB medium was incubated on a shaker (225 rpm) at 37°C over-night. About 4 ml of the overnight culture was inoculated into 100 ml of the LB medium (antibiotics are not required for expression). The culture was incubated on a shaker (225 rpm) at 37°C for 2-4 h or until OD_{600} = 0.6–0.8. A 0.5 ml sample was immediately taken before induction (non-induced control) and was stored at –20°C until SDS-PAGE analysis. Then IPTG was added to a final concentration of 1 mM. The culture was grown at 25°C with vigorous shaking for 3-4 hours. A second 0.5 ml sample (induced control) was collected and was stored at –20°C until SDS-PAGE analysis. The aliquots of induced and control cultures were then analysed for expression of the recombinant protein by SDS-PAGE followed by Coomassie blue staining or silver staining as described in (2.11.8). After the culture had been treated with IPTG, the cells were harvested by centrifugation and frozen at -20°C for further use.

b. 6xHis-tagged proteins

The procedure was performed as described above.

2.11 Biochemical Methods

2.11.1 Extraction of Expressed Proteins from *E. coli* Cells

a. GST-fusion proteins

Mechanical disruption of the cell membrane (sonication) is a common method for breaking the cell membrane and isolating the soluble protein. The frozen cell pellet from 50 ml culture (see 2.10.2.a) was re-suspended in 1.6 ml of 0.1 M potassium phosphate buffer, pH 7.2 at 4°C. Sonication of the cells was carried out on ice for 5 min at 50% pulses using a Branson Sonifier B15 (Heinemann, Schwäbisch Gmünd,

Germany). After centrifugation at 10000 g and 4ºC for 10 min, the supernatant is stored on ice until it is applied to an affinity column (GSTrap FF column, Amersham Biosciences) or to the glutathione agarose protein purification system (Invitrogen).An aliquot of the supernatant had been taken as expressed protein control and stored at –20°C until SDS-PAGE (see 2.11.8).

b. 6xHis tagged proteins

The frozen cell pellet from a 50 ml culture (see 2.10.2.b) was re-suspended in 1.6 ml of lysis buffer, pH 8.0 (see 2.4) at 4°C. Sonication of the cells was carried out on ice for 5 min at 50 % pulses using a Branson Sonifier B15 (Heinemann, Schwäbisch Gmünd, Germany). After centrifugation at 10000 g and 4ºC for 10 min, the supernatant was stored on ice until it was applied to a Ni-NTA protein purification system (QIAGEN). An aliquot of the supernatant had been taken as expressed protein control and stored at -20°C until SDS-PAGE (see 2.11.8).

2.11.2 Purification and Factor Xa Cleavage of GST-Fusion Proteins

2.11.2.1 Purification of GST-Fusion Proteins and On-Column Cleavage using GSTrap FF Column

The following purification procedure was performed using a Biologic®-System for protein purification (FPLC; Bio Rad). Supernatants (2.11.1.a) containing the GST-fusion proteins (GST-BPS / GST-CHS) were loaded on a pre-equilibrated GSTrap FF 1 ml column in series with PBS, pH 7.3 as binding buffer (see 2.4). The pump tubing “drop to drop” was used to avoid introducing air into the column. Sample loading onto the column was by pumping at a reduced flow rate (1ml / min) to optimize the binding interactions with the GST affinity medium (Glutathione Sepharose™ 4 Fast

Flow). Following GST-fusion protein binding to the column, bound material was washed with PBS, pH 7.3 until the baseline returned to zero. Once the baseline had stabilized, buffer was substituted with factor Xa cleavage buffer (see 2.4). This buffer was used to more stringently wash the GST-fusion protein bound to the GSTrap FF column and to pre-equilibrate the column. Equilibration with Factor Xa cleavage buffer was continued until both the UV absorbance baseline and the conductivity baseline stabilized, after which the buffer flow was stopped. The Factor Xa mix was prepared according to the concentration of GST-tagged protein bound. For 1 mg GST-tagged protein, mix 10 µl factor Xa solution (see 2.3) with 990 µl factor Xa cleavage buffer and manually inject onto the column. Following injection, the column was sealed with the top cap and incubated at room temperature (22 to 25°C) for 2-16 h. The cleaved protein eluted immediately upon flow startup with factor Xa cleavage buffer. The eluted fraction contained the protein of interest and factor Xa, while the GST moiety of the fusion protein remained bound to GSTrap FF column. Following target protein elution and return to baseline, a GST affinity competitor (reduced glutathione elution buffer, see 2.4) was applied to elute GST and unbound GST-fusion protein.

2.11.2.2 Purification of GST-Fusion Proteins and Off-Column Cleavage using GSTrap FF Column

As described in (2.11.1.a), supernatants containing GST-fusion protein (GST-BPS / GST-CHS) were loaded on a GSTrap FF 1 ml column and GST-fusion proteins were bound to the column (see 2.11.2.1). Following a wash with binding buffer, GST-fusion proteins were eluted with elution buffer (see 2.4). Then the reduced glutathione was removed from the eluate using a quick buffer exchange against factor Xa cleavage buffer (see 2.4) on a PD-10 Desalting Column (Amersham Biosciences) as described in (2.11.7.1) or on a Microsep™ Cenrifugal Device “50 K, green” (PALL life Sciences) as described in (2.11.7.2). Following desalting, 10 µl of factor Xa solution (see 2.4) per 1 mg of tagged protein in the eluate were mixed and incubated

at room temperature (22 to 25°C) for 2-16 h. Once digestion has completed, the sample was applied to an equilibrated GSTrap FF column to remove the GST moiety. The eluted fraction contained the protein of interest and factor Xa.

2.11.2.3 Purification of GST-Fusion Proteins using Glutathione Agarose Protein Purification System

The following purification procedure was performed on a glutathione agarose protein purification system (Invitrogen). Glutathione slurry (200 µl) was added to 3.5 ml of the cleared lysate (supernatant which contained either GST-BPS or GST-CHS) as described in (2.11.1.a). After mixing gently by shaking (200 rpm on a rotary shaker) at 4°C for 1 h, the lysate-glutathione mixture was loaded into a column, the outlet of which was capped. After removing the outlet cap, the column was washed four times with 1 ml washing buffer each (see 2.4). The GST-tagged-fusion protein was eluted using 3.5 ml elution buffer (see 2.4). The glutathione was removed from the eluate using a quick buffer exchange against PBS, pH 7.3 (see 2.4) on a PD-10 desalting column (Amersham Biosciences) as described in (2.11.7.1).

2.11.3 Purification of 6xHis-Tagged Proteins

The following purification procedure was performed on a nickel-nitrilotriacetic acid "Ni-NTA" protein purification system (QIAGEN). Ni-NTA slurry (200 µl) was added to 4 ml of the cleared lysate (supernatant which contained either 6xHis-BPS or 6xHis-CHS) as described in (2.11.1.b). After mixing gently by shaking (200 rpm on a rotary shaker) at 4°C for 1 h, the lysate-Ni-NTA mixture was loaded into a column the outlet of which was capped. After removing the outlet cap, the column was washed four times with 1 ml washing buffer each (see 2.4). The 6xHis-tagged-fusion protein was eluted using 3.5 ml elution buffer (see 2.4). The imidazol was removed from the eluate using a quick buffer exchange against PBS, pH 7.3 (see 2.4.) on a PD-10 desalting column (Amersham Biosciences) as described in (2.11.7.1).

2.11.4 Extraction of Proteins from Plant Tissues

Two alternative extraction procedures were used. The procedure involved either grinding of the plant tissue in liquid nitrogen followed by extracting proteins into extraction buffer or direct homogenization with extraction buffer. Generally, plants produce a wide range of proteases which might interfere with extraction of intact proteins. It might therefore be important to use protease inhibitors during extraction to prevent the degradation of the protein of interest.

2.11.4.1 Grinding Plant Tissue in Liquid Nitrogen and Solving Proteins in Extraction Buffer

All steps were carried out at 0- 4°C. Fresh or material stored at -80°C (1 g) was ground in a mortar with liquid nitrogen, until a fine powder was produced. Two ml of extraction buffer (PBS buffer, pH 7.3, containing Polyclar® AT, see 2.4) were added to the powder and grinding was continued for additional 30 sec. Polyclar® AT is used as an inhibitor of phenolic oxidation and sodium ascorbate is used as an antioxidant substance. The homogenized mixture was transferred to a Falcon tube and agitated for 30 min, followed by centrifugation for 30 min at 13000 rpm, 4°C (Universal 32R centrifuge, Hettich). The pellet containing plant debris was thrown away. The supernatant contained the soluble protein fraction (crude extract) and was stored at -20°C.

An alternative method of protein extraction from plant tissue was suitable for enzyme assay application. The proteins extracted in this way were more active, because a protease inhibitor was added to the extraction buffer. All steps were carried out at 0-4°C. Fresh or frozen (-80°C) leaves (1 g) were placed in a cooled mortar and ground for 2-3 min in liquid nitrogen, until a fine powder was produced. This powder was mixed with 0.1 g Polyclar® AT and homogenized in 1 ml of 50 mM Tris-HCl buffer, pH 7.4 containing PMSF as protease inhibitor (see 2.4). However, PMSF is extremely toxic and had to be used with care during extraction of proteins. The homogenized mixture was transferred to a Falcon tube and centrifuged for 15 min at

13000 rpm, 4°C. The pellet containing plant debris was thrown away. The supernatant contained the soluble protein fraction (crude extract) and was stored at -20°C.

2.11.4.2 Plant Tissue Directly Homogenized in Extraction Buffer

All steps were carried out at 0-4°C. Fresh or frozen (-80°C) leaves (1 g) were mixed with 0.1 g Polyclar® AT and homogenized in 0.1 M potassium phosphate buffer, pH 7.5, containing 1 mM dithiothreitol (DTT). DTT is used to protect cystein residues of proteins from oxidation. The homogenized mixture was transferred to a Falcon tube and centrifuged for 15 min at 13000 rpm, 4°C (Universal 32R centrifuge, Hettich). The pellet containing plant debris was thrown away. The supernatant contained the soluble protein fraction (crude extract) and was stored at -20°C.

2.11.5 Fractionation of Complex Protein Solutions

2.11.5.1 Purification of Fusion Proteins after Cleavage by Gel Filtration (Size Exclusion Chromatography)

Gel filtration is used to separate molecules according to their molecular masses. In a column filled with porous beads, larger molecules move through the column much faster than small molecules. The purified cleaved fusion protein was fractionated on a HiPrep 16/60 Sephacryl S-200 HR column (Amersham Biosciences) at 0.3 ml/min in binding buffer (PBS buffer, pH 7.3, see 2.4.) using fast protein liquid chromatography (FPLC, Biologic®-System, Bio Rad). Calibration was done using size exclusion chromatography standards (Bio Rad). After elution was completed, fractions were further examined separately by SDS-PAGE (see 2.11.8).

2.11.5.2 Purification of Fusion Proteins after Cleavage by Native Polyacrylamide Gel Electrophoresis

This technique is inversed when compared to gel filtration, the smaller molecules move faster through the cross-linked gel than the larger molecules. Protein purification by gel electrophoresis has been used in various applications such as antigen preparation for antibody generation. Many systems for native (non-denaturing) protein electrophoresis have been developed. The charge of the proteins comes into play in this separation, because native gel electrophoresis is run in the absence of SDS. While in SDS-PAGE (see 2.11.8) the electrophoretic mobility of proteins depends exclusively on their molecular masses, the mobility in native PAGE depends on both the protein's charge and hydrodynamic size. Native gel electrophoresis allows for rapid screening of protein mixtures for bioactive fractions. The native PAGE method was based on the gel system first described by Davis, 1964 (Walker, 1996).

The preparation of native polyacrylamide gels using either an acidic or a basic buffer system is described in the following.

Acidic native gel for basic proteins (pI >7.0):

	Separating gel		**Stacking gel**
	10% [ml]	**7% [ml]**	**4% [ml]**
H_2O	2.10	3.30	3.20
30 % Acrylamide solution	4.40	3.20	0.50
1.5 M Acetate-KOH pH 4.3	3.35	3.35	-
0.25 M Acetate-KOH pH 4.3	-	-	1.25
50 % (v/v) Glycerol solution	3.00	3.00	-
10 % (w/v) APS	0.16	0.16	0.05
TEMED	0.02	0.02	0.005

Basic native gel for acidic proteins (pI <7.0):

	Separating gel		Stacking gel
	12% [ml]	7% [ml]	4% [ml]
H_2O	3.72	5.64	3.20
30 % Acrylamide solution	4.52	2.60	0.50
1.5 M Tris-HCl pH 8.9	2.80	2.80	-
0.5 M Tris-HCl pH 6.8	-	-	1.25
10 % (w/v) APS	0.04	0.04	0.05
TEMED	0.0092	0.0092	0.005

Polyacrylamide creates a network; the size of the lattice depends on the acrylamide concentration. Acrylamide mixed with bisacrylamide forms a cross-linked polymer network when the polymerizing agent (ammonium persulfate “APS”) is added. APS produces free radicals faster in the presence of TEMED. The concentration of acrylamide was below 12% and changed to separate proteins of different molecular weight rang. The mixture for the separating gel was allowed for 30 minutes to polymerize, and immediately poured between two vertically oriented glass plates in a gel-casting stand to make a gel of 1.0 mm thickness. This was followed by addition of the collecting gel layer on top of the separating gel. Protein samples to be analysed were mixed with protein stock sample buffer (loading buffer, see 2.4) (ratio 1:1). The prepared samples were pipetted into individual wells of the collecting gel including a known protein (Bovine Serum Albumin “BSA”). Then the electrodes were already plumbed into the holder above and below the gel and contacted the gel via 1x electrode buffer (see 2.4).

The power leads were attached, so that in the basic-native gel the proteins were running towards the anode. In an acidic native gel the proteins were positively charged, and therefore run toward the cathode, so the polarity of the leads to the gel was reversed to prevent sample loss (see Fig. 2-1). Analysis of multiple samples is accomplished using a Multigel-Long Electrophoresis system (Biometra). The running conditions were at 30 mA /200 V max. supplied by a Standard Power Pack P25 (Biometra). The gel was run until the dye front reached the bottom (about 3 hrs).

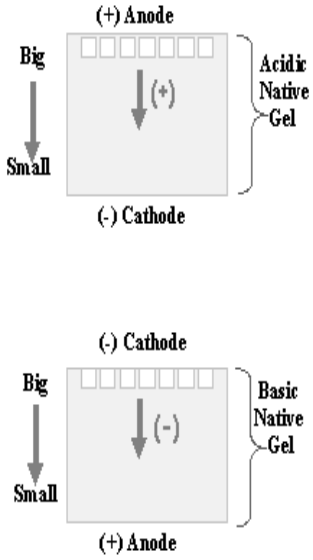

Fig. 2- 1: Acidic and basic native PAGE principles.

After electrophoresis, the protein band of interest (antigen) must be located in the gel, and the gel slice was excised for immunizing rabbits by using a reversible staining method. The entire gel was stained using the E-zinc reversible stain kit (Pierce). The E-zinc reversible stain is a negative stain that produced an opaque white background and left the protein bands as a clear band. The relevant band was excised, and then the gel slice was placed in a non-stick 1.5 ml tube with a few drops of water. The concentration of antigen in the gel slice was 300 µg or more in less than 0.5 µl volume. The maximum size of the gel slice allowed per injection was 1.5 inches long by 4 mm wide by 1 mm thick. The gel slices were stored at -20°C until use for immunization.

2.11.5.3 Purification of Proteins by Centrifugal Devices

Centrifugal devices provided rapid and convenient concentration, purification, and desalting of small volumes of biological samples. Protein samples were concentrated and purified by filtration using a highly selective ultra filtration membrane. This

membrane was made from polyethersulphone specifically modified to minimize protein binding. The centrifugal device was selected to have a molecular weight cutoff (MWCO) 3 to 6 times less than the molecular mass of the protein to be purified. The driving force for filtration was provided by centrifugation at 3000 to 7500 g. The protein molecules larger than the MWCO of the membrane were retained in a sample reservoir, while solvent and low molecular mass proteins passed through the membrane into the filtrate reservoir.

The following cenrifugal devices were used:

a. Microsep™ Cenrifugal Devices
b. Vivaspain Centrifugal Concentrators with patented vertical membrane technology.

2.11.6 Protein Assays

2.11.6.1 Quantitative Determination of Proteins

2.11.6.1.1 Dye-Binding (Bradford) Assay

The total protein concentration was determined by the binding of proteins to Coomassie® brilliant Blue G 250 (Bradford, 1976). In the photometric assay, the binding ability causes a shift in the absorbance from 465 nm to an intense band at 595 nm. In the assay, 10 µl sample was mixed with 990 µl Bradford-dye solution (see 2.3). The assay was performed in a cuvett of one cm width at 595 nm in an UV/VIS-spectrophotometer (Pharmacia Biotech Ultraspec 1000). Protein concentrations were calculated from a calibration curve which was prepared for each determination using 1 µg to 10 µg /ml bovine serum albumin (BSA) as standard.

2.11.6.1.2 Spectrophotometric (Absorbance) Assay (280 nm)

This is an alternative approach to measure protein concentrations, e.g. in antibody solutions (IgGs). The protein was directly assayed by measurement of the absorbance at 280 nm. This assay is rapid, simple and allows full recovery of the protein for subsequent analyses. The sample was simply filled into a quartz cuvette and the absorption at 280 nm was measured. Each species of protein has a unique extinction coefficient (ε). The extinction coefficient of rabbit IgG for a 1% solution at 280 nm is "13.5" (Harlow and Lane, 1988). The concentration of the sample is simply calculated by *Beer's law.*

2.11.6.2 Concentration of Proteins from Dilute Solutions

2.11.6.2.1 Precipitation of Protein by Deoxycholate (DOC) and Trichloro-acetic acid (TCA)

This method provided rapid precipitation of low protein concentrations, to enhance sensitivity for electrophoresis or protein determination. One volume of protein solution (about 20 µg) was mixed with 1/10 volume of 0.1% DOC solution (see 2.3). DOC forms complexes with proteins to enhance precipitation at low pH. Then, one volume of the previous solution was mixed with 1/10 volume of 55% TCA solution (see 2.3). TCA is used for precipitation of DOC-protein complexes. Then the solution was mixed and incubated overnight at 4°C. The precipitated protein was centrifuged for 30 min at 4°C at 15000 g. The supernatant was carefully removed and the pellet (concentrated protein) was re-suspended in 10 µl Tris-HCl, pH 8.5.

2.11.6.2.2 Protein Concentration by Cenrifugal Devices

The principle of Cenrifugal Devices (Microsep™ Cenrifugal Devices and Vivaspain Centrifugal Concentrators with patented vertical membrane technology) is described in (2.11.5.3).

2.11.7 Buffer Change and Desalting of Protein Samples

Protein desalting is an important preparation step for many biological samples. It is necessary for controlling enzyme activity as well as for purification and cleavage steps.

2.11.7.1 Disposable PD-10 Desalting Columns

The PD10 column (Amersham) was equilibrated with 25 ml standard buffer to desalt the soluble protein. Then 2.5 ml of the protein sample was loaded onto a PD10 column. Soluble proteins were eluted with 3.5 ml standard buffer .

2.11.7.2 Cenrifugal Filter Devices

The principle of centrifugal devices is described in (2.11.5.3). The sample was concentrated. The new buffer was added to the concentrated sample and centrifuged for a second time. The dilution /concentration steps were repeated until the required amount of salt is removed /replaced.

2.11.8 Molecular Mass Determination of Protein Subunits by SDS Polyacrylamide Gel Electrophoresis (SDS-PAGE)

Sodium Dodecyl Sulfate Polyacrylamide Gel Electrophoresis (SDS-PAGE) served the analysis of protein mixtures to confirm the successful expression of recombinant proteins in heterologous expression systems (2.11.1) Besides protein isolation and molecular mass determination of protein subunits, SDS-PAGE is a commonly used method in molecular biology which also allows for the separation of proteins for Western Blotting (see 2.11.9.3.1).

Proteins were separated based on their mass as they migrated through a polyacrylamide gel matrix. Acrylamide gel preparation involves the crosslinking of acrylamide monomers with the use of catalysts. APS produced free radicals faster in the presence of TEMED. SDS was a detergent that dissociates and unfolds oligomeric proteins into its subunits. Protein extracts were denatured by heating at 95°C for 5 min in the presence of the anionic detergent SDS and a reducing agent such as *β*-mercaptoethanol. In this step the proteins were bound to SDS and became negatively charged, thereby disrupting their subunits. Many systems for gel electrophoresis have been developed, as well as systems for setting up gel cassettes. In the typical Laemmli sodium dodecyl sulphate system, the proteins were separated according to their molecular mass while migrating towards the anode. This gel electrophoresis method was based on the gel system first described by Laemmli (1970), and was used according to the modified regulations of Gordon (1972) and Sambrook *et al.* (1989). Once the gel has set, protein samples can be loaded into the gel and separated along an electric field. The electrophoretic migration rate through a gel was determined by simultaneously running marker proteins of known molecular mass.

The Laemmli Sodium Dodecyl Sulphate System (SDS-PAGE):

	Separating gel 12% [ml]	Stacking gel 4% [ml]
H_2O	3.3	3.40
30 % Acrylamide solution	4.0	0.83
1.5 M Tris-HCl pH 8.8	2.5	-
0.5 M Tris-HCl pH 6.8	-	0.63
10 % (w/v) SDS solution	0.1	0.05
10 % (w/v) APS solution	0.1	0.05
TEMED	0.004	0.005

The concentration of acrylamide and bisacrylamide in the separating gel was 12 % which allowed the highest resolution of proteins between 10 and 200 kDa. The above composition was used for preparing a 12 % separating gel. After addition of APS and TEMED, the mixture for the separating gel was allowed for 30 min to polymerize, and immediately poured between two vertically oriented glass plates in a gel-casting stand to make a gel of 1.0 mm thickness. This was followed by addition of the collecting gel layer on top of the separating gel. Protein samples to be analysed were mixed with protein stock sample buffer (loading buffer, see 2.4), (ratio 1:1) and denatured at 95°C for 5 min. The prepared samples were pipetted into the individual wells of the collecting gel including known proteins (PageRuler™ Protein ladder, 10 kDa to 200 kDa, or Unstained Protein Molecular Weight Marker, 14.4 kDa to 116 kDa, Fermentas). Then the electrods were plumbed into the holder above and below the gel and contacted the gel via 1x electrode buffer (see 2.4). The power leads were attached and the proteins ran towards the anode. Analysis of multiple samples is accomplished using a Multigel-Long Elecrrophoresis System (Biometra). The running conditions were 35 mA / 200 V max supplied by a Standard Power Pack P25 (Biometra). The gel was run until the dye front reached the bottom (about 3 hrs). After electrophoresis, the protein bands of interest must be located in the gel by using staining techniques.

a. Coomassie Blue Staining Technique:

The Coomassie blue stain was used to check the successful separation of proteins in the gel. The gel was incubated at a room temperature in Coomassie blue staining solution (see 2.3) for 30-60 min, followed by de-staining the gel in fast de-staining solution for 30 min and then slow de-staining solution for 60 min. The de-staining solutions were described on (2.3).

b. Silver Staining Technique:

In addition, the silver stain was used to check the successful separation of proteins. The silver stain method was described by Heukeshoven and Dernick (1988). The reagents for silver stain (see 2.3) were prepared freshly.

The silver staining procedure is described as follows:

Solution	Incubation Time
1. Fixing Solution	ð 40-60 min
2. Sensitizing Solution	ð 60 min or over night
3. Washing with water	ð 3 x 5 min
4. Silver Solution	ð 30 min
5. Washing with water	ð 2 x 2 min
6. Developing Solution	ð To band visibility
7. Stop Solution	ð 10 min

The SDS gel was documented by photographing with visible light in a Multi Image Light Cabinet (Biozym) and was stored in sealed plastic bags at 4°C.

2.11.9 Immunochemistry Methods

2.11.9.1 Immunization

Production of antisera (polyclonal antibodies) in rabbits against polyketide synthases (cloned CHS and BPS from cell cultures of *Hypericum androsaemum*) (Liu *et al*., 2003) was accomplished by the company SEQLAB Sequence Laboratories (Göttingen).

- **Standard Immunization Protocol**

F **Two months**

Day	Immunization Protocol
0	ð 1st Injection (Preimmune sera > 5ml)
21	ð 2nd Injection
35	ð 1st Bleeding (10 - 20 ml)
49	ð 3rd Injection
53	ð 2nd Bleeding (2 ml + 10 to 20 ml)
60	ð Final Bleeding (>50 ml)

F **Three months**

Day	Immunization Protocol
0	ð 1st Injection (Preimmune sera >5m
21	ð 2nd Injection
35	ð 1st Bleeding (10 - 20 ml)
49	ð 3rd Injection
63	ð 2nd Bleeding (2 ml + 10 to 20 ml)
77	ð 4th Injection
98	ð Final Bleeding (>50 ml)

- **Suggested Doses of Immunogens for Rabbits**

F **Two months**

Form of Antigens	1st Injection	Following injections
Purified BPS included in PAGE-slice	ð 200 µg	100 µg
Purified CHS included in PAGE-slice	ð 150 µg	100 µg

F **Three months**

Form of Antigens	1st Injection	Following injections
Purified 6xHis-BPS included in PBS buffer, pH 7.2	ð 500 µg	250 µg
Purified 6xHis-CHS included in PBS buffer, pH 7.2	ð 500 µg	250 µg

For antibody titer determination, a test-aliquot of 2 ml was received from the company after each bleeding. In addition, about 10 ml pre-immune serum was received from the company prior to immunization to test for and to avoid cross-reactions.

- **Serum Storage and Handling**

A serum aliquot (10 ml) was stored at -20°C and was expected to be stable for many years.

2.11.9.2 Purification of IgG by Affinity Chromatography

The following purification procedure was performed on a Biologic®-FPLC-System (Bio Rad). The serum containing the antibodies was loaded on a pre-equilibrated HiTrap Protein A HP column (1 ml) in series with sodium phosphate, pH 7.0 as binding buffer (see 2.4) using the pump tubing "drop to drop" to avoid introducing air into the column. Sample loading to the column was run at a reduced flow rate (1 ml/min) to optimize the binding interactions with the protein A affinity medium (protein A-spherical agarose). The antibodies (IgGs) that recognize the protein A were retained in the column and serum proteins that do not recognize the protein A were flowed through the column. Following IgG binding to the column, the column was washed with sodium phosphate buffer, pH 7.0 until the baseline returned. Then, the IgGs were eluted with elution buffer (see 2.4). The purified IgGs were collected in tubes containing 60-200 µl of 1 M Tris-HCl, pH 9 per 1 ml of fraction to be collected. The elution buffer was exchanged using a quick buffer exchange against PBS buffer (see 2.4) on a PD-10 desalting column (Amersham Biosciences) as described (2.11.7.1).

- **Storage and Handling of Purified IgGs**

The purified antibodies were aliquoted (25-50 µl, $OD_{280} > 0.6$) and stored at -20°C for long-term storage. Antibody solutions under use were stored at 4°C for at least 6 months.

2.11.9.3 Immunoblotting

2.11.9.3.1 Western Blotting

A western blot was used to detect a given protein in a sample by using the antibody specificity to that protein. It is also used to determine a number of important characteristics of protein antigens, including its presence and quantity in a sample, its molecular mass, and the efficiency of antigen extraction. Polyclonal antibodies were raised in rabbits against polyketide synthases as described in (2.11.9.1) and used to detect proteins transferred from an SDS-PAGE gel onto a membrane.

The basic western blotting procedure was performed as indicated in the following steps:

1. Protein sample preparation (Extraction of soluble protein from plant tissue)

The extraction procedures were described in (2.11.4). The extract contains the soluble proteins, whose concentration was determined as described in (2.11.6.2.1). It was stored at -20°C up to further use.

2. Proteins were separated by SDS-PAGE

The proteins of the samples were separated according to their size in a SDS-PAGE gel as described in (2.11.8).

3. Proteins resolved by SDS-PAGE were transferred to a solid support membrane

After separation of the proteins of the sample by SDS-PAGE, the proteins in the gel were transferred onto a membrane made from a polyvenylidene fluoride (PVDF) (Immobilon P, Millipore). Either a semi-dry blotting system (Fig.2-2) or a wet (tank) blotting system (Fig.2-3) was used. The membrane was sticky and all proteins bound

equally well on the membrane. The membrane was moistened firstly with methanol and then equilibrated together with 4 x Whatman papers 3MM of the same size in 1x blot buffer (see 2.4). The transfer sandwich was then placed in the transfer apparatus using a semi-dry western blot apparatus (Pharmacia LKB Multiphor II) and subjected to an electric current, 120 mA for one gel and 160 mA for two gels. The voltage increased from 5 to 15 V during one hour supplied with the electrophoesis apparatus (Pharmacia LKB Multi Drive XL). An alternative transfer apparatus was a Mini Trans-Blot Electrophoretic Transfer Cell (Bio-Rad), used at an electric current of 350 mA for two gels and a voltage of 100 V during one hour. Here, the electrophoresis apparatus was Power Pack 300 (BioRad).

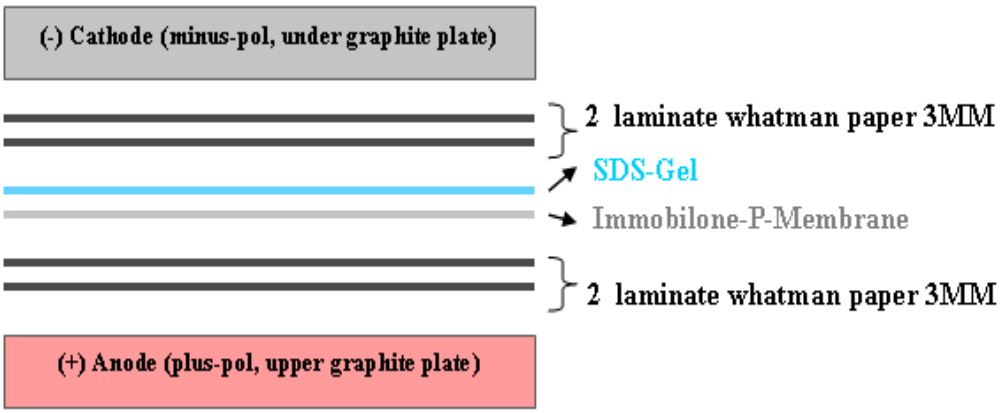

Fig. 2- 2: The order of the semi-dry electroblotting components in the apparatus.

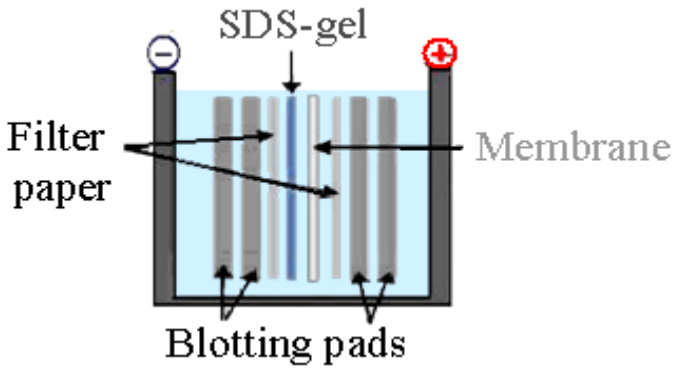

Fig. 2- 3: The order of the tank electroblotting components in the apparatus.

4. The non-specific binding sites on the membrane were blocked by a suitable blocking protein solution

The membrane was incubated with TBS-T + 5 % milk powder for 30 min at 37˚C (or 1 h at room temperature, or over night at 4˚C) with shaking to reduce background and prevent binding of the primary antibody to the membrane itself.

5. The membrane was incubated with the first antibody (often called the primary antibody)

The primary antibody (specific to protein of interest) was diluted in milk-blocking solution (see 2.3) by 1:5000 to 1:100000 dilutions. After the blocking solution was decanted from the blot, the membrane was incubated with diluted primary antibody for 1 h at room temperature with gentle agitation.

6. The membrane was incubated with the second antibody (often called the secondary antibody)

Following incubation with primary antibody, the blot was washed in several changes of 1xTBS-T buffer (see 2.4) to remove unbound primary antibody. After that, the membrane was incubated with 1:3300 diluted Goat anti-Rabbit antibody, which was conjugated with horseradish peroxidase (Dianova) for 45 min at room temperature with gentle agitation.

7. Proteins of interest were detected by using the ECL western blotting detection reagent which contains the substrate luminol

Following incubation with secondary antibody, the blot was washed in several changes of 1xTBS-T buffer (see 2.4) to remove unbound secondary antibody, then for 5 minutes in PBS buffer (see 2.4). After that, the membrane was incubated in a 1:1 mixture of two supplemented solutions in the ECL western blotting detection reagent

Kit (Amersham Bioscience) for 1 minute. The conjugated horseradish peroxidase catalyzes the oxidation of luminol. Directly following the oxidation, the luminol is in an excited state (intermediate reaction product), which decays to the ground state by emitting light, so that the position of membrane-bound secondary antibody will become visible. The emitted light was detected by using a radiographic film (Kodak). The membrane was put between two transparent plastic sheets and exposed to radiographic film X-Omate (Kodak) for 30 sec. to 2 min. After that, the films were developed with KODAK RP X-OMAT Developer and Replenisher. Bands corresponding to the detected protein of interest will appear as dark regions on the developed film. Films were washed with acidic water and then normal water. The films were fixed for 1 hour with KODAK RP X-OMAT LO Fixer and Replenisher. Then the membrane was stained with Indian ink solution (see 2.3) and the gel was stained with Coomassie blue solution (see 2.3). Both served as controls whether or not an efficient protein transfer had taken place during the blotting.

2.11.9.3.2 Dot Blot

Dot blotting was used to detect a given protein in samples by using an antibody specific to that protein. Similar to the western blot technique, but differing in that protein samples are not separated electrophoretically but spotted through circular templates directly onto the membrane. Two µl of protein solution containing 0.04 - 2.00 µg protein were directly spotted onto a membrane by using narrow mouth pipet tip. After that, the membrane was left in air for drying. Then the procedure was performed as described before in (2.11.9.3.1).

2.11.9.4 Immunotitration

Immunotitration was used to detect a given enzyme activity by using a specific antibody. The amount of non-precipitated protein remaining in the supernatant after addition of decreasing quantities of antibodies was removed from antibody-antigen complex and examined for enzyme activity. The mixtures between 50 µl of constant

quantity of enzyme solution and 50 µl of decreasing quantities of an antiserum (from 1:2 to 1: 512 dilution) were incubated (Beerhues and Wiermann, 1988a). After 20 min of incubation at room temperature, 50 µl PBS containing 6% (w/v) polyethyleneglycol 8000 were added. Following incubation at 4˚C over night, the mixtures were centrifuged at the same temperature for 10 min at 8700 g. One hundred µl of the supernatant were used to determine the non-precipitated enzyme activity. The enzyme activity assay was carried out as described in (2.11.10). Two controls were run in parallel: one without any antibody; the other one with preimmune serum in the same concentration range as in the assays.

2.11.9.5 Immunohistochemical Technique

In this technique, antibodies raised against PKSs (BPS/CHS) were linked to a cellular antigen in plant tissues that can thus be detected readily with a microscope. The basic procedure to obtain thin transverse sections of plant tissues was as follows.

2.11.9.5.1 Specimen Preparation

Two types of sections were used in this study.

2.11.9.5.1.1 Resin (Technovit) Sectioning Technique

Resin (Technovit) is routine embedding material and used in immunohistochemical techniques because it provides for excellent morphological details and high resolution.

The basic protocol for Resin embedded sctions was as follows:

	Resin (Technovit) Sectioning Technique
1. Pre-Embedding Technique	**a. <u>Fixation</u>** The fixation step served to preserve cells and tissues in a reproducible and life-like manner. Glutaraldehyde and formaldehyde are two fixatives in most common use, which were also employed for fixation of plant tissues. Either reagent causes transverse cross-linking of proteins. Plant tissues were cut into small pieces (about 1.2 mm^2) and immediately fixed on ice for 2 hours under reduced pressure (under vacuum 0.3 mbar) with fixative solution (see 2.3). Then the tissues were washed twice for 10 min with PBS to remove any remains of the fixative solution. **b. <u>Dehydration</u>** Water should be removed from the tissues of the plant parts for complete and good penetration of the fixative solution. Water was gradually removed by 30, 50, 70, and 90% aqueous ethanol and finally 3x 100 % ethanol. Each step of incubation took 30 min at room temperature. **c. <u>Infiltration</u>** After dehydration, the plant tissue was pre-infiltrated in a mixture (1:1) of Technovit 7100 (Heraeus-Kulzer) and ethanol (100 %) for 30 min. Subsequently, it was infiltrated in Technovit 7100 (100 %) for 1 hour and then incubated over-night in a mixture of Technovit 7100 hardener I (0.05 g hardener I in 5 ml Technovit 7100).

	Resin (Technovit) Sectioning Technique
2. Embedding Technique	At the end, the plant tissues were embedded in a mixture of 0.05 g Technovit 7100 hardener I, 5 ml Technovit 7100 and 333 µl Technovit 7100 hardener II and left at room temperature till hardness. An upper layer of the Technovit 3040 was added, which is a hard layer that the sample could be caught from it. The fixed tissues were stored in cool and dry place until microtome cutting.
3. Sectioning Technique	After embedding the plant tissues in Technovit® 7100 resin (Heraeus-Kulzer), the specimens were cut into thin segments (3.5 µm) using a microtome (HM 355 S, Microme). The sections were transferred onto diagnostic microscope slides (Diagnostic slides, standard type Teflon®, Roth) using a drop of distilled water and left to dry.

2.11.9.5.1.2 Cryo-sectioning Technique

In certain cases in immunohistochemical studies, it may be useful to use a technique that preserves maximum antigenicity such as the cryo-sectioning technique.

The basic protocol for cryostate embedded sctions was as follows:

	Cryo-sectioning Technique
1. Pre-Embedding Technique	**Fixation** The procedure was performed as described in (2.11.9.5.1.1)
2. Embedding Technique	The plant tissues were embedded in cryo-embedding compound (plano).The fixed tissues were stored in cool and dry place until microtome cutting.
3. Sectioning Technique	After embedding the plant tissues in cryo-embedding coumpound (plano), the specimens were cut into thin segments (18-20 µm) using a microtome (HM 500 O cryostate, Microme). The sections were transferred onto poly-laysin coated slides (roth) and left to dry.

2.11.9.5.2 Tissue Processing for Immunofluorescence Histochemistry using the Indirect Labeling Technique

The indirect labeling technique (Coons *et al.* 1955) is powerful in detecting antigens *in situ*. It is often preferred over the direct method, in which the primary antibody is conjugated, because secondary antisera can be used to detect a wide range of primary antibodies. One limitation of the indirect technique in immunohistochemistry is an increase in background staining (Hierck *et al.* 1994).

The non-specific background binding in the sections was reduced by floating them on a bleaching solution. The thin sections were incubated on a 50 mM ammonium chloride solution at 37˚C for 15 min, washed with water, incubated in 50 mM glycin solution at 37˚C for 15 min and washed again with water. Then the sections were

blocked at 37˚C for 1 h with BSA-blocking solution (see 2.3), washed with water and three times (10 min each) with PBS buffer. After that, the sections were incubated with either pre-immune serum or affinity-purified primary antibody (1:10 – 1:100 dilution) with 1% BSA in PBS buffer at 37˚C for 1 hour. They were washed with water and three times (10 min each) with PBS buffer. Finally, the sections were incubated in the dark with fluorescence dye-conjugated goat anti-rabbit antibody as secondary antibody (Alexa Fluor® 488 goat anti-rabbit IgG (H+L), Molecular Invitrogen) diluted 1:100 with 1% BSA in PBS buffer at 37˚C for 1 hour. They were washed three times (15 min each) with PBS buffer and then water and left in the dark at 37˚C until dryness.

2.11.9.5.3 Immunodetection and Documentation

Following immunochemical staining of the tissue, mounting medium (Citifluor Glycerol / PBS solution; Agar Scientific) was used to adhere the coverslip (a thin piece of glass) to the tissue section. This is predominantly to protect the specimen and the immunochemical staining from physical damage, but also helps to improve the clarity and contrast of the image during microscopy (Renshaw, 2007).

The tissues were viewed using a fluorescence microscope set up according to the excitation and emission characteristics of the fluorochrome label. Fluorescein isothiocyanate (FITC) (absorbance of blue light at 495 nm, emission of green light at 518 nm) is commonly used to label and track cells in fluorescence microscopic applications. This fluorochrome has a good quantum yield, however, FITC exhibits weaker intensity of fluorescence and less photo-stability. Furthermore, the intensity of the FITC fluorescence is affected by the pH value. Nowadays, more photo-stable alternatives to the fluorochrome FITC are available, such as Alexa Flour 488. It is a fluorochrome with similar spectral characteristics as FITC (absorbance of blue light at 494 nm, emission of green light at 517 nm). The tissues were examined under an immunoflourescence (IF) microscope (Zeiss III photomicroscope). The Alexa 488-labeled sections were excitated by blue light of 494 nm. A FITC filter was used to visualize the green immunoflourescence label. The imaging of whole-mount specimens was recorded using a digital camera (Axioskop 2, Zeiss) and the software

Axio Vision 3.0 (Zeiss). In addition, tissues were examined under the laser scanning microscope (LSM) (Zeiss LSM 510). A 488-nm argon laser line and 505-550 nm emission band pass (FITC channel) were used to visualize the Alexa 488-conjugated secondary antibody. A high-contrast final image as lambda mode or channel mode with good resolution was obtained by using LSM 510 META software (Zeiss).

2.11.10 Enzyme Assays and Product Analysis

2.11.10.1 Benzophenone Synthase Assay

The enzyme assay (Liu *at al.*, 2003) was performed in a total volume of 250 µl containing 15 µM benzoyl-CoA as starter CoA, 56 µM malonyl-CoA as extender CoA, 0.1 M potassium phosphate buffer pH 7.0 and approximately 2 µg protein. The mixture was incubated at 35˚C for 30 min and centrifuged at 13000 rpm for 10 min. The supernatant which contained the product was extracted twice with 250 µl ethyl acetate and centrifuged at 13000 rpm for 10 min. The combined organic phases were dried under vacuum, and the residue was dissolved in 50 µl of methanol. Analysis of the enzymatic products was performed by HPLC as described on (2.11.12). The detection wavelength was 306 nm (benzophenones). Standard solutions of reference compounds served for quantification.

2.11.10.2 Chalcone Synthase Assay

The enzyme assay (Liu *at al.*, 2003) was performed in a total volume of 250 µl containing 15 µM *p*-coumaroyl-CoA or 15 µM cinnamoyl-CoA as starter CoA, 56 µM malonyl-CoA, 0.1 M potassium phosphate buffer pH 7.0 and approximately 2 µg protein. The mixture was incubated at 35˚C for 30 min and centrifuged at 13000 rpm for 10 min. The supernatant which contained the reaction product was extracted twice with 250 µl ethyl acetate and centrifuged at 13000 rpm for 10 min. The combined organic phases were dried under vacuum, and the residue was dissolved in 100 µl of methanol. Analysis of the enzymatic products was performed by HPLC as described in (2.11.12). The detection wavelength was 289 nm (flavanones). Standard solutions of reference compounds served for quantification.

2.11.11 Extraction and Analysis of Secondary Products from *H. perforatum* Fruits

Freshly harvested fruits of various developmental stages (10 g) were homogenised in 15 ml methanol. After centrifugation at 7000 rpm for 10 min, a 50 µl aliquot of the supernatant was analysed by HPLC as described on (2.11.12).

2.11.12 Analysis of Enzymatic Products and Secondary Products by HPLC

Analysis of enzymatic products and secondary products was performed by HPLC.

2.11.12.1 HPLC Instruments

	Type	Manufacturer
Pump	ð Waters ™ 616	Millipore
Detector	ð Waters ™ 996-Photodiode Array	
Auto sampler	ð Waters ™ 717 Plus	
Controller	ð Waters ™ 6oo S	
Software	ð Millennium 2010 Chromatograhy Manager	
Pump	ð 1090 Series II	Hewlett Packard
Detector	ð 1090 Series II-Dual Absorbance Detector (DAD)	
Auto sampler	ð 1090 Series II	
Controller	ð 1090 Series II	
Software	ð Chemstation(Pascal series) on Windows 95 platform	

2.11.12.2 HPLC Columns

Column type	Supplier
Hyperclone C_{18} 3 µm column (3.20 mm x 150 mm)	ð Phenomenex
Hyperclone C_{18} 5 µm column (4.60 mm x 150 mm)	ð Phenomenex

2.11.12.3 Mobile Phases

The eluents were bidistilled water (2.2) containing 1% o*rtho*-phosphoric acid (A) and methanol (B) at a flow rate of 0.5 ml min^{-1} or 0.3 ml min^{-1} according to the column size.

2.11.12.4 Solvent Gradients

The enzymatic products or secondary products were analyzed by HPLC using either gradient of solvents A and B or isocratic elution (constant mixture of the solvents). The flow rate was 0.5 ml min^{-1} or 0.3 ml min^{-1} according to the column type.

The following gradients were used:

Gradient	Gradient parameter			Applications
1	Time [min]	Water[%]	Methanol[%]	Determination of BPS and CHS activities
	0	50	50	
	2	50	50	
	12	30	70	
	20	10	90	
	21	5	95	
	23	5	95	
	25	50	50	
	30	50	50	
2	Time [min]	Water[%]	Methanol[%]	Determination of BPS and CHS activities
	0	80	20	
	3	80	20	
	17	50	50	
	20	50	50	
	23	0	100	
	25	0	100	
	28	80	20	
	34	80	20	
3	Time [min]	Water[%]	Methanol[%]	Determination of secondary products from *H. perforatum* fruits.
	0	95	5	
	3	95	5	
	25	0	100	
	28	0	100	
	30	95	5	
	33	95	5	

2.11.13 Induction of Benzophenone Synthase in *H. perforatum* Leaves

2.11.13.1 Treatment of Excised Leaves with Methyl Jasmonate

Hypericum perforatum leaves (0.5-2 cm) were freshly harvested and immediately floated on 50, 100, or 200 µM ethanolic methyl jasmonate solution under reduced pressure (vacuum of 0.6 mbar) with occasional swirling for 1 hour. After the vacuum was broken, leaves were incubated for 15 hours at 25˚C under constant light. As a negative control, leaves were floated on water. At the end of the incubation period, leaves were washed with water und used immediately for protein extraction as described in (2.11.4).

2.11.13.2 Treatment of Excised Leaves with Salicylic Acid

The leaves were treated with Salicylic acid solution (1.0, 2.5, or 5.0 mM). The procedure was performed as described before in (2.11.13.1).

2.11.13.3 Treatment of Excised Leaves by Wounding

Hypericum perforatum leaves (0.5-2 cm) were freshly harvested. They were immediately wounded by slightly crushing with a metal forceps. For systemic wound induction, five wounds were made per leaf in a way that each wound site was overlapping a secondary vein without affecting the larger primary veins. The leaves were incubated in water for 15 hours at 25˚C under constant light. Leaves without wounds were floated on water and used as a negative control. At the end of the incubation period, leaves were used immediately for protein extraction as described on (2.11.4).

2.11.14 Preparation of Sterile *Hypericum perforatum* Plants

After a first sterilization step of *H. perforatum* seeds for 3 minutes in 70% ethanol, the seeds were incubated for 5 min in 6 % sodium hypochlorite /0.1% Tween 20. The seeds were washed twice with sterile water and spread on Petri dishes as a suspension made with a sterile solution of 8 % sucrose in water with 0.8 % agar. Fifteen-day-old seedlings were transferred to MS medium (without phytohormones). After 5 to 6 weeks the plants were completely developed (Fig. 2-4).

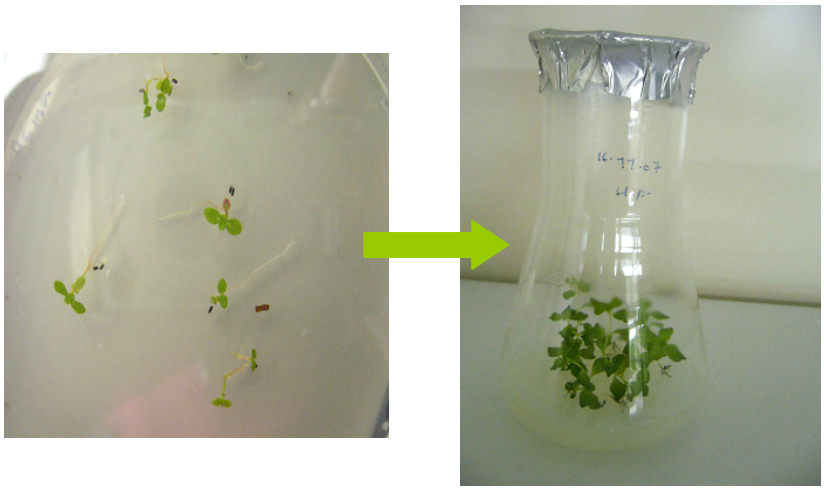

Fig. 2- 4: *Hypericum perforatum*: (left) seedlings, (right) *in vitro* plant.

3 Results

All pharmacologically active constituents of the well-known medicinal plant *Hypericum perforatum* (Clusiaceae) are derivatives of polyketide metabolism. *Hypericum* species are ideal model systems to study the biosynthesis of aromatic polyketides, due to the variety of compounds formed and the ease of *in vitro* cultivation. Plants synthesize polyketides via the acetate-malonate pathway using enzymes called type III polyketide synthases (PKSs). Two type III PKSs involved are benzophenone synthase (BPS) and chalcone synthase (CHS). cDNAs encoding these PKSs were cloned and the recombinant proteins characterized (Liu *et al*., 2003). This work describes immunochemical studies of the PKSs and their immunofluorescence localization in *H. perforatum* tissues.

3.1 Heterologous Expression and Affinity Purification of PKSs

To perform immunochemical studies of PKSs, it is vital to obtain the recombinant proteins at high levels of yield and purity. BPS and CHS were previously cloned and characterized from *H. androsaemum* (Liu *et al*., 2003). Both proteins are homodimers with subunit molecular masses of about 43 kDa. CHS shared 60.1% amino acid sequence identity with BPS. Both enzymes were heterologously expressed in *E. coli* as GST-fusion proteins (Liu *et al.,* 2003) and as 6xHis-tagged proteins (Liu *et al*., unpublished).

In this work, both the GST-fusion proteins and the His-tagged proteins were used for immunization. Unfortunately, the antisera raised against the PKSs resulting from the cleavage of the GST fusion proteins did not recognize their antigens. Nevertheless, the procedures of production and cleavage of the GST-PKSs are described.

3.1.1 Isolation of GST-PKS Fusion Proteins from *E. coli*

The production and purification protocol for GST-PKSs consisted of several steps as described in (2.10 and 2.11). Following bacterial growth (see 2.10.1.a), induction of expression (see 2.10.1.a) and extraction of the proteins from *E. coli* cells (see 2.11.1.a), the GST-tagged proteins were purified and cleaved by factor Xa as described in (2.11.2).

3.1.1.1 Purification of GST-PKSs using a GSTrap FF Column

The method of purification of GST-PKSs using a GSTrap FF column was described in (2.11.2.1 and 2.11.2.2). GST-tagged PKSs were purified from large-scale cultures. Fig. 3-1 displays the purification of GST-BPS using a glutathione sepharose fast flow column (1 ml). The soluble fraction (30 ml) from *E. coli* cells (850 ml culture) was loaded on a pre-equilibrated GSTrap column, to which GST-BPS was bound. Unbound material was eluted by washing with binding buffer until the baseline had returned and GST-BPS was eluted with elution buffer (5 ml). The yield of fusion protein was 2.75 mg, as measured by the Bradford assay (see 2.11.6.1.1).

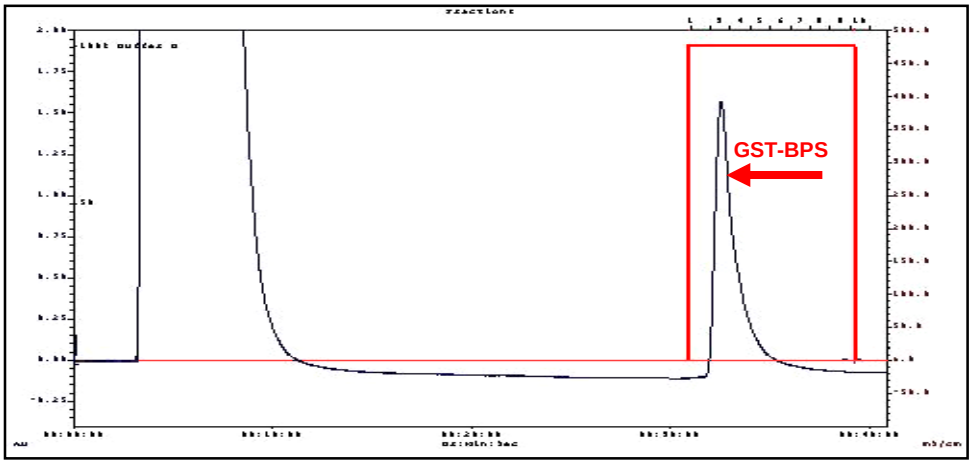

Fig. 3- 1: Purification of GST-BPS using a GSTrap FF column (1 ml). The sample consists of 30 ml soluble fraction from *E. coli*. The binding buffer is phosphate buffered saline, pH 7.3. The elution buffer is reduced glutathione, pH 8.0.

Fig. 3-2 shows the purification of GST-CHS using the same procedure as above, except that 45 ml *E. coli* extract from 1250 ml culture were applied. The yield of the eluted fusion protein was 3.8 mg.

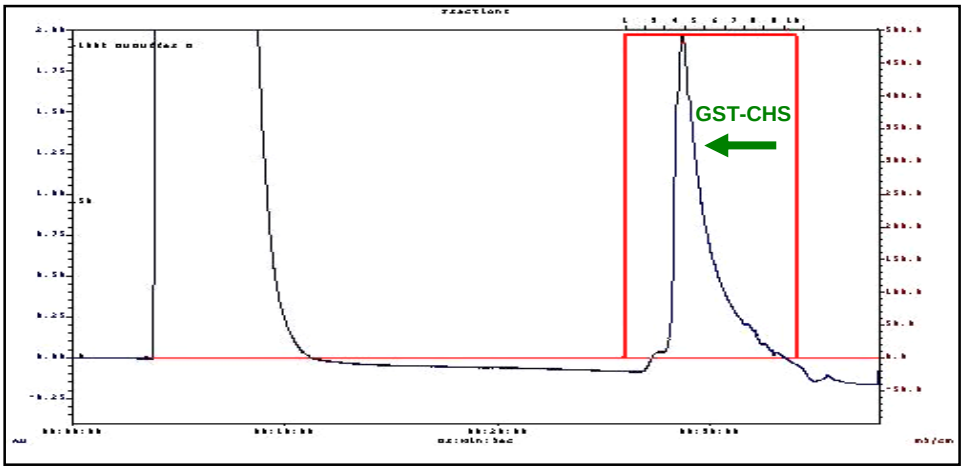

Fig. 3- 2: Purification of GST-CHS. For details, see Fig. 3-1.

3.1.1.2 Cleavage of GST-PKSs and Purification of the PKS Moiety

The GST-PKS fusions were cleaved using factor Xa (see 2.11.2.1 and 2.11.2.2). Factor Xa specifically recognizes the tetrapeptide Ile-Glu-Gly-Arg and cleaves in front of the first amino acid following the tetrapeptide. During the incubation of GST-PKS fusions with factor Xa, cleavage occurred directly in front of the PKS start methionine, thereby releasing the mature enzymes without any overhang at the N-terminus (Liu *et al*., 2003).

Native polyacrylamide gel electrophoresis was used for separation of GST and PKS after cleavage by factor Xa (2.11.5.2). Because BPS (*pI* = 5.78) and CHS (*pI* = 6.55) are acidic proteins, they were fractionated in a basic native gel. Acidic native PAGE was found to give poor resolution. The acrylamide concentration was adjusted to

10%, which allowed best resolution of the PKSs. Generally, native PAGE separates proteins in an electric field according to their size, shape, and charge. Fig. 3-3 shows a Coomassie blue-stained gel (2.11.8.a) with the separation of BPS, GST and factor Xa. BSA was used to estimate the quantity of protein recovery. GST and Factor Xa were used as references. BPS was well separated from GST and factor Xa.

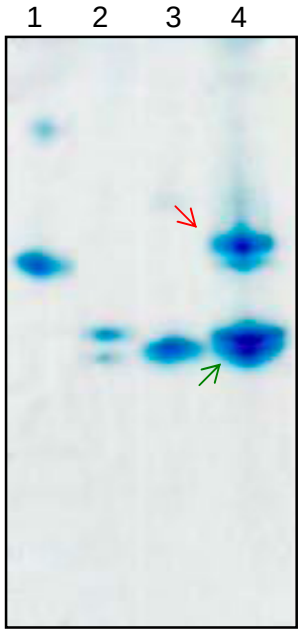

Fig. 3- 3: Separation of factor Xa-cleaved GST-BPS in a 10 % basic native gel followed by Coomassie blue staining.
Lane 1: BSA (5 µg) (MW 66 kDa),
lane 2: Factor Xa (2 µg) (MW ~ 45-50 kDa) consisting of two subunits of 28-30 and 17-20 kDa,
lane 3: GST (5 µg) (MW 52 kDa),
lane 4: GST-BPS after cleavage (35 µg) (BPS: MW 85.6 kDa).

The poor separation of CHS from GST and factor Xa in a 10% basic native gel was solved by using preceding affinity chromatography. The diagram (Fig. 3-4) explains the removal of the GST moiety from CHS and factor Xa using a glutathione sepharose fast flow column (1 ml) (2.11.2.2). GST-CHS (2 mg) cleaved with factor Xa was loaded on a pre-equilibrated GSTrap column. While the GST moiety bound to the column, CHS and factor Xa were collected during the washing period. Thereafter, elution buffer eluted the GST moiety. The recovery of protein was 0.6 mg/4 ml, as measured by the Bradford assay (2.11.6.1.1).

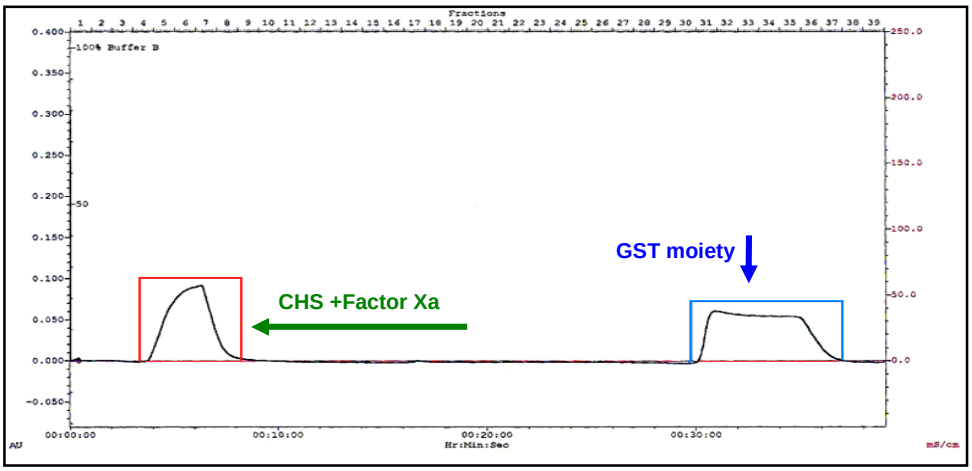

Fig. 3- 4: Separation of GST and CHS after GST-CHS cleavage by factor Xa using a GSTrap FF 1 ml column. The sample is 2 mg/3 ml of GST-CHS after incubation with factor Xa. Binding buffer is phosphate buffered saline, pH 7.3. Elution buffer is reduced glutathione buffer, pH 8.0.

Fig. 3-5 shows a silver-stained gel (2.11.8.b) with the separation of CHS, GST and factor Xa. CHS was not separated from factor Xa.

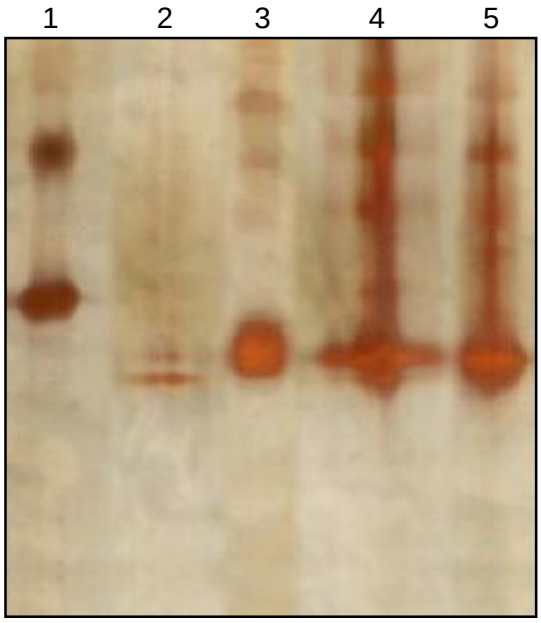

Fig. 3- 5: Separation of factor Xa-cleaved GST-CHS in a 10 % basic native gel followed by silver staining.
Lane 1: BSA (5 µg) (MW 66 kDa),
lane 2: Factor Xa (2 µg) (MW ~ 45-50 kDa) consisting of two subunits of 28-30 and 17-20 kDa,
lane 3: GST (5 µg) (MW 52 kDa),
lane 4: GST-CHS after cleavage (2 µg) (CHS: MW 85.4 kDa),
lane 5: GST-CHS after cleavage and separation of GST moiety (15 µg).

The successful expression and purification of GST-tagged PKSs are summarized in Fig. 3-6 and Fig. 3-7

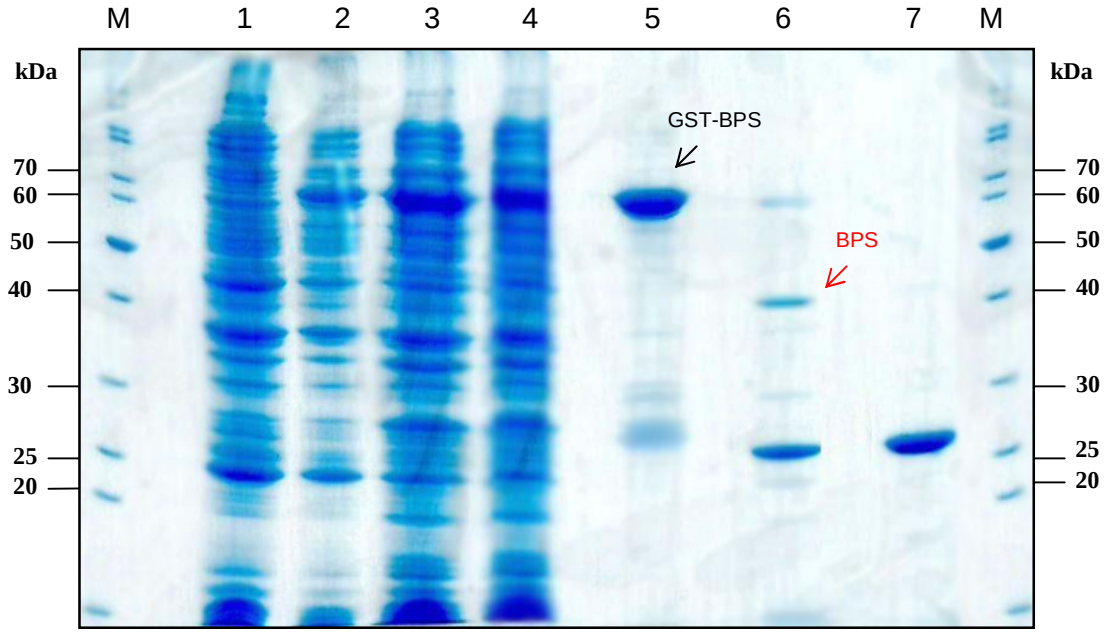

Fig. 3- 6: SDS-PAGE analysis of GST-BPS purification followed by coomassie blue staining.
Lane M: Protein marker (PageRuler™ Protein ladder, 10 kDa to 200 kDa, Fermentas),
lane 1: Pre-induction (total proteins extract of non-induced culture),
lane 2: Post-induction (total proteins extract of induced culture),
lane 3: Pellet (insoluble fraction),
lane 4: Supernatant (soluble fraction),
lane 5: GST-BPS (15 µg) (MW 68.8 kDa),
lane 6: GST-BPS after cleavage (10µg) (BPS: MW 42.8kDa and factor Xa: MW ~ 22-25 kDa),
lane 7: GST (5 µg) (MW 26 kDa).

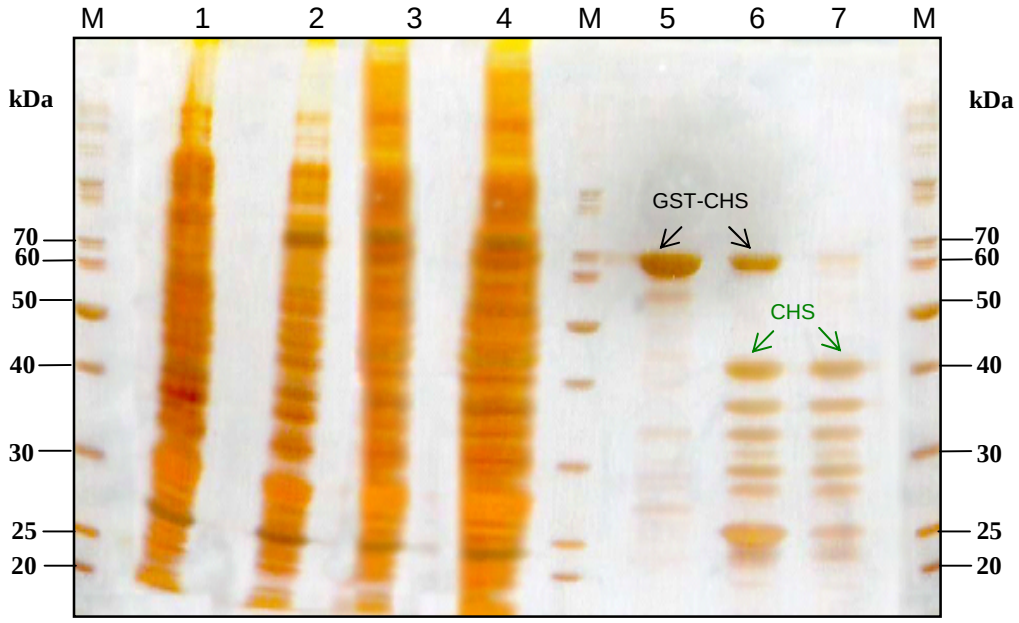

Fig. 3- 7: SDS-PAGE analysis of GST-CHS purification followed by silver staining.
Lane M: Protein marker (PageRuler™ Protein ladder, 10 kDa to 200 kDa, Fermentas),
lane 1: Pre-induction (total proteins extract of non-induced culture),
lane 2: Post-induction (total proteins extract of induced culture)
lane 3: Pellet (insoluble fraction),
lane 4: Supernatant (soluble fraction),
lane 5: GST-CHS (15 µg)(68.7 kDa),
lane 6: GST-CHS after cleavage (15 µg)(CHS: MW 42.7 kDa, GST: MW 26 kDa and factor Xa: MW ~ 22.5-25 kDa). The GST-CHS was not completely cleaved by factor Xa. In addition, the amino acids sequence of CHS was degraded by factor Xa.
lane 7: GST-CHS after cleavage and separation of GST moiety (15 µg).

Finally, BPS and CHS were purified for immunization by excising their protein bands from a basic native polyacrylamide gel after reversible staining (2.11.5.2). Fig. 3-8 explains how the BPS and CHS bands from the cleaved GST-fusion proteins were cut off from the basic native gel after they had been located by E-zinc reversible staining. GST-BPS after cleavage (1 mg/60 µl) and GST-CHS (0.4 mg/240 µl) after cleavage and separation of GST moiety were loaded into the gel. The amount of BPS in the excised gel slice was about 450 µg, while the amount of CHS in the gel slice was about 350 µg. These gel slices were used for immunizing rabbits (see 2.11.9.1).

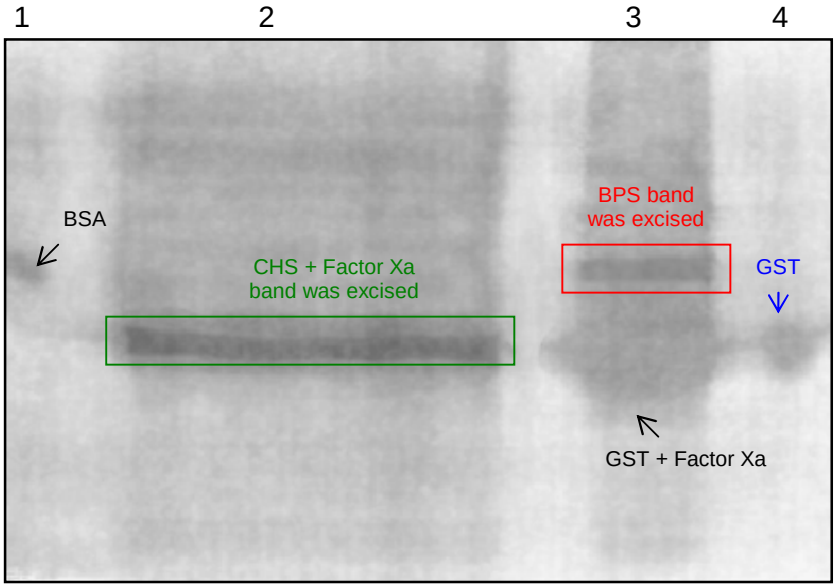

Fig. 3- 8: Cutting the BPS and CHS bands (cleaved GST-fusion proteins) located in native gel after they were fractionated by electrophoresis followed by E-zinc reversible staining.
Lane 1: BSA (5 µg) (MW 66 kDa),
lane 2: GST-CHS after cleavage and separation of GST moiety (0.4 µg/240 µl))(CHS: MW 42.7 kDa and factor Xa: MW ~ 22.5-25 kDa),
lane 3: GST-BPS after cleavage (1mg/60 µl) (BPS: MW 85.6 kDa),
lane 4: GST (5 µg) (MW 52 kDa).

3.1.1.3 Purification of GST-PKS Fusion Proteins using a Glutathione Agarose Protein Purification System

The GST-PKS fusions which were purified by this method (2.11.2.3) were used for studies of immunological cross-reactivity. It is a simple and rapid method for the purification of GST-fusion proteins. GST-tagged PKSs were purified from small-scale cultures. The soluble fraction (3.5 ml) from *E. coli* cells (100 ml culture) containing GST-BPS was purified, GST-BPS was eluted with elution buffer (3.5 ml). The yield of fusion protein was 0.8 mg, as measured by the Bradford assay (see 2.8.6.1.1).
The GST-CHS was purified using the same procedure as above. The yield of the eluted fusion protein was 0.35 mg. The successful expression and purification of GST-tagged PKSs are summarized in Fig. 3-9 and Fig. 3-10.

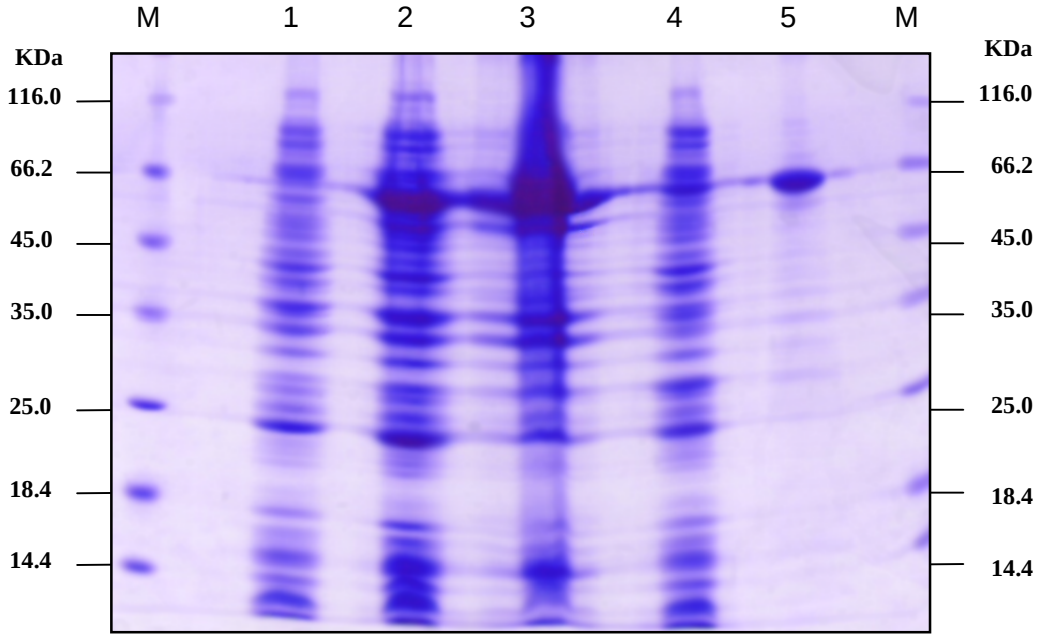

Fig. 3- 9: SDS-PAGE analysis of GST-BPS purification followed by coomassie blue staining. Lane M: Protein marker (Unstained Protein Molecular Weight Marker, 14.4 kDa to 116 kDa, Fermentas).
lane 1: Pre-induction (total proteins extract of non-induced culture),
lane 2: Post-induction (total proteins extract of induced culture),
lane 3: Pellet (insoluble fraction),
lane 4: Supernatant (soluble fraction),
lane 5: GST-BPS (15 µg) (68.8 kDa).

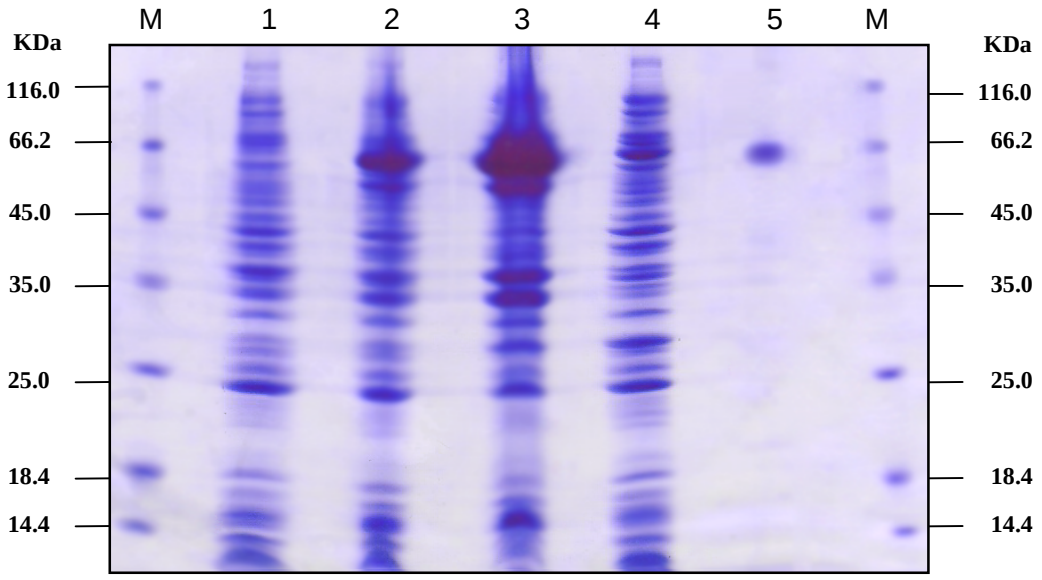

Fig. 3- 10: SDS-PAGE analysis of GST-CHS purification followed by coomassie blue staining.
Lane M: Protein marker (Unstained Protein Molecular Weight Marker, 14.4 kDa to 116kDa, Fermentas),
lane 1: Pre-induction (total proteins extract of non-induced culture),
lane 2: Post-induction (total proteins extract of induced culture),
lane 3: Pellet (insoluble fraction),
lane 4: Supernatant (soluble fraction),
lane 5: GST-CHS (15 µg) (68.7 kDa).

3.1.2 Purification of 6xHis-tagged PKS fusion proteins using the Ni-NTA System

His-tag-BPS and -CHS were used for raising antibodies. The His-tag was not cleaved off. The general production and purification protocol for 6xHis tagged PKSs was described in (2.10.1, 2.10.2.b, 2.11.1.b and 2.11.3). 6xHis-tagged PKSs were purified from large-scale cultures. The soluble fraction (9 ml) from *E. coli* cells (1050

ml culture) containing 6xHis-BPS was purified, 6xHis-BPS was eluted with elution buffer (2.5 ml). The yield of fusion protein after buffer change (using PD-10 desalting column) was 12 mg, as measured by the Bradford assay (see 2.8.6.1.1).

The 6xHis-CHS was purified using the same procedure as above. The yield of the eluted fusion protein was 7 mg. The successful expression and purification of 6xHis-tagged PKSs are summarized in Fig. 3-11 and Fig. 3-12.

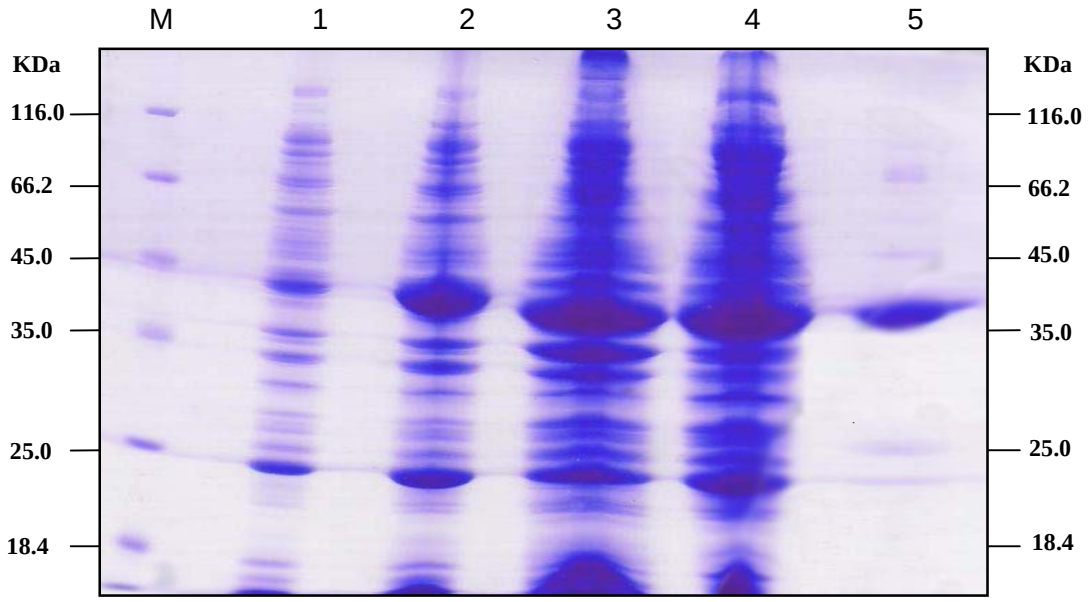

Fig. 3- 11: SDS-PAGE analysis of 6xHis-BPS purification followed by coomassie blue staining.
Lane M: Protein marker (Unstained Protein Molecular Weight Marker, 14.4 kDa to 116kDa, Fermentas),
lane 1: Pre-induction (total proteins extract of non-induced culture),
lane 2: Post-induction (total proteins extract of induced culture),
lane 3: Pellet (insoluble fraction),
lane 4: Supernatant (soluble fraction),
lane 5: 6xHis-BPS (15 µg) (43.8 kDa).

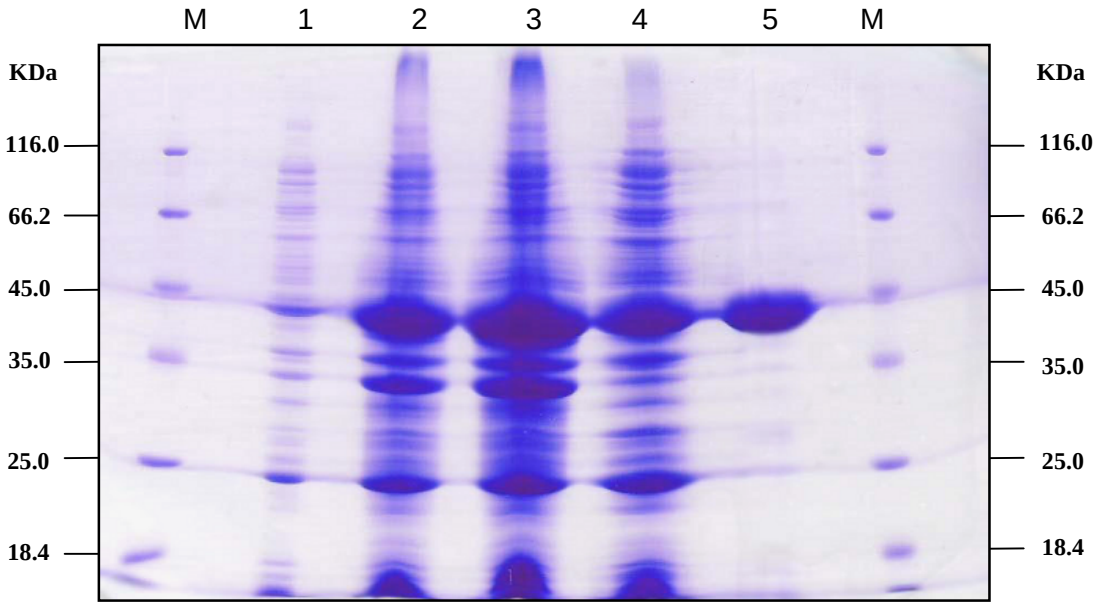

Fig. 3- 12: SDS-PAGE analysis of 6xHis-CHS purification followed by coomassie blue staining.
Lane M: Protein marker (Unstained Protein Molecular Weight Marker, 14.4 kDa to 116kDa, Fermentas),
lane 1: Pre-induction (total proteins extract of non-induced culture),
lane 2: Post-induction (total proteins extract of induced culture),
lane 3: Pellet (insoluble fraction),
lane 4: Supernatant (soluble fraction),
lane 5: 6xHis-CHS (15 µg) (43.7 kDa).

3.2 Antisera Production and IgG Purification

The generation of polyclonal antibodies against the PKSs in rabbits was accomplished by the company SEQLAB Sequence Laboratories (Göttingen) as described in (2.11.9.1). The isolation of the IgG fractions was done by antibody affinity chromatography using a protein A sepharose column as described in (2.11.9.2).

The successful isolation of IgG fractions against 6xHis-tagged PKSs is summarized in Fig. 3-13 and Fig. 3-14.

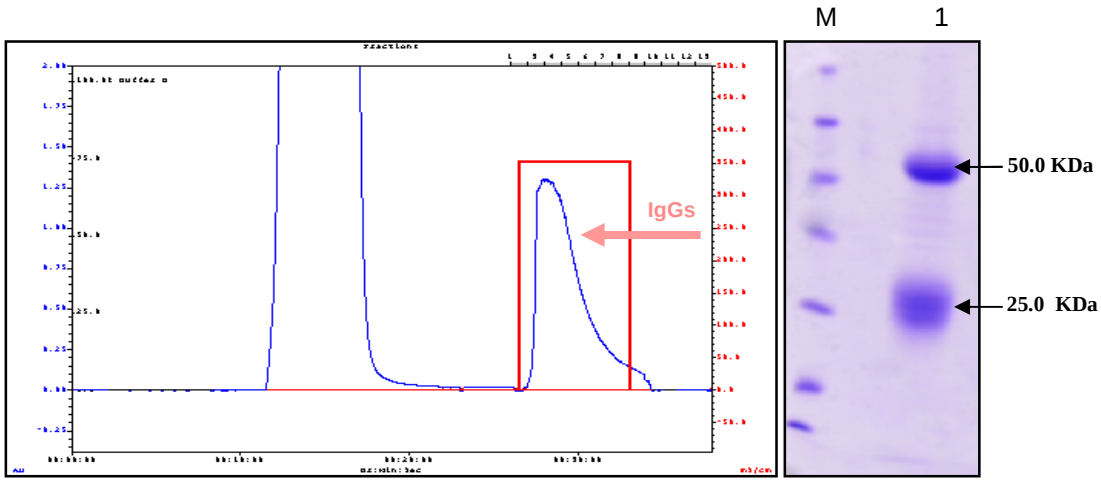

Fig. 3- 13: Purification of preimmune 6xHis-BPS IgG using HiTrap-Protein A HP column (1 ml) (left). The sample consists of 2 ml serum. The binding buffer is 20 mM sodium phosphate, pH 7.0.The elution buffer is 0.1 M citric acid, pH 4.5.
The SDS-PAGE analysis of isolated IgG fractions was followed by coomassie blue staining (right).
Lane M: Protein marker (Unstained Protein Molecular Weight Marker, 14.4 kDa to 116 kDa, Fermentas),
lane 1: Pre-immune 6xHis-BPS IgG (25 µg).

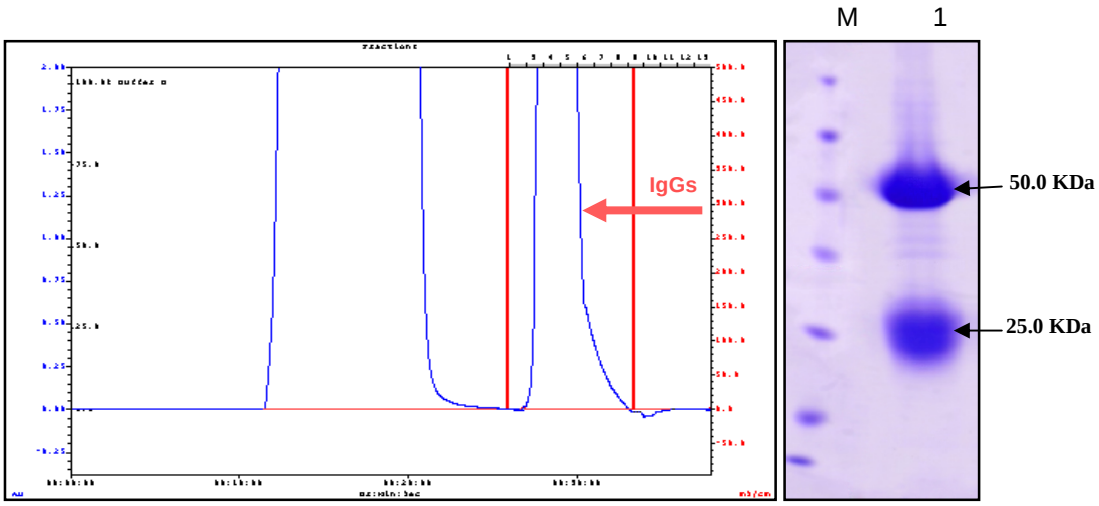

Fig. 3- 14: Purification of anti 6xHis-BPS IgG (2nd bleeding) using HiTrap-Protein A HP column (1 ml) (left). The sample consists of 2 ml serum. The binding buffer is 20 mM sodium phosphate, pH 7.0.The elution buffer is 0.1 M citric acid, pH 4.5.
The SDS-PAGE analysis of isolated IgG fractions was followed by coomassie blue staining (right).
Lane M: Protein marker (Unstained Protein Molecular Weight Marker, 14.4 kDa to 116 kDa, Fermentas),
lane 1: Anti 6xHis-BPS IgG (2nd bleeding) (25 µg).

3.3 Analysis by Immunoblotting of Antibody Specificity

The specificity of the polyclonal antibodies was examined using immunoblotting following SDS-PAGE (Western blotting) as described in (2.11.9.3.1). Since the antisera were raised against the His-tagged PKSs, immunoblotting was performed using the GST-PKSs in order to avoid cross-reaction with the tag. Fig. 3-15 shows the immunoblotting of recombinant GST-PKSs and 6xHis-tagged PKSs, the blots were either stained with Indian black ink or incubated with anti-6xHis-BPS or preimmune 6xHis-BPS (The primary antibodies were diluted in milk-blocking solution by 1:100000). Anti-6xHis-BPS detected GST-BPS, but anti-6xHis-CHS did not. Conversely, anti-6xHis-CHS stained GST-CHS whereas anti-6xHis-BPS gave only a poor immunoreaction with GST-CHS. No immunoreactions were found in the presence of the pre-immune IgG preparations.

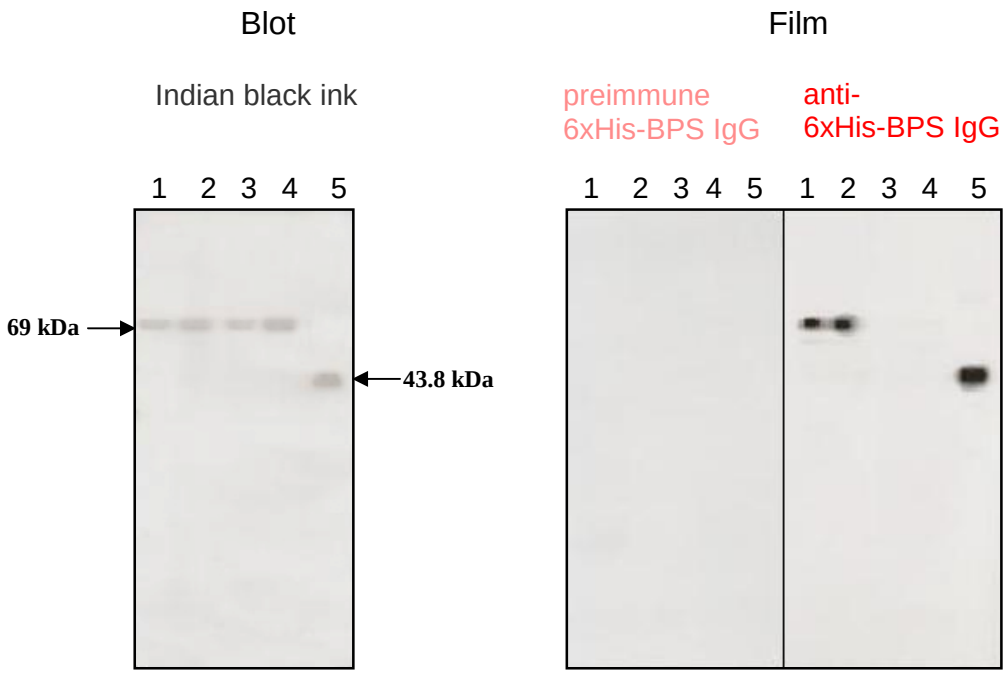

Fig. 3- 15: Immunoblotting of recombinant GST-PKSs and 6xHis-tagged PKSs. The SDS gel (12 %) was performed with protein applied per lane as follows.
Lane 1 is 0.15 µg GST-BPS,
lane 2 is 0.3 µg GST-BPS,
lane 3 is 0.15 µg GST-CHS,
lane 4 is 0.3 µg GST-CHS,
lane 5 is 0.1 µg 6xHis-BPS.
The blots were either stained with Indian black ink or incubated with anti- 6xHis-BPS or pre-immune 6xHis-BPS (The primary antibodies were diluted in milk-blocking solution by 1:100000).

Fig. 3-16 documents the results obtained with anti-6xHis-CHS or pre-immune 6xHis-CHS (The primary antibodies were diluted in milk-blocking solution by 1:10000).

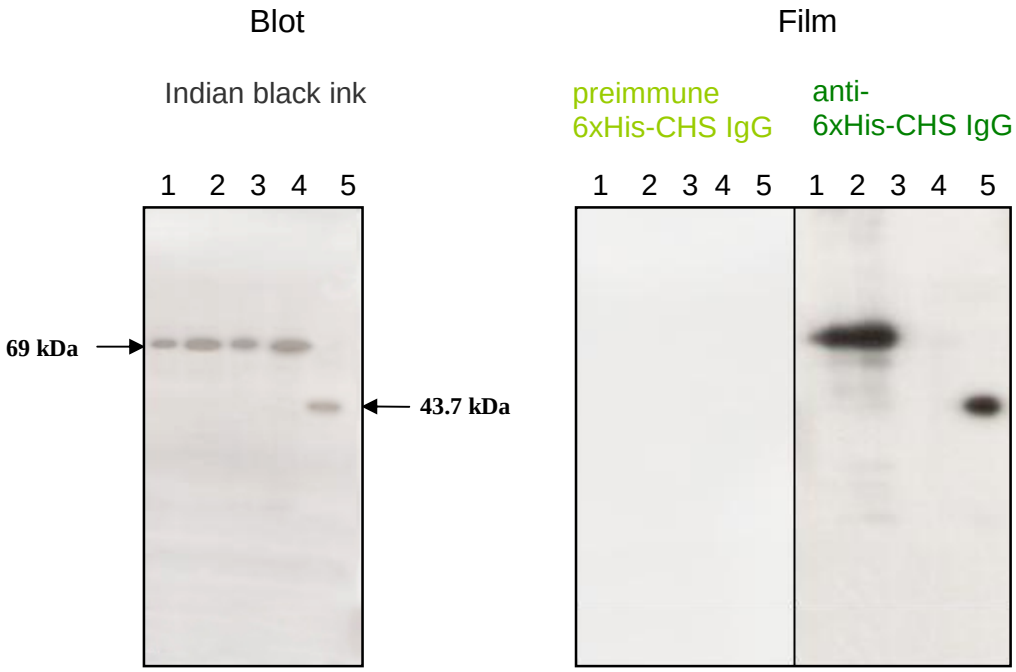

Fig. 3- 16: Immunoblotting of recombinant GST-PKSs and 6xHis-tagged PKSs. The SDS-gel (12 %) was performed with protein applied per lane as follows.
Lane 1 is 0.2 µg GST-CHS,
lane 2 is 0.6 µg GST-CHS,
lane 3 is 0.3 µg GST-BPS,
lane 4 is 0.6 µg GST-BPS,
lane 5 is 0.1 µg 6xHis-CHS.
The blots were either stained with Indian black ink or incubated with anti- 6xHis-CHS or preimmune 6xHis-CHS (The primary antibodies were diluted in milk-bloking solution by 1:10000).

3.4 Immunological Relationship between BPS and CHS

Insight into the immunological cross-reactivity between the antisera and the PKSs was provided by immuno-dot blotting as described in (2.11.9.3.2) and immunotitration coupled to enzyme activity measurement as described in (2.11.9.4).

3.4.1 Immuno-Dot Blotting Assay

The negligible cross-reactivities observed under 3.3 were confirmed by dot blotting with decreasing amounts of the GST-PKSs that were stained with either anti-6xHis-BPS or anti-6xHis-CHS. Fig. 3-17 explains the estimation of the immunological relationship between the two PKSs. Decreasing amounts from 2.0 µg to 0.004 µg of GST-BPS and GST-CHS were dotted onto a PVDF membrane, followed by immunostaining with anti 6xHis-BPS (diluted in milk-blocking solution by 1:100000) and anti-6xHis-CHS (diluted in milk-blocking solution by 1:10000) . The staining of GST-BPS by anti-6xHis-BPS was saturated by amounts around 0.063 µg GST-BPS protein. Lower protein amounts were stained to lesser extents but still clearly detectable. Otherwise, the staining of GST-BPS by anti-6xHis-CHS failed to produce any immunoreaction. The staining of GST-CHS by anti-6xHis-BPS produced insignificant immunoreactions. The staining of GST-CHS by anti-6x His-CHS was saturated by amounts around 0.032 µg GST-CHS protein. Lower protein amounts were stained to lesser extents but still clearly detectable. No immunoreactions occurred in the presence of the preimmune IgG preparations.

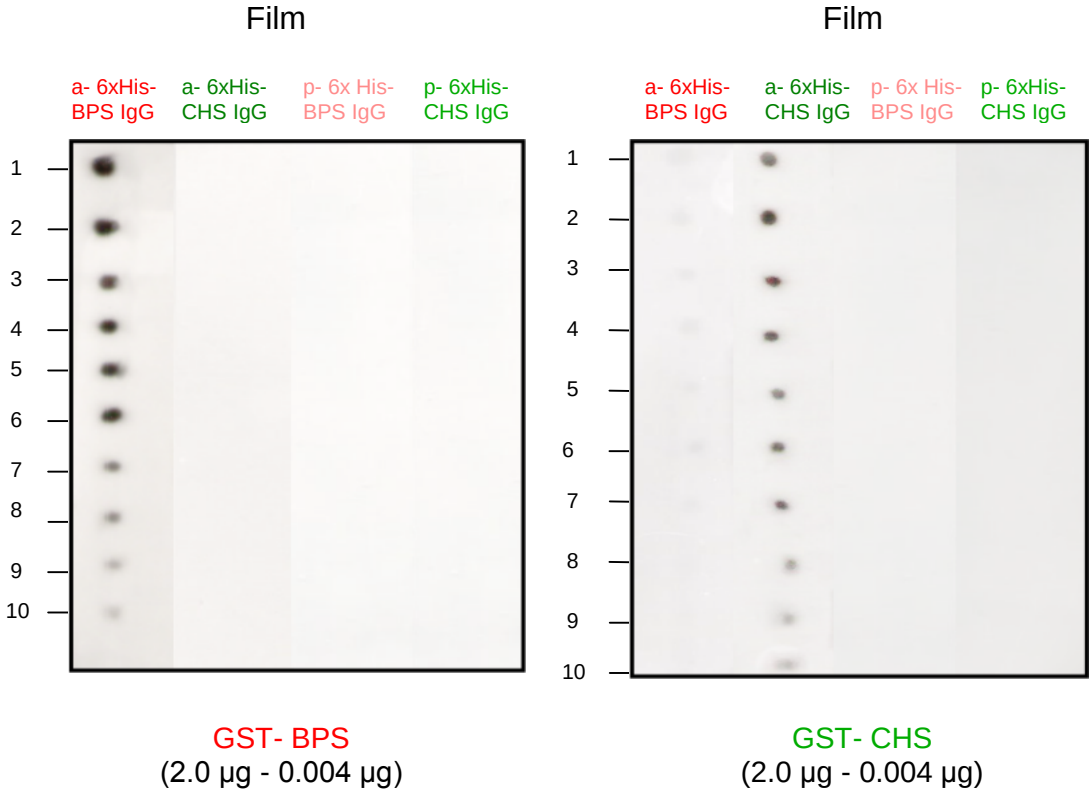

Fig. 3- 17: Estimation of the immunological relationship between the two PKSs (BPS and CHS): Decreasing amounts (numbers 1-10) 2.0, 1.0, 0.5, 0.25, 0.125, 0.063, 0.032, 0.016, 0.008, and 0.004 µg of GST-BPS (left) and GST-CHS (right) were dotted onto a PVDF membrane, followed by immunostaining with anti-6xHis-BPS, anti-6xHis-CHS, preimmune 6xHis-BPS or preimmune 6xHis-CHS. *a* is anti-IgG, *p* is pre-immune.

3.4.2 Immunotitration Coupled to Enzyme Activity Measurement

3.4.2.1 Stability of the Enzyme Activities

To perform immunotitration analysis with the PKSs, it is vital to study first their time- and temperature-dependent stability.

Both enzymes were heterologously expressed in *E. coli* as GST-fusion proteins (Liu *et al.,* 2003). The GST-PKS fusions (GST-BPS and GST-CHS) were purified using a glutathione agarose protein purification system (2.11.2.3 and 3.1.1.3). The enzyme assays and the product analysis were described in (2.11.12). Fig. 3-18 shows the stability of BPS activity. The enzyme is relatively stable at 4º C. During one day, it looses approx. 20% of its original activity. Only 6% of the original enzyme activity were lost during 20 min at 37º C.

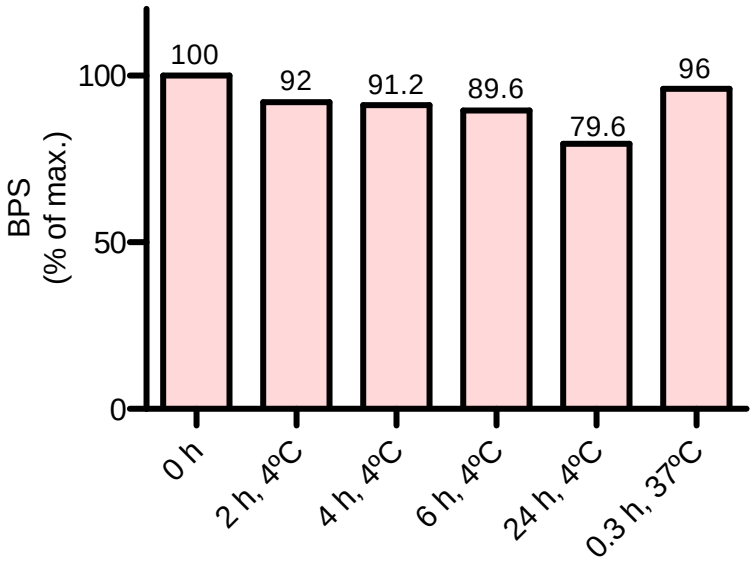

Fig. 3- 18: Effect of time and temperature on BPS activity.

Fig. 3-19 and 3-20 show the stability of CHS activity. The enzyme is relatively stable at 4º C. During one day, it looses approx. 55% of its original activity and about 20% of the original activity were lost during 20 min at 37º C. The enzyme lost 30% of its activity following freezing for one day in the absence of glycerol, and it lost about 20% of its activity in the presence of 15 % or 30 % (v/v) glycerol.

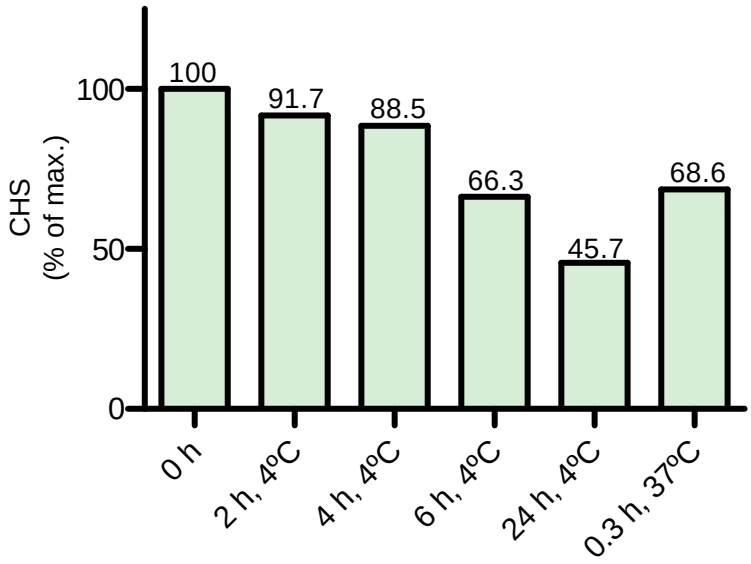

Fig. 3- 19: Effect of time and temperature on CHS activity.

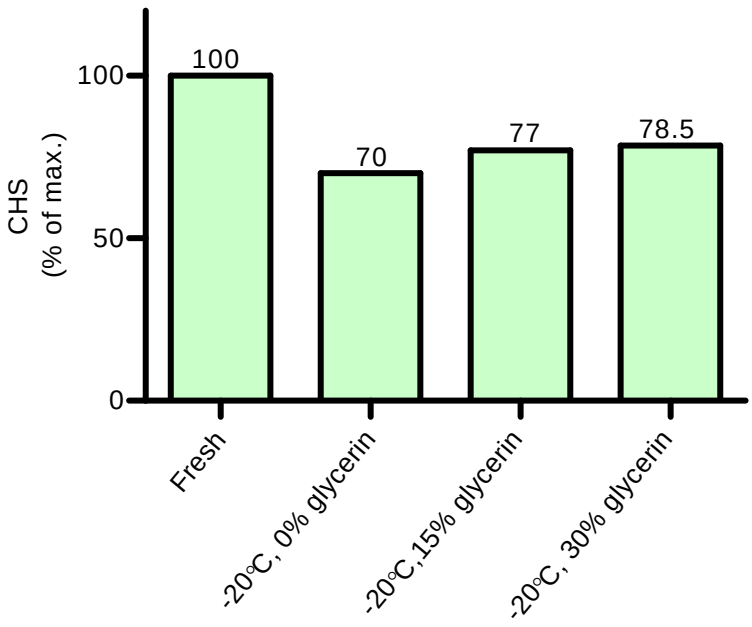

Fig. 3- 20: Effect of glycerol content on CHS activity.

3.4.2.2 Immunotitration

Immunotitration was performed after the IgG fractions had been isolated from the crude sera (2.11.9.2) (Fig. 3-21). GST-BPS and GST-CHS were used as antigens in constant quantities throughout the experiment (2 µg). Decreasing quantities (from 1:2 to 1 :512 dilution) of pre-immune 6xHis-BPS IgG, anti-6xHis-BPS IgG, pre-immune 6xHis-CHS IgG, and anti-6xHis-CHS IgG were added and the PKS activities remaining in the supernatants of the titration mixtures were determined. Weak precipitation of the PKS activities occurred with the pre-immune IgGs. Anti-6xHis-CHS IgG precipitated GST-CHS and did not cross-react with GST-BPS. Anti-6xHis-BPS IgG precipitated GST-BPS and cross-reaction with GST-CHS was only observed with the undiluted IgG preparation.

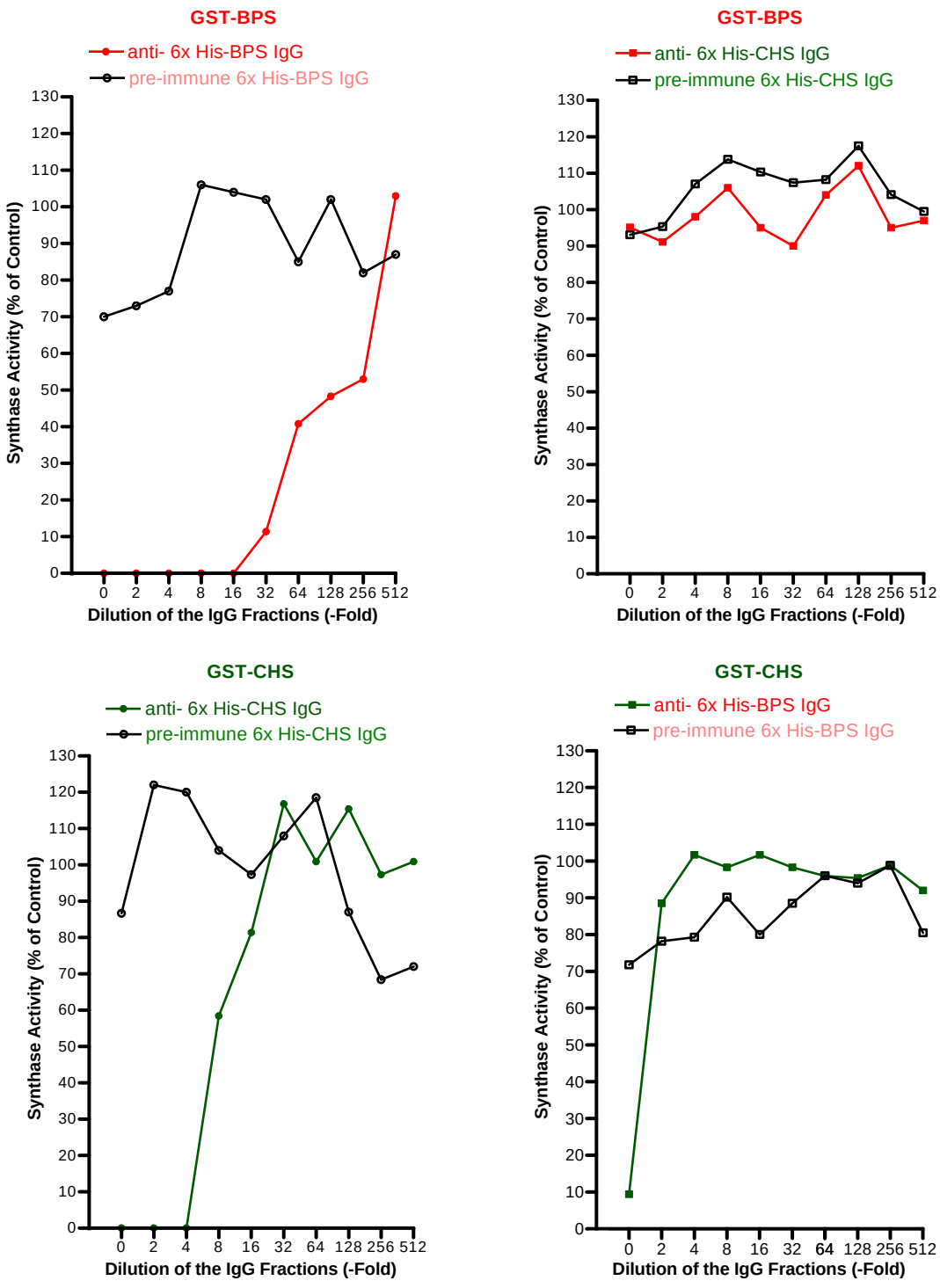

Fig. 3- 21: Immunotitrations of recombinant GST-fusion PKSs activities. The amounts of the enzyme activity remaining in the supernatants after addition of decreasing quantities (from 1:2 to 1 :512) of the pre-immune 6xHis-BPS IgG, anti-6xHis-BPS IgG, pre-immune 6xHis-CHS IgG, anti-6xHis-CHS IgG were determined.

3.5 Detection by Immunoblotting of BPS and CHS in Organs of *H. perforatum*

Protein extracts from various organs of *H. perforatum* and various developmental stages of these organs (2.11.4) were subjected to SDS-PAGE (2.11.8) and subsequent immunoblotting (2.11.9.3.1). The result is shown in Fig. 3-22. Anti-6xHis-BPS-IgG markedly stained a protein band with a molecular mass of 43 kDa in crude extracts from fruits. This molecular mass corresponds to a BPS subunit. Pre-immue IgG failed to stain this band. During fruit development, BPS was immunodetected in the middle-aged fruit. Weak bands were detected in young buds.

In addition, no induction of BPS was immunochemically observed after treatment of excised leaves from *in-vitro* or *in-vivo* plants with elicitors such as methyl jasmonate (2.11.13.1) and salicylic acid (2.11.13.2). The same was true for wounding (2.11.13.3).

Anti 6xHis-CHS-IgG stained a protein band with a molecular mass of 43 kDa in crude extracts from young leaves and flower buds. The molecular mass corresponds to a CHS subunit. Pre-immue IgG failed to stain this band. During leaf development, CHS was immunodetected in 0.3-0.5 cm long leaves only. Furthermore, CHS was not immunodetected in *in-vitro* plants.

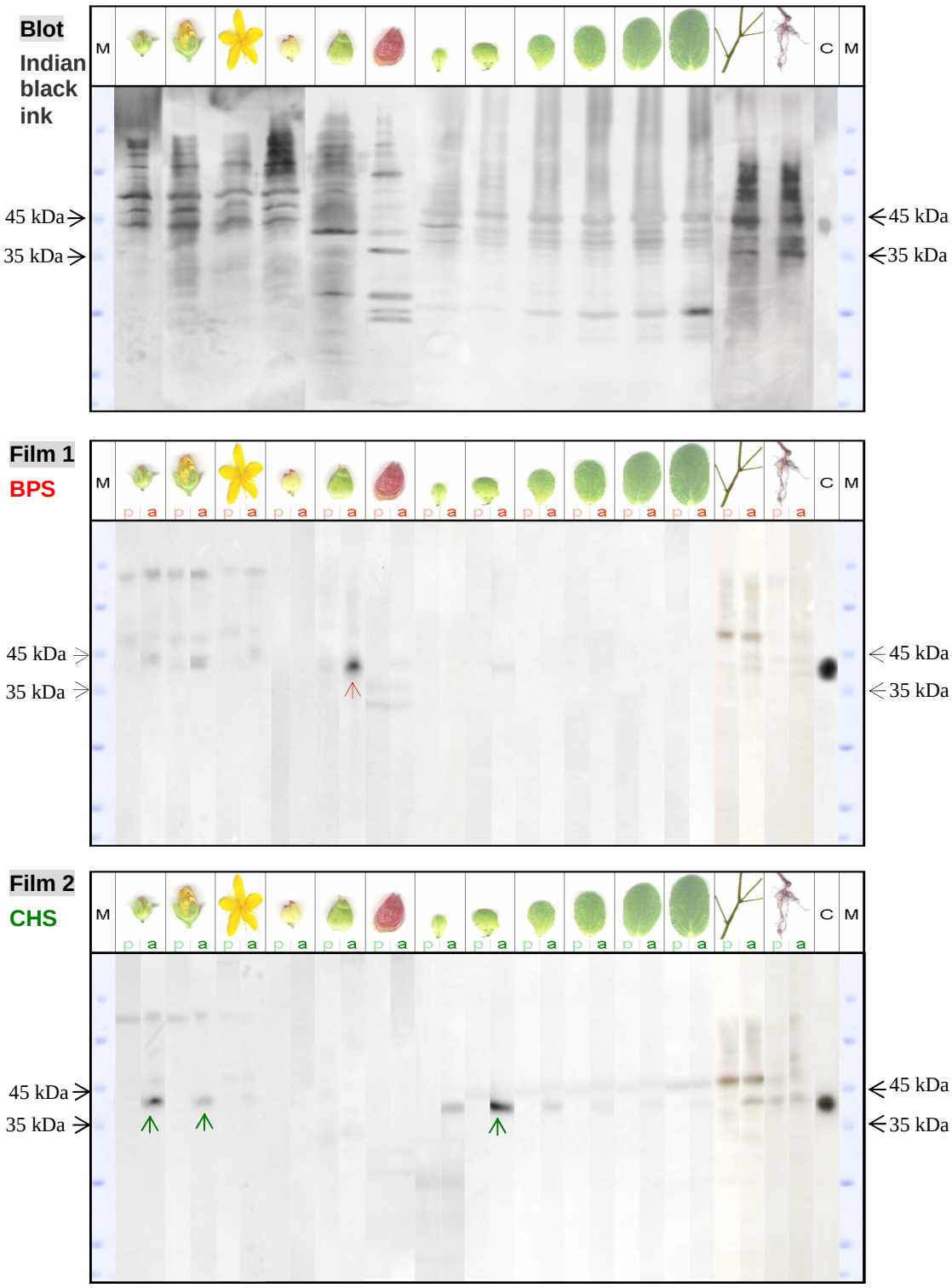

Fig. 3- 22: Immunoblotting of crude protein extracts from various *H. perforatum* organs. The SDS gel (12 %) was performed with 45 µg of protein applied per lane.The blots were (from top to bottom) either stained with Indian black ink or anti-6xHis-BPS and anti-6xHis-CHS. *p*, pre-immune control (pre-immune 6xHis-BPS, *film 1;* pre-immune 6xHis CHS, *film 2*), *a*, antiserum (anti-6xHis-BPS, *film 1;* anti- 6xHis-CHS, *film 2). M*, protein marker, *C*, positive control (0.1 µg 6xHis-BPS or CHS).

3.6 Analysis of Secondary Products from *H. perforatum* Fruits

Methanolic extracts from three developmental stages of *H. perforatum* fruits (2.11.11) were analyzed by HPLC (2.11.12). The gradient used is described in (2.8.12.4). The extracts from the ripe and old fruits contained an additional, so far unidentified secondary metabolite (R_t 16 min), which was not found in the methanolic extract from young fruits (Fig. 3-23). This result suggests that the biosynthesis of this unidentified secondary metabolite was related to the immunodetected occurrence of BPS (Fig. 3-22). Large-scale isolation and structure elucidation of the new compound are in progress.

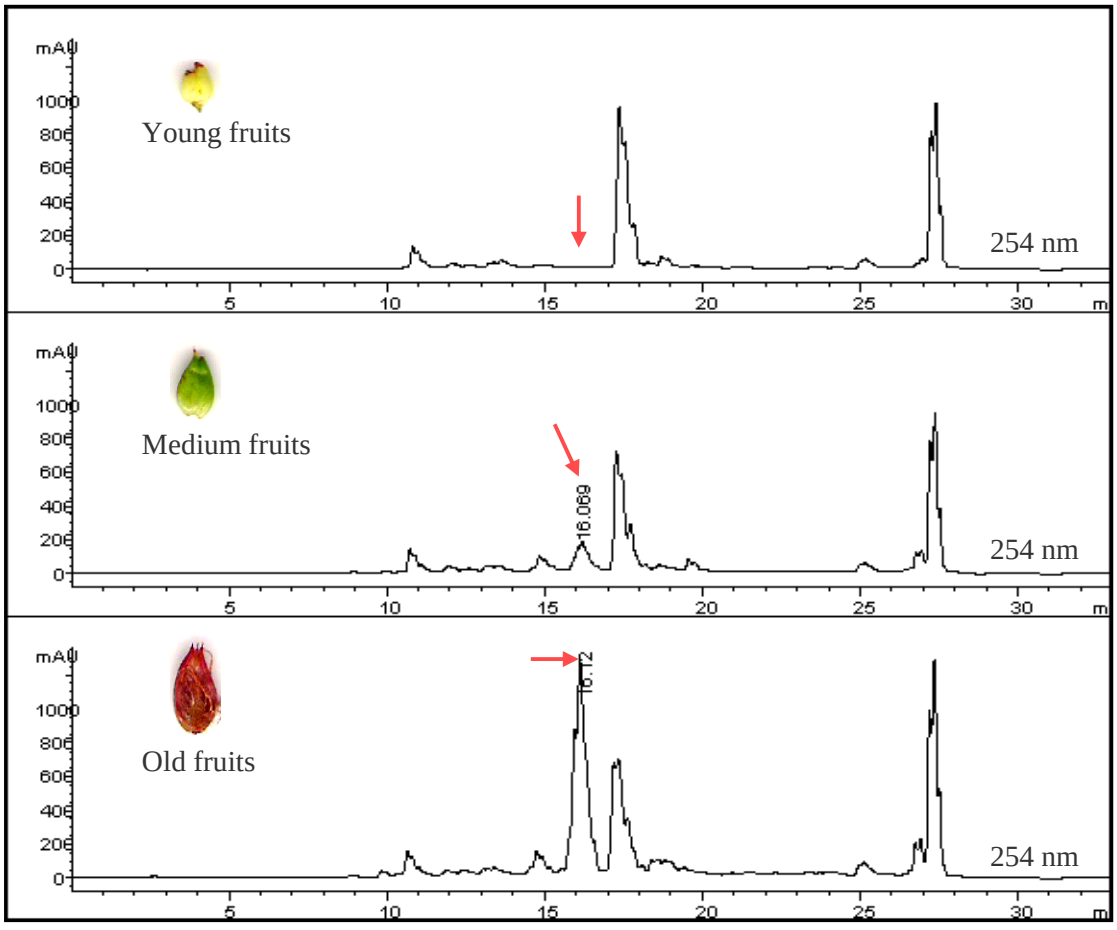

Fig. 3- 23: HPLC analysis of methanolic extracts from three developmental stages of *H. perforatum* fruits. Detection wavelength: 254 nm. Similar results were obtained in two other independent experiments.

3.7 Immunolocalization of PKSs in *H. perforatum* Organs

The tissue-specific localization of BPS and CHS was studied in field-grown *Hypericum perforatum* plants (medicinal plant garden of the Institute of Pharmaceutical Biology) using the immunofluorescence technique (2.11.9.5). Two types of section preparation were tested, the resin (Technovit) sectioning technique (2.11.9.5.1.1) and the cryo-sectioning technique (2.11.9.5.1.2). Compared to the cryo-sections, the resin-embedded sections showed dramatically decreased PKS antigenicity and strong non-specific background labeling. Thus, this work describes only the results of the immunofluorescence localization of the PKSs using cryo-sectioning. Imaging of whole-mount specimens was performed on a Zeiss LSM 510 laser scanning confocal microscope (2.11.9.5.3). The immunostaining of BPS in the plant sections was performed using affinity-purified anti-6xHis-BPS IgG diluted 1:10-1:100. The immunostaining of CHS in the plant sections was performed using affinity-purified anti-6xHis-CHS IgG diluted 1:10-1:100. The best dilution of both affinity-purified antibodies was 1:25.

3.7.1 Immunofluorescence Localization of PKSs in Leaf and Stem Tissues

BPS and CHS were observed in leaf tissues but not in stem tissues. *H. perforatum* leaves are characterized by the presence of different types of secretory tissues including translucent glands and black nodules. From the morphological standpoint, a whole leaf shows numerous translucent dots (translucent glands) of different size dispersed throughout the lamina. In contrast, black dots (black nodules) are much less numerous. They are mostly arranged around the leaf margin and fewer elsewhere in the lamina (Figure 3- 24).

Fig. 3- 24: Secretory tissues present in *H. perforatum* leaf. Light spots are translucent glands and black spots are black nodules.

From the anatomical point of view, translucent glands and black nodules in mature leaves differ remarkably from each other. According to a study by Ciccarelli *et al*. (2001), the translucent glands are spherical or oblong glands consisting of a sub-epidermal cavity delimited by two layers of cells. The internal layer consists of very flattened, thin-walled secretory cells. The external layer consists of thicker-walled parenchymatous cells. The translucent glands are present within the lamina of the leaf, close to the lower surface, and extend from the abaxial to the adaxial epidermis (Figure 3- 25).

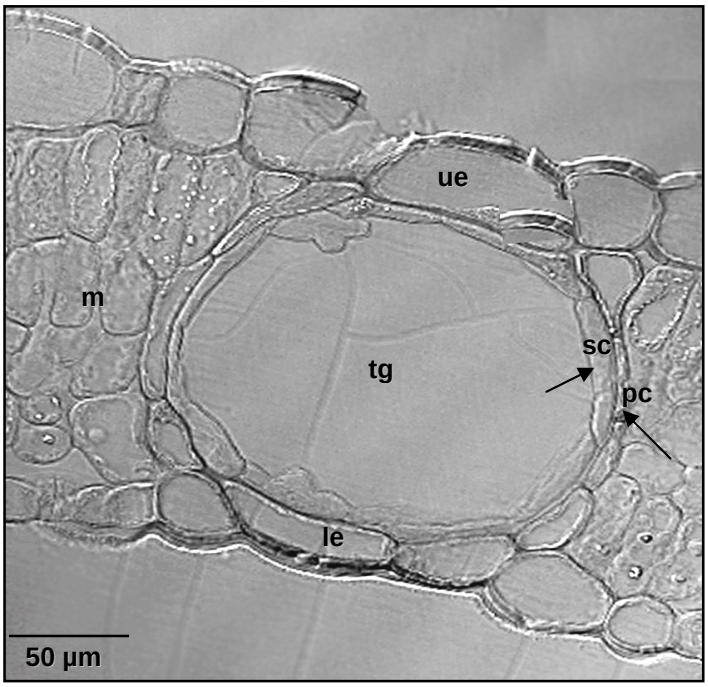

Fig. 3- 25: Anatomical structure of a mature translucent gland in a *H. perforatum* leaf cross-section. *Le*, lower epidermis, *m*, mesophyll, *pc*, parenchymatous cell, *sc*, secretory cell, *tg*, translucent gland, *ue*, upper epidermis.

The black nodules (Figure 3-26) are multicellular nodules and consist of a core of large secretory cells surrounded by two layers of flattened sheath cells. Mature nodules are initiated as small clusters of cells in contact with the abaxial epidermis. They accumulate a black or red homogeneous content (Wen-Zhe et *al*. 2002). The

nodules do not quite span the entire height of the mesophyll, being separated from the adaxial epidermis by a layer of flattened palisade parenchyma cells (Curtis and Lersten, 1990).

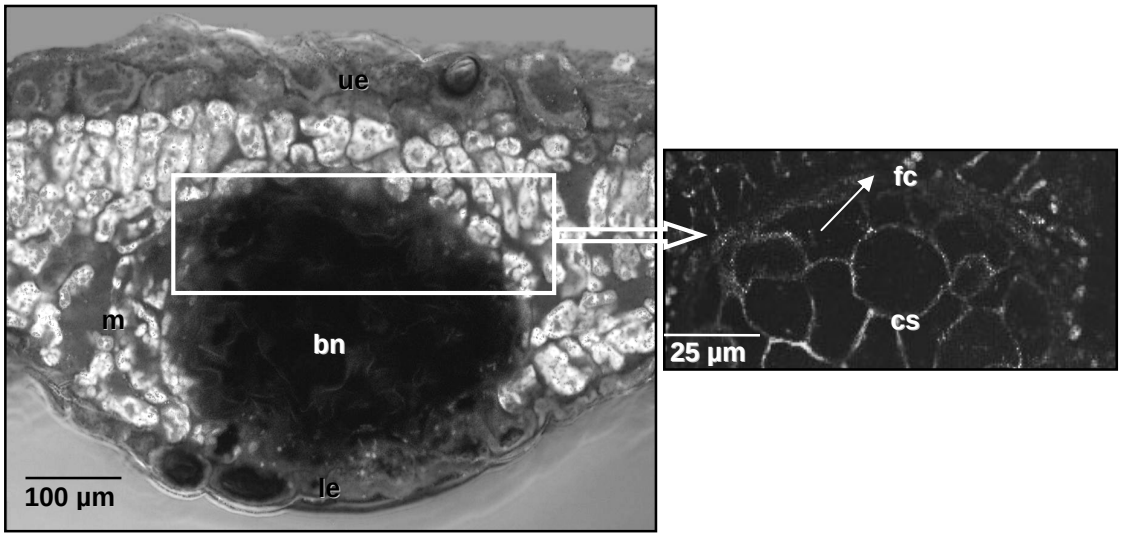

Fig. 3- 26: Anatomical structure of a mature black nodule in a *H. perforatum* leaf cross-section. *bn*, black nodule, *cs*, cluster cells, *fc*, flattened cell, *le*, lower epidermis, *m*, mesophyll, *tg*, translucent gland, *ue*, upper epidermis.

BPS is located in the translucent glands but not in the black nodules, while CHS is present in neither secretory structure. Figure 3-27 shows a specific fluorescence photography of an Alexa Fluor 488-labeled leaf after treatment with anti-6xHis-BPS IgG. Strong antibody labeling was detected in the internal cell layer of large translucent glands present within the lamina. In addition, relatively weak antibody labeling was detected in the leaf mesophyll (Figure 3-27, B). To confirm the specificity of this labeling, control experiments were performed with pre-immune IgG, which gave no labeling (Figure 3-27, A). The lambda-signature (META) of Alexa Fluor 488 labeling of BPS in leaf cells is documented in Figure 3-27, C. The Alexa 488-labeled section was excited by blue light of 488 nm and emitted green light of approximately 520 nm.

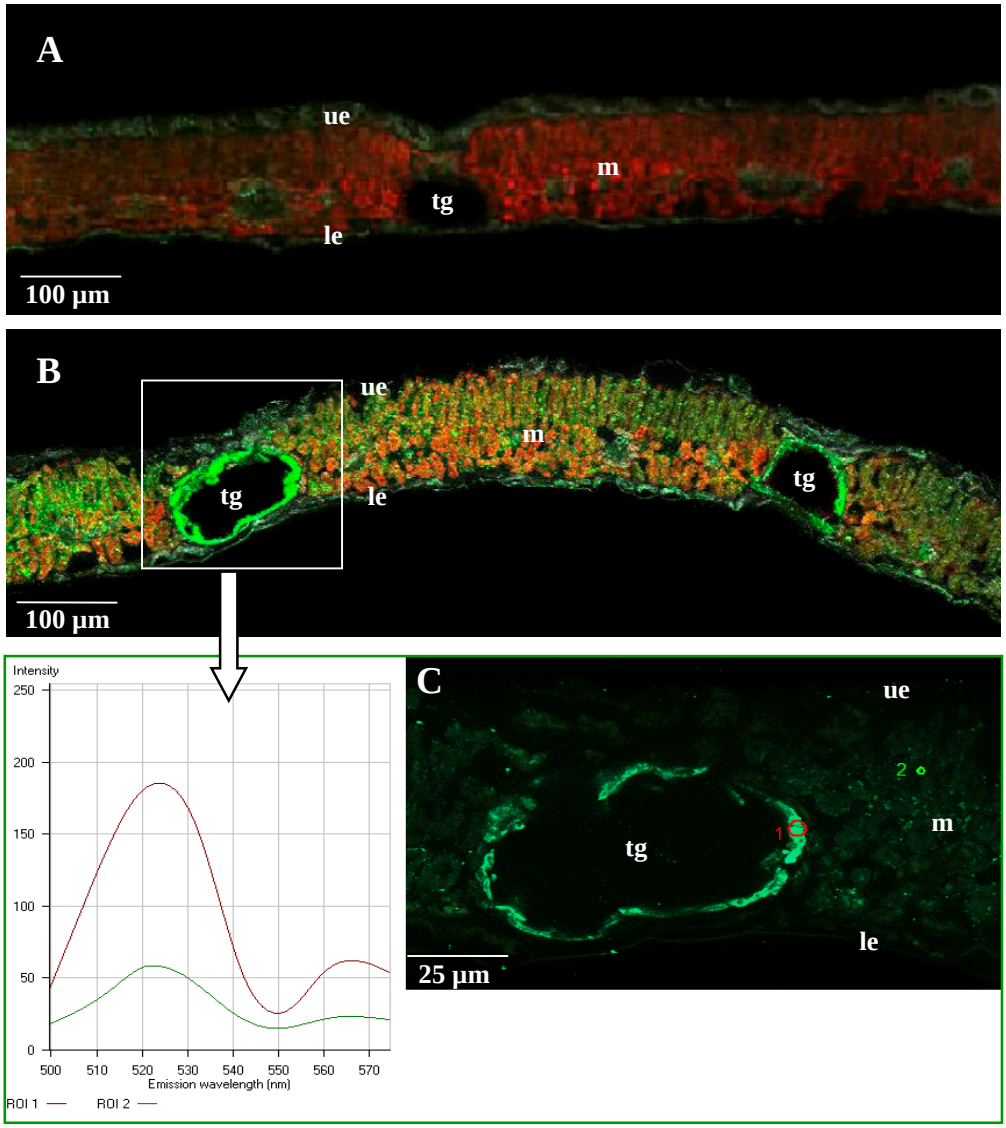

Fig. 3- 27: Immunofluorescence localization of benzophenone synthase in leaves of *H. perforatum*. A, cross-section incubated with preimmune IgG. B, cross-section incubated with anti-6xHis-BPS-IgG. C, Lambda-signature (META) of Alexa Fluor 488 labeling of BPS in leaf cells. The scan modes are channel scan (A and B) and lambda scan (C). *le*, lower epidermis, *m*, mesophyll, *tg*, translucent gland, *ue*, upper epidermis.

The intensity of specific fluorescence in the leaf mesophyll after treatment with anti-6xHis-BPS IgG was dependent on the leaf age (Figure 3-28). During leaf development, maximum labeling of BPS was observed in approximately 1.5 cm long leaves (Figure 3-28, C). The mesophyll layer in very young leaves and in very old leaves did not contain BPS (Figure 3-28, A and D).

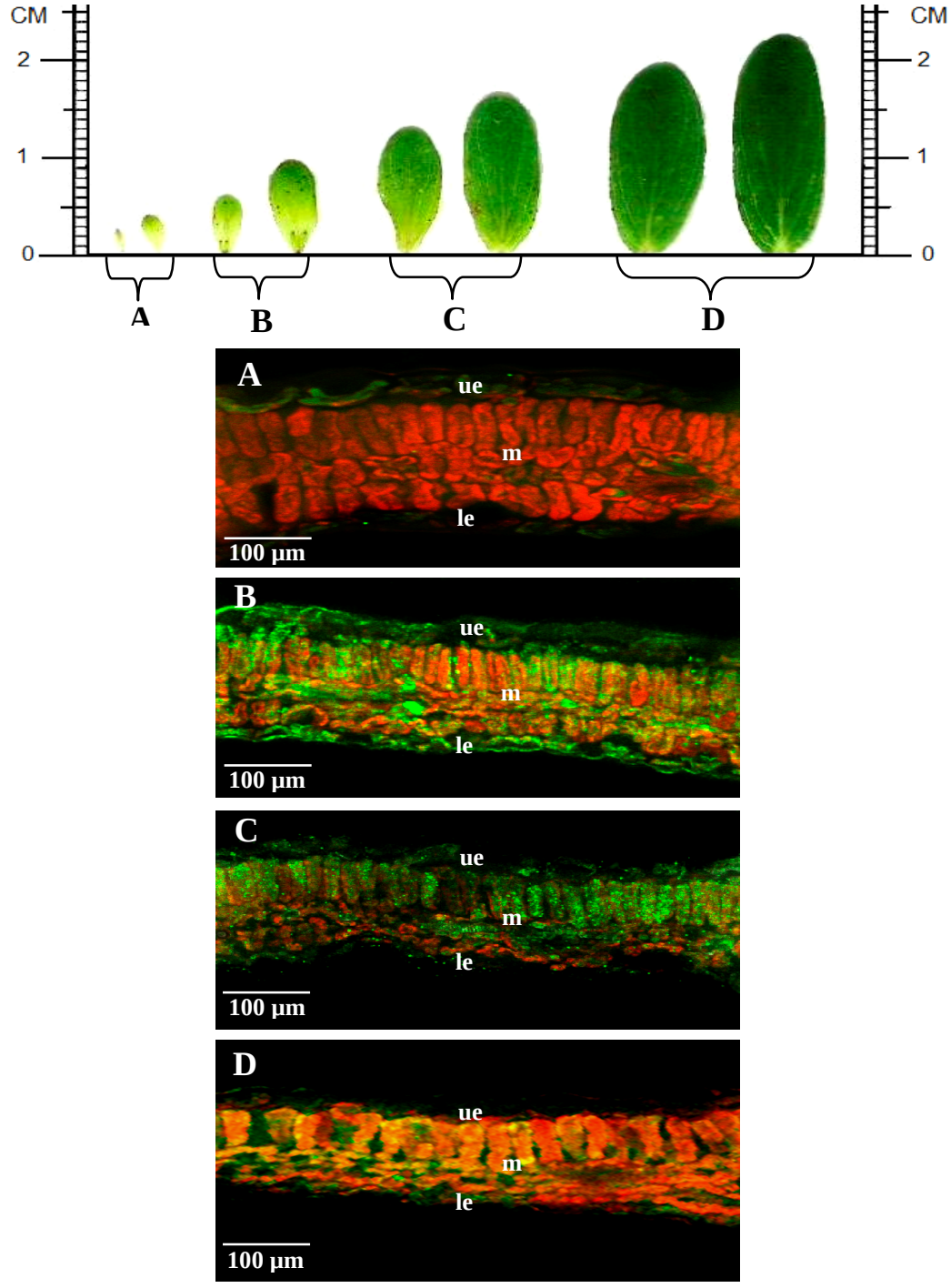

Fig. 3- 28: Immunofluorescence localization of benzophenone synthase in *H. perforatum* leaves of varying ages. The sections A-D are from leaves with a blade length of approximately 0.3, 0.7, 1.5 and 2.0 cm, respectively. The scan mode is channel scan. *le*, lower epidermis, *m*, mesophyll, *ue*, upper epidermis.

Figure 3-29 shows a specific fluorescence photography of an Alexa Fluor 488-labeled leaf after treatment with anti-6xHis-BPS IgG. Strong antibody labeling was detected in the internal cell layer of a translucent gland present within the lamina. In contrast, specific labeling was not detected in the black nodule. In addition, some mesophyll cells exhibit weak antibody labeling.

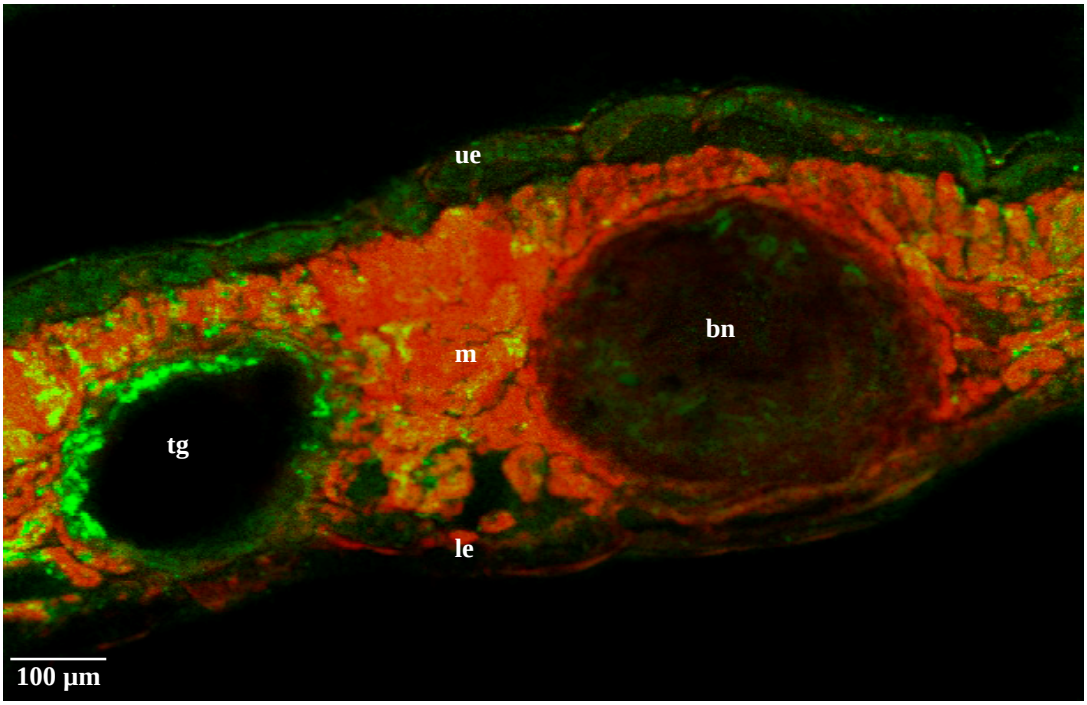

Fig. 3- 29: Immunofluorescence localization of benzophenone synthase in a leaf of *H. perforatum*. Cross-section incubated with anti-6xHis-BPS-IgG. The scan mode is channel scan. *bn*, black nodule, *le*, lower epidermis, *m*, mesophyll, *tg*, translucent gland, *ue*, upper epidermis.

The intensity of the specific fluorescence in the internal cell layer of translucent glands after treatment with anti-6xHis-BPS IgG was dependent on the developmental stage of the gland (Figure 3-30). In the course of gland development, maximum labeling of BPS was found in large glands with a diameter of approximately 80 µm (Figure 3-30, D). Small glands (Ø 20 µm) did not contain BPS (Figure 3-30, A). Medium-sized glands (Ø 55 µm) and very large glands (Ø 90 µm) contained traces of BPS (Figure 3-30, B and E).

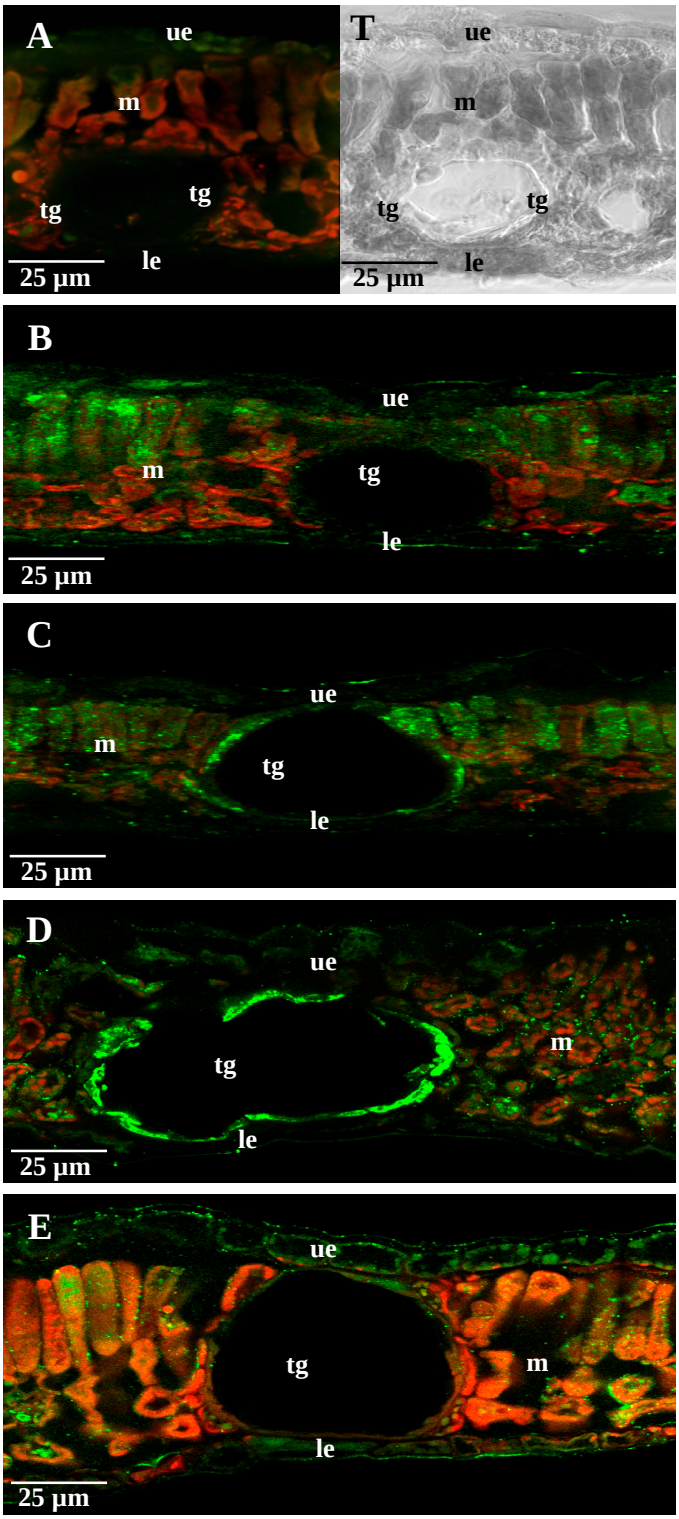

Fig. 3- 30: Immunofluorescence localization of benzophenone synthase in translucent glands of varying developmental stages present within the lamina of *H. perforatum* leaves. The sections A-E contain translucent glands with diameters of approximately 20, 55, 70, 80 and 90 µm, respectively. The scan mode is channel scan. T is transmitted channel of A. *le*, lower epidermis, *m*, mesophyll, *tg*, translucent gland, *ue*, upper epidermis.

Figure 3-31 shows specific fluorescence photographies of Alexa Fluor 488-labeled leaves after treatment with anti-6xHis-BPS IgG. BPS was not observed in black nodules, irrespective of the developmental stage.

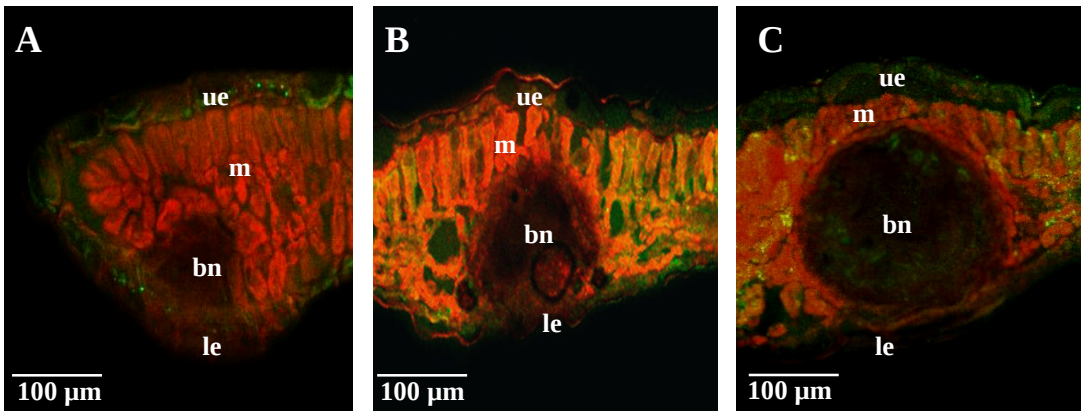

Fig. 3- 31: Immunofluorescence of benzophenone synthase was not localized in black nodules, irrespective of the developmental stage. The sections A-C are from *H. perforatum* leaves containing black nodules with diameters of approximately 20, 50 and 90 µm, respectively. The scan mode is channel scan. *bn*, black nodule, *le*, lower epidermis, *m*, mesophyll, *ue*, upper epidermis.

Figure 3-32 shows a specific fluorescence photography of Alexa Fluor 488-labeled young leaves after treatment with anti-6xHis-CHS IgG. Strong antibody labeling was detected in the leaf mesophyll (Figure 3-32, B). To confirm the specificity of this labeling, control experiments were performed with pre-immune IgG, which gave no labeling (Figure 3-32, A). The lambda-signature (META) of Alexa Fluor 488 labeling of CHS in leaf cells is documented in Figure 3-32, C. The Alexa 488-labeled sections were excitated by blue light of 488 nm and emitted green light of approximately 520 nm.

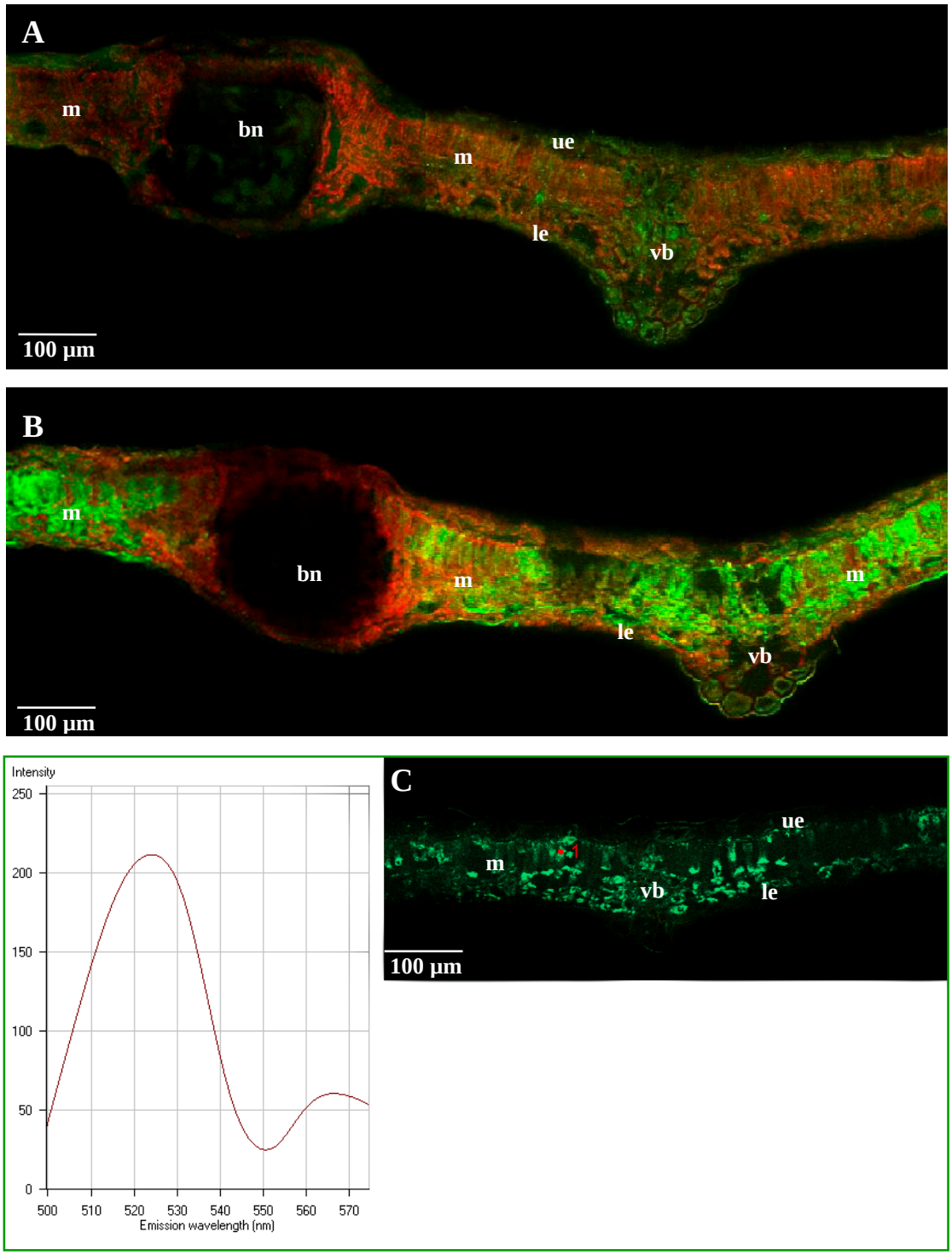

Fig. 3- 32: Immunofluorescence localization of chalcone synthase in leaves of *H. perforatum*. A, cross-section incubated with preimmune IgG. B, Cross-section incubated with anti-6xHis-CHS-IgG. C, Lambda-signature (META) of Alexa Fluor 488 labeling of CHS. The scan modes are channel scan (A and B) and lambda scan (C). *bn*, black nodule; *le*, lower epidermis; *m*, mesophyll; *ue*, upper epidermis*; vb*, vascular bundle.

The intensity of the specific fluorescence in the leaf mesophyll after treatment with anti-6xHis-CHS IgG depended on the leaf age (Figure 3-33). During leaf development, maximum labeling of CHS was observed in approximately 0.5 cm long leaves (Figure 3-33, B). Young leaves contained traces of CHS (Figure 3-33, A). In elder leaves, the CHS level in the mesophyll cells continuously decreased (Figure 3-33, C-D).

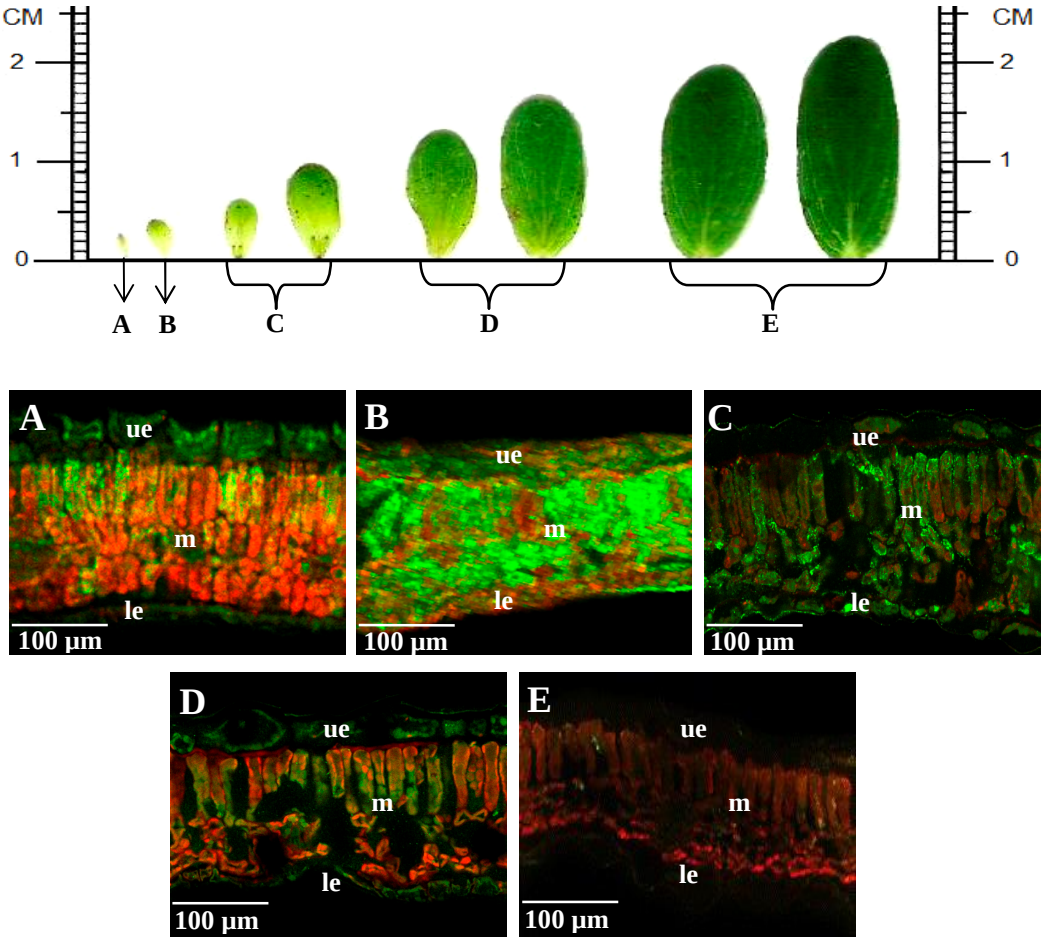

Fig. 3- 33: Immunofluorescence localization chalcone synthase in *H. perforatum* leaves of varying ages. The sections A-E are from leaves with a blade length of approximately 0.3, 0.5, 0.7, 1.5 and 2.0 cm, respectively. The scan mode is channel scan. *le*, lower epidermis, *m*, mesophyll, *ue*, upper epidermis.

CHS was not observed in any secretory tissue present in leaves. Figure 3-34 shows a specific fluorescence photography of Alexa Fluor 488-labeled leaves after treatment with anti-6xHis-CHS IgG. CHS was not detected in any developmental stage of translucent glands which are present in the lamina of *H. perforatum* leaves.

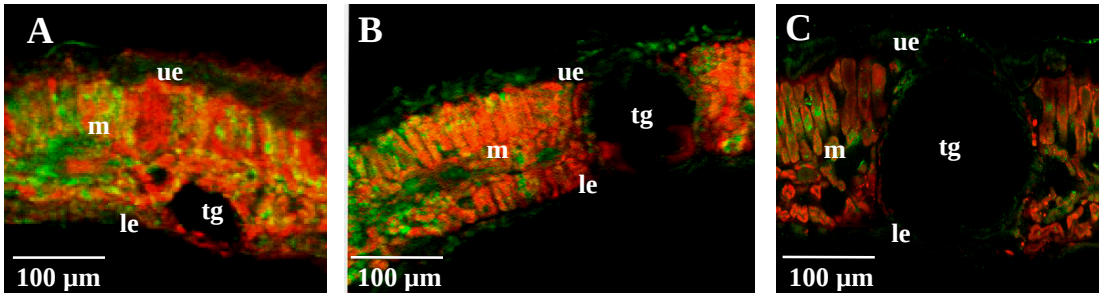

Fig. 3- 34: Immunofluorescence of chalcone synthase was not observed in translucent glands, irrespective of the developmental stage of the glands. The sections A-C are from leaves containing translucent glands with diameters of approximately 25, 60 and 80 µm, respectively. The scan mode is channel scan. *le*, lower epidermis, *m*, mesophyll, *tg*, translucent gland, *ue*, upper epidermis.

Figure 3-35 shows a specific fluorescence photography of Alexa Fluor 488-labeled leaves after treatment with anti-6xHis-CHS IgG. CHS was not observed at any developmental stage of black nodules which are also present in the leaf lamina.

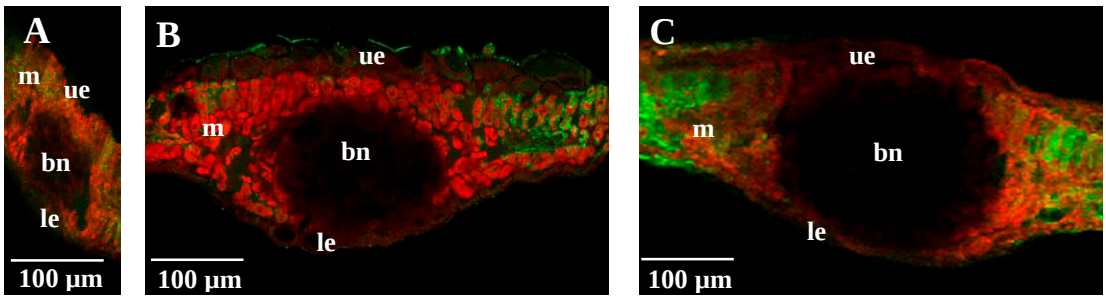

Fig. 3- 35: Immunofluorescence of chalcone synthase was not found in black nodules, irrespective of the developmental stage of the nodules. The sections A-E are from leaves containing black nodules with diameters of approximately 30, 60, and 90 µm, respectively. The scan mode is channel scan. *le*, lower epidermis, *m*, mesophyll, *bn*, black nodule, *ue*, upper epidermis.

3.7.2 Immunofluorescence Localization of PKSs in Rhizome and Root Tissues

BPS and CHS were not observed in rhizome tissues. In contrast, BPS is expressed in roots, while CHS is not.

Figure 3-36 shows a specific fluorescence photography of Alexa Fluor 488-labeled roots after treatment with anti-6xHis-BPS IgG. Strong antibody labeling was detected in the root cortex (Figure 3-36, B). The root cap, the exodermis, and the vascular cylinder were devoid of fluorescence. To confirm the specificity of this labeling, control experiments were performed with preimmune IgG. These sections showed no labeling (Figure 3-36, A).

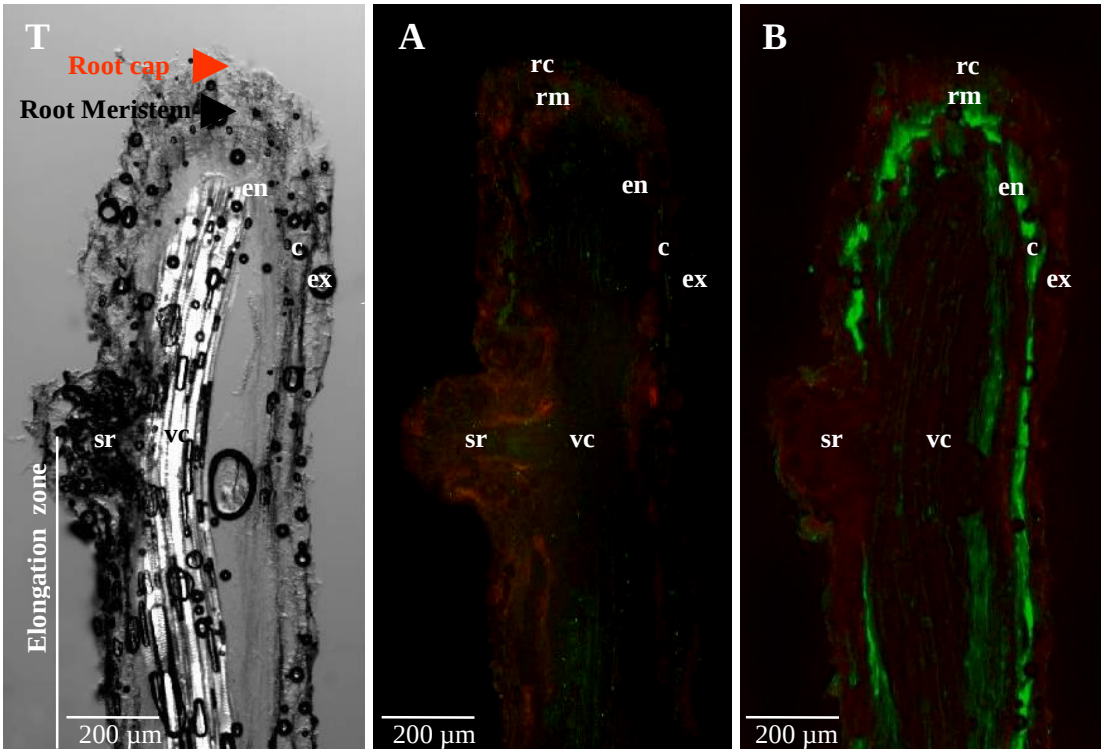

Fig. 3- 36: Immunofluorescence localization of benzophenone synthase in roots of *H. perforatum*. A, longitudinal section incubated with preimmune IgG. B, longitudinal section incubated with anti-6xHis-BPS-IgG. T, transmitted channel of B. The scan mode is channel scan. *c*, cortex, *en*, endodermis, *ex*, exodermis, *rc*, root cap, *rm*, root meristem, *sr*, secondary root, *vc*, vascular cylinder.

The cortex of *H. perforatum* roots is relatively thin and consists of only few layers of storage parenchyma cells. The distribution of the specific fluorescence of Alexa Fluor 488-labeling after treatment with anti-6xHis-BPS IgG is uneven (Figure 3-37). Some portions of cortex cells are labeled while others are not. This finding was also obtained with cross sections.

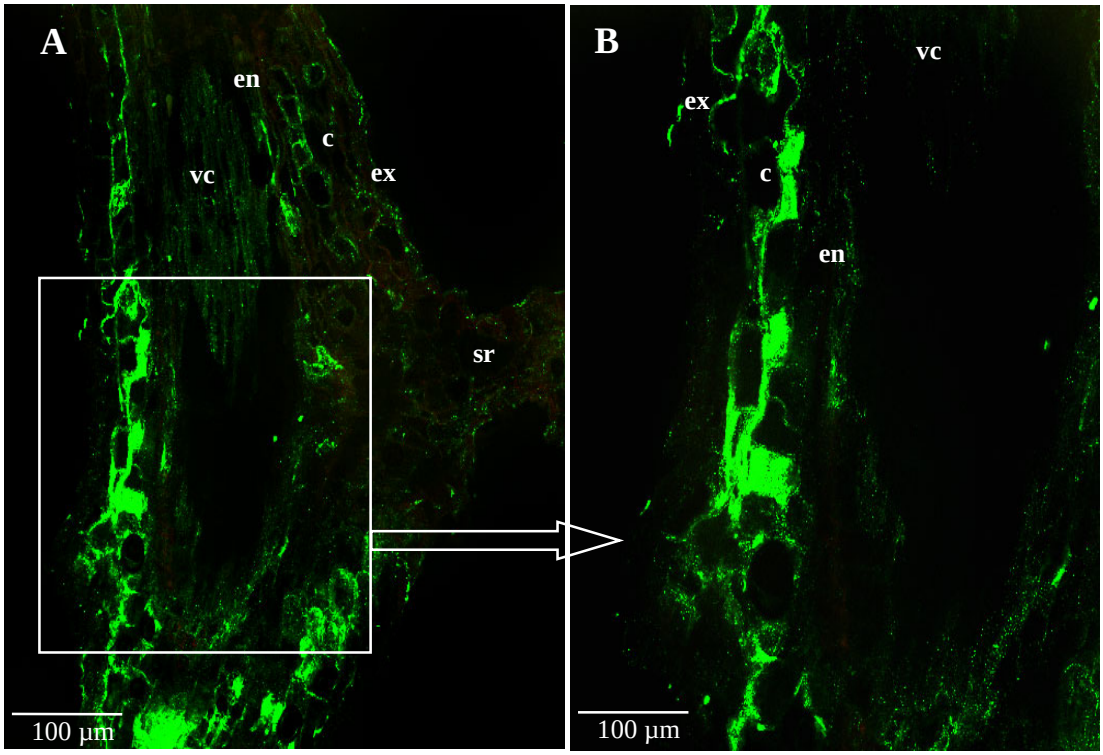

Fig. 3- 37: Immunofluorescence localization of benzophenone synthase in roots of *H. perforatum*. A, longitudinal section incubated with anti-6xHis-BPS-IgG. B, detail from A. The scan mode is channel scan. *c*, cortex, *en*, endodermis, *ex*, exodermis, *sr*, secondary root, *vc*, vascular cylinder.

Figure 3-38 shows a specific fluorescence photography of Alexa Fluor 488-labeled roots after treatment with anti-6xHis-BPS IgG. Strong antibody labeling was detected in the root cortex (Figure 3-38, B). To confirm the specificity of this labeling, control experiments were performed using preimmune IgG, which gave no labeling (Figure 3-38, A). The lambda-signature (META) of Alexa Fluor 488 labeling of CHS in root

cells is documented in Figure 3-38, C. The Alexa 488-labeled sections were excitated by blue light of 488 nm and emitted green light of approximately 520 nm.

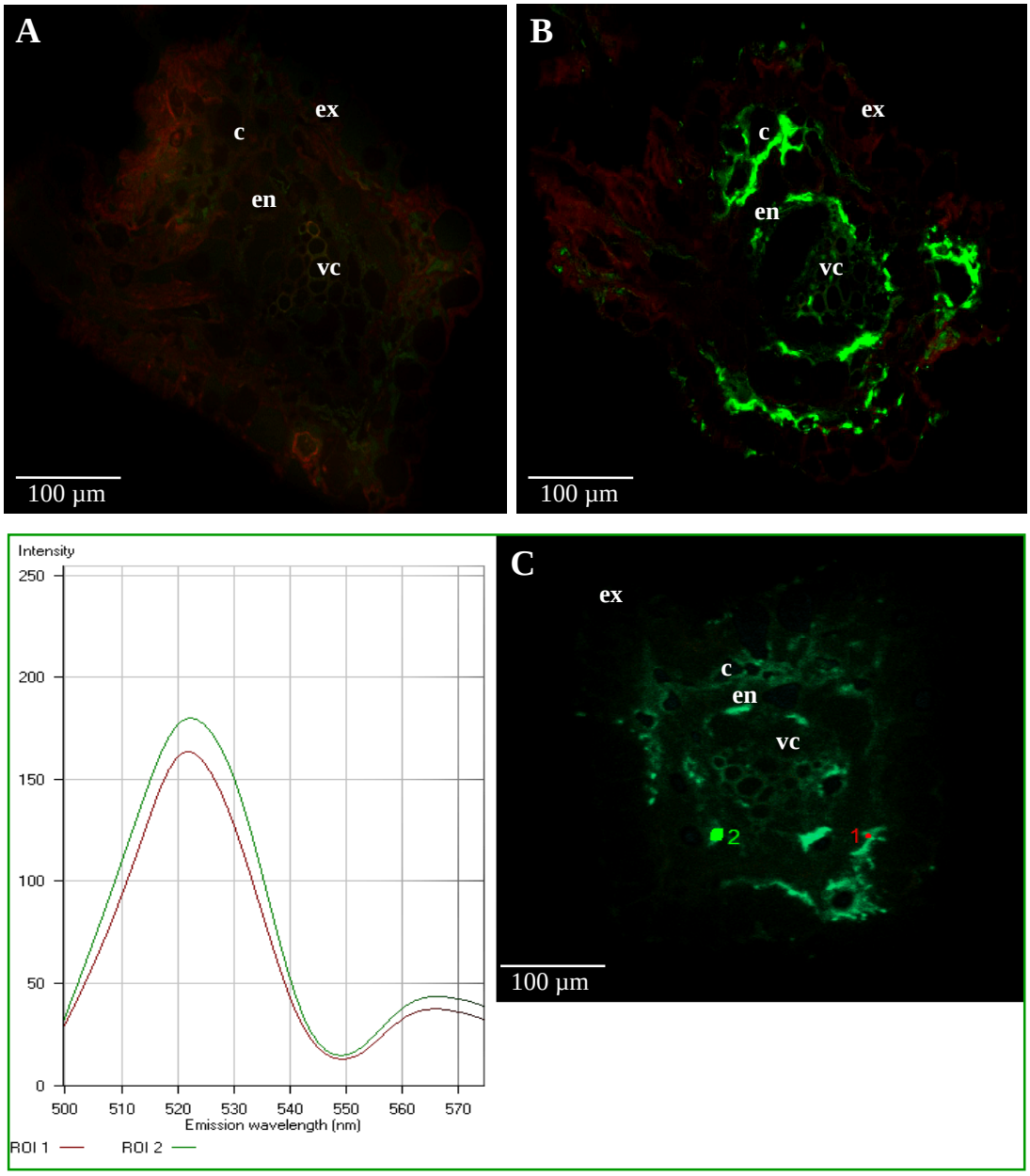

Fig. 3- 38: Immunofluorescence localization of benzophenone synthase in roots of *H. perforatum*. A, cross-section incubated with preimmune IgG. B, cross-section incubated with anti-6xHis-BPS-IgG. C, Lambda-signature (META) of Alexa Fluor 488 labeling of BPS. The scan modes are channel scan (A, B) and lambda scan (C). *c*, cortex, *en*, endodermis, *ex*, exodermis, *vc* , vascular cylinder.

3.7.3 Immunofluorescence Localization of PKSs in Floral Tissues

According to the immunoblotting detection of PKSs at various developmental stages of *H. perforatum* floral organs (Figure 3-22), the tissue-specific immunofluorescence localization of PKSs was carried out in young sepals and middle-aged fruits. Immunolocalization of PKSs in other floral parts will be future work. So far, BPS was found in secretory tissue which is present in young bud sepals and middle-aged fruits, while CHS is located in mesophyll cells of young buds.

According to Ciccarelli *et al.* (2001), sepals contain oblong translucent glands (Figure 3-25), albeit fewer than leaves. In addition, sepals contain type B canals. Both translucent glands and type B canals have schizogenous origin (Ciccarelli *et al.*, 2001). Figure 3-39 shows a specific fluorescence photography of Alexa Fluor 488-labeled young sepals after treatment with anti-6xHis-BPS IgG. Strong antibody labeling was detected in secretory gland cells (Figure 3-39, B-D). To confirm the specificity of this labeling, control experiments were performed with pre-immune IgG and gave no labeling (Figure 3-39, A).

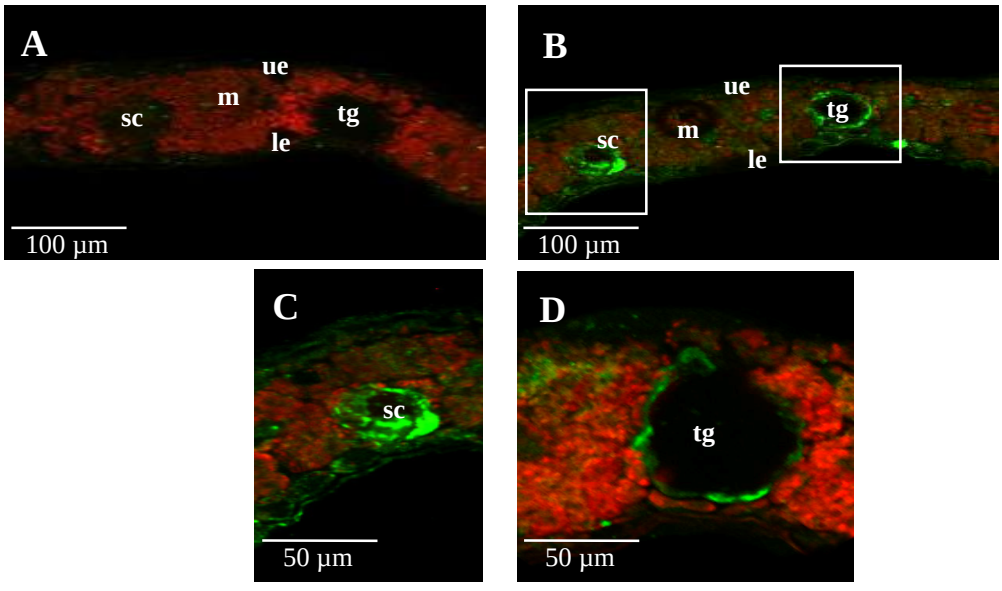

Fig. 3- 39: Immunofluorescence localization of benzophenone synthase in bud sepals of *H. perforatum*. A, cross-section incubated with preimmune IgG. B, cross- section incubated with anti-6xHis-BPS-IgG. C and D, magnifications of B. The scan mode is channel scan. *le*, lower epidermis, *m*, mesophyll, *sc*, secetory canal, *tg*, translucent gland, *ue*, upper epidermis.

Figure 3-40 shows a specific fluorescence photography of Alexa Fluor 488-labeled young bud sepals after treatment with anti-6xHis-CHS IgG. Strong antibody labeling was detected in the mesophyll (Figure 3-40 B, C). To confirm the specificity of this labeling, control experiments were performed. Incubation of sections with pre-immune IgG gave no labeling (Figure 3-40 A).

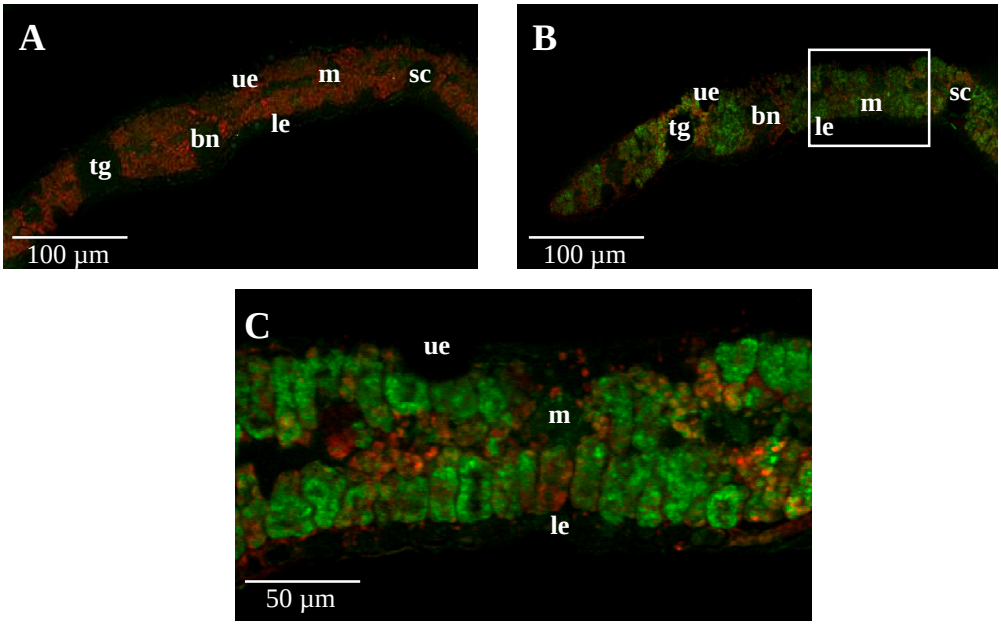

Fig. 3- 40: Immunofluorescence localization of chalcone synthase in bud sepals of *H. perforatum*. A, cross-section incubated with preimmune IgG. B, cross-section incubated with anti-6xHis-CHS-IgG. C, magnification of B. The scan mode is channel scan. *bn*, black nodule, *le*, lower epidermis, *m*, mesophyll, *sc*, secetory canal *tg*, translucent gland, *ue*, upper epidermis.

Figure 3-41 shows the anatomical structure of a *H. perforatum* fruit. According to Ciccarelli *et al.* (2001), type C canals consist of a wide cavity delimited by one or more layers of secretory cells. They were located in the fruit wall along the midrib of each carpel.

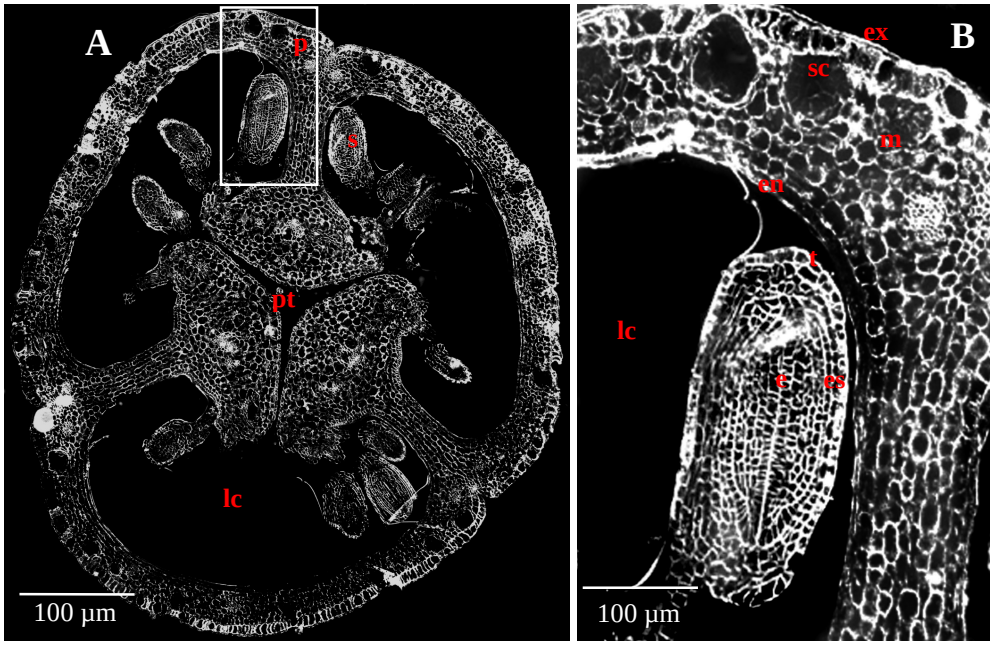

Fig. 3- 41: Anatomical structure of a *H. perforatum* fruit. A, cross-section of a middle-aged fruit. B, detail from A. *e*, embryo, *en*, endocarp, *es*, endosperm, *ex*, exocarp, *lc*, locular cavity, *m*, mesocarp, *p*, pericarp, *pt*, placenta tissue, *s*, seed, *sc*, secretory canal, *t*, testa.

Figure 3-42 shows a specific fluorescence photography of an Alexa Fluor 488-labeled middle-aged fruit after treatment with anti-6xHis-BPS IgG. Strong antibody labeling was detected in secretory gland cells present in the ovary wall and in seed cells (Figure 3-42 B, C). To confirm the specificity of this labeling, control experiments were performed. Incubation of sections with pre-immune IgG gave no labeling (Figure 3-42, A). The lambda-signature (META) of the Alexa Fluor 488 labeling of BPS in middle-aged fruit cells was determined (Figure 3-42, C). The Alexa 488-labeled sections were excitated by blue light of 488 nm and emitted green light of approximately 520 nm.

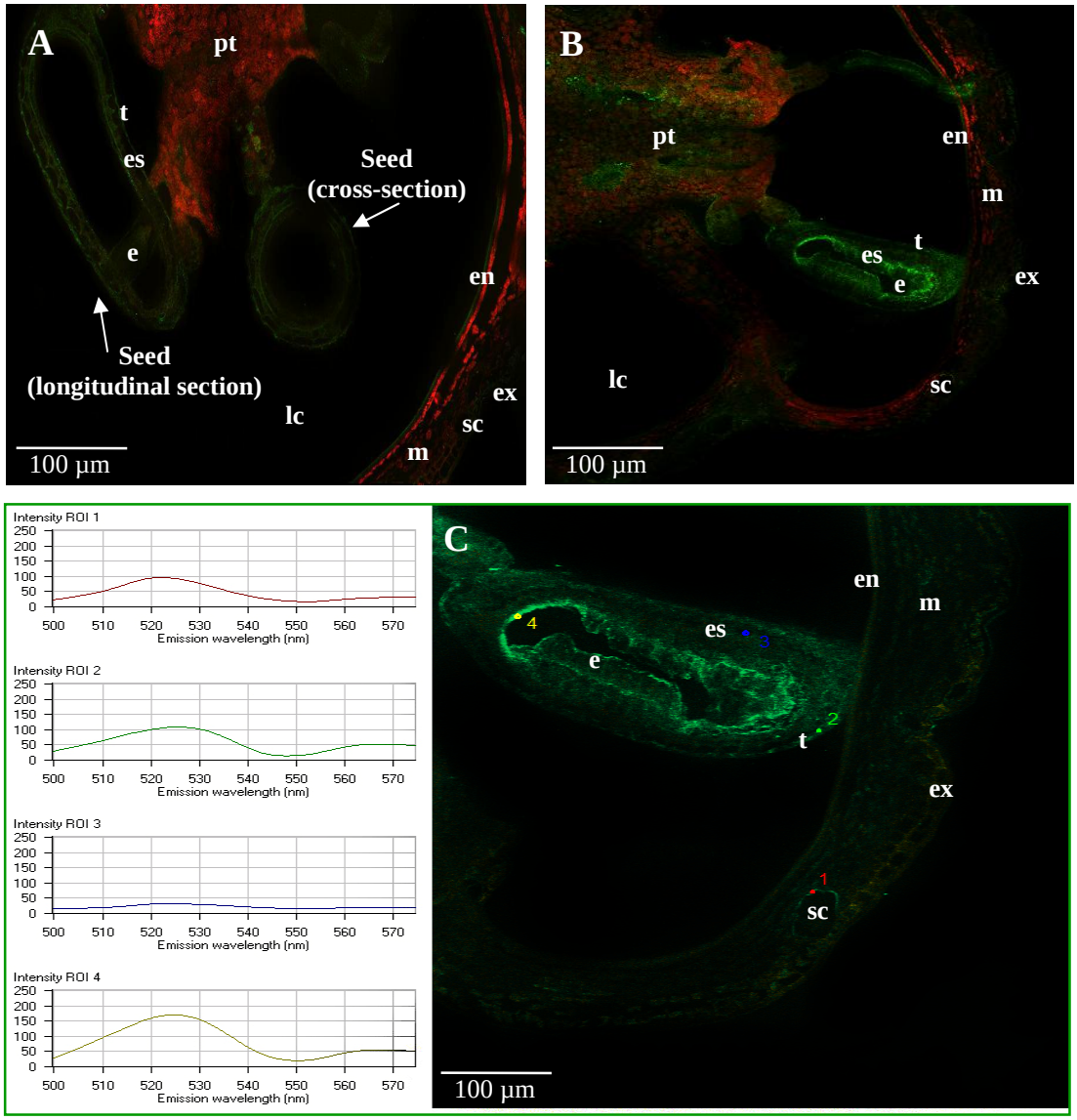

Fig. 3- 42: Immunofluorescence localization of benzophenone synthase in a middle-aged fruit of *H. perforatum*. A, cross-section incubated with preimmune IgG. B, cross-section incubated with anti-6xHis-BPS-IgG. C, Lambda-signature (META) of Alexa Fluor 488 labeling of BPS in middle-aged fruit cells. The scan modes are channel scan (A and B) and lambda scan (C). *e*, embryo, *en* is endocarp, *es*, endosperm, *ex*, exocarp, *lc*, locular cavity, *m*, mesocarp, *p*, pericarp, *pt*, placenta tissue, *s*, seed, *sc*, secretory canal, *t*, testa.

Figure 3-43 shows a specific fluorescence photography of an Alexa Fluor 488-labeled middle-aged fruit carpel after treatment with anti-6xHis-BPS IgG. Strong antibody labeling was detected in the internal cell layer of type B canals present in the fruit wall (Figure 3-43, B, C). To confirm the specificity of this labeling, control experiments were performed. Incubation of the sections with pre-immune IgG gave

no labeling (Figure 3-43, A). The lambda-signature (META) of the Alexa Fluor 488 labeling of BPS in middle-aged fruit carpel cells was recorded (Figure 3-43, C). The Alexa 488-labeled sections were excitated by blue light of 488 nm and emitted green light of approximately 520 nm.

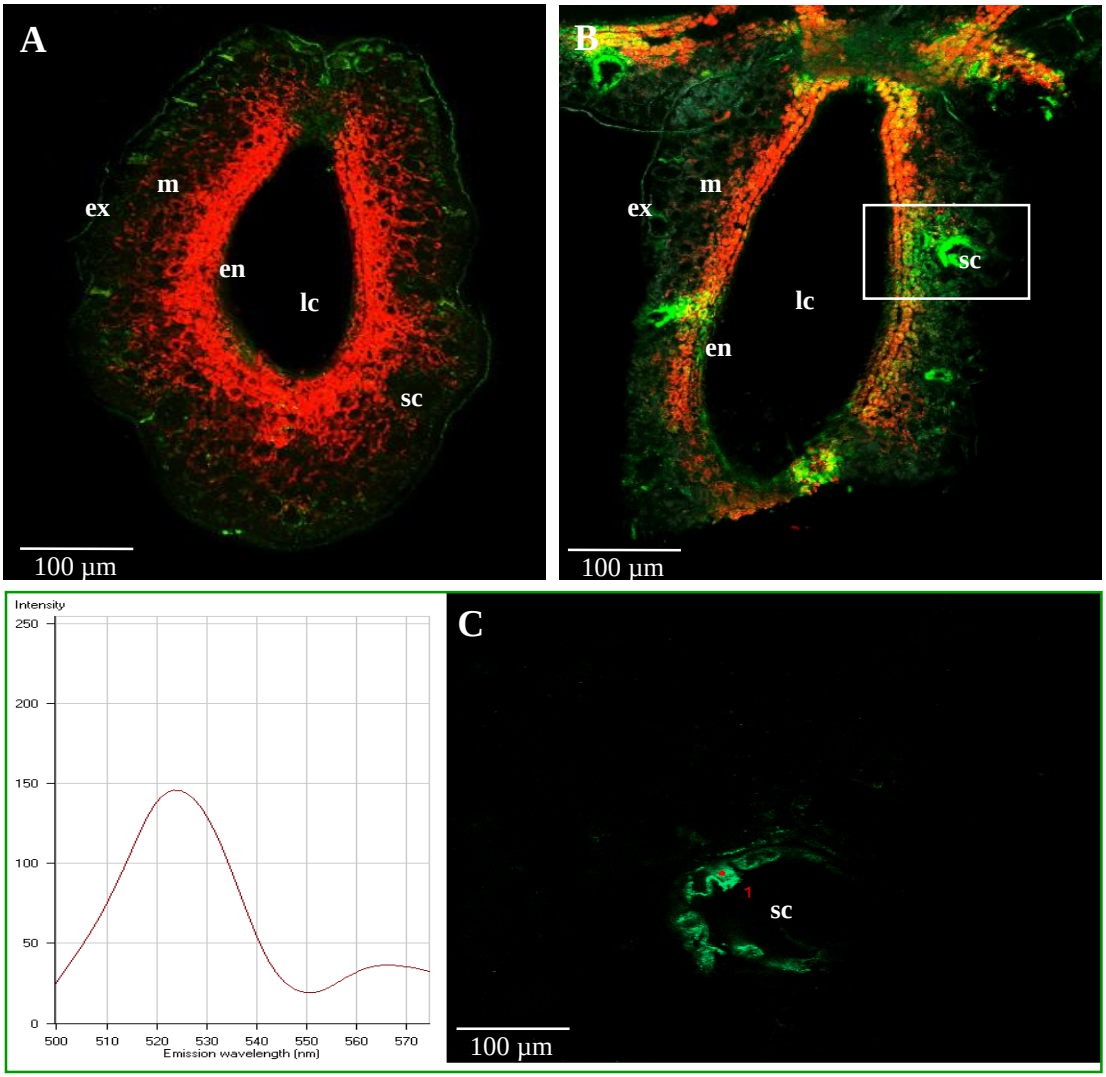

Fig. 3- 43: Immunofluorescence localization of benzophenone synthase in middle-aged fruits of *H. perforatum*. A, cross-section incubated with preimmune IgG. B, cross-section incubated with anti-6xHis-BPS-IgG. C, Lambda-signature (META) of the Alexa Fluor 488 labeling of BPS in the internal cell layer of type B canals present in the fruit wall. The scan modes are channel scan (A and B) and lambda scan (C). *en*, endocarp, *ex*, exocarp, *lc*, locular cavity, *m*, mesocarp, *p*, pericarp, *sc*, secretory canal (type C).

The intensity of the specific immunofluorescence in the internal cell layer of type C canals in fruit walls after treatment with anti-6xHis-BPS IgG depended on the developmental stage of the glands (Figure 3-44). In the course of secretory canal development, maximum labeling of BPS was observed in glands with a diameter of approximately 60 µm (Figure 3-44, C). Larger glands, e.g. Ø 90 µm in Figure 3-44 D contained only traces of BPS**.**

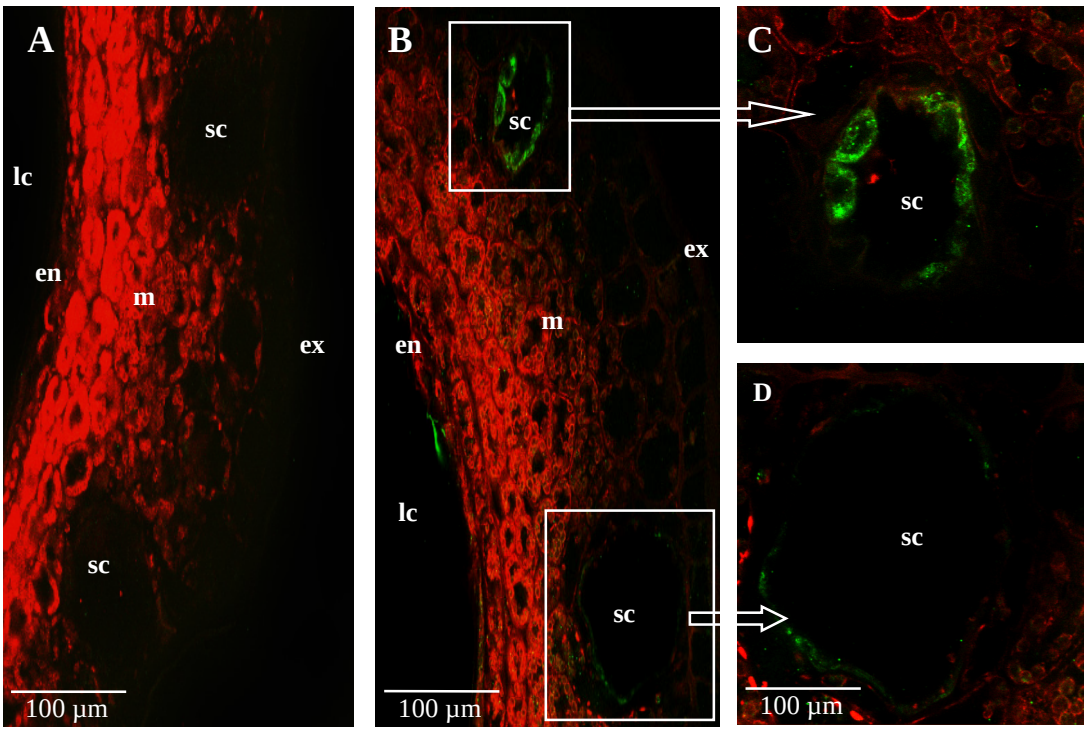

Fig. 3- 44: Immunofluorescence localization of benzophenone synthase in middle-aged fruits of *H. perforatum*. A, cross-section incubated with preimmune IgG. B, cross-section incubated with anti-6xHis-BPS-IgG. C and D are detail from B showing young and old glands, respectively. The scan mode is channel scan. *ex*, exocarp, *lc*, locular cavity, *m*, mesocarp, *p*, pericarp, , *sc*, secretory canal (type C).

4 Discussion

Hypericum perforatum is one of the best studied medicinal plants regarding pharmacological investigations and clinical trials (Müller, 2003). In contrast, little is known about the biochemistry and the physiology of the active constituents. The antidepressant activity of extracts from *H. perforatum* is attributed to hyperforins, hypericins, and flavonoids (Butterweck, 2003). Indian populations of the medicinal plant were found to contain high amounts of xanthones, some of which act as selective monoamine oxidase A inhibitors (Muruganandam *et al.,* 2000). In addition, hyperforins exhibit antibacterial and antitumoral activities (Beerhues, 2006), and hypericins are promising agents for a photodynamic cancer therapy (Ebermann *et al.,* 1996; Court, 2003). Thus, *H. perforatum* contains a number of pharmacologically attractive compounds.

Interestingly, all four classes of pharmacologically relevant constituents are derivatives of polyketide metabolism (see Scheme 1-2) (Beerhues, 2006; Dias, 2003). Four type III PKSs are responsible for the formation of the carbon skeletons, which can subsequently undergo substitution reactions, such as prenylation, methylation, and glycosylation. Where the PKSs are located at the tissue level and intracellularly, is so far unknown. However, understanding a metabolic pathway does not only include knowledge of the biochemical and molecular biological processes but also involves insight into the temporal and spatial regulation. The goal of the present work was to study the localization of two of the four PKSs using immunofluorescence microscopy. BPS and CHS were available as recombinant proteins, their cDNAs had been cloned from cell cultures of the related species *H. androsaemum* (Liu *et al.,* 2003). Here, polyclonal antibodies were raised against BPS and CHS and the IgG fractions were isolated by affinity purification. The exclusive specificity of the IgG fractions for either BPS or CHS was proven by immunobloting. The lack or negligibility of cross-reactivity between the antibodies and the respective heterologous antigens was confirmed by dot blotting and immunotitration coupled with the determination of enzyme activities. The absence of immunological relationship between BPS and CHS finally allowed for a separate immunocytochemical localization of the two PKSs. Interestingly, different spatial expression patterns were observed, which are related to

differential functions and biological roles of the respective metabolic pathways in the plant.

Unlike localization of CHS, the distribution pattern of BPS was studied for the first time in vegetative and generative plant organs. The immunofluoresence analysis of *H. perforatum* leaves demonstrated that BPS is weakly and more sporadically expressed in mesophyll cells of young leaves. However, a strong expression was observed in large translucent glands present inside the leaves. In roots, BPS is located in the cortical cells. In floral parts, as far as studied, BPS was found in secretory structures present in sepals of young buds and middle-aged fruits. Seeds in middle-aged fruits also expressed BPS. At present, it is difficult to correlate these immunohistochemical findings with the accumulation of BPS products, such as prenylated benzophenones and xanthones. The knowledge of the occurrence of BPS products in vegetative and generative tissues of *Hypericum* species and of plants belonging to other genera of Clusiaceae = Guttiferae is rather limited, although the recent widespread interest in the antidepressant activity of *H. perforatum* has stimulated the investigation of the secondary metabolites in *Hypericum* species. In general, a fundamental characteristic of secondary metabolism is that secondary products are not uniformly distributed throughout the plant but are frequently limited to particular organs and particular cells and tissues within that organ (Rhodes, 1994). The expression of secondary pathways is often a feature of cell specialization and is integrated into the pattern of differentiation of those cells or tissue types.

The quantitatively major constituents of extracts from upper parts of *H. perforatum* are flavonoids and hyperforins, the structures of which were elucidated by mass spectrometry and NMR spectroscopy (Hansen *et al*., 1999 and literature cited therein). Recently, HPLC coupled to diode array detection and mass spectrometry has been used for investigation of extracts (Hansen *et al*., 1999). Unlike flavonoids and hyperforins, xanthones occur in small amounts (less than 1%) in *H. perforatum*. Aerial parts contain trace amounts of 1,3,6,7-tetrahydroxyxanthone (norathyriol) and kielcorin (Fig. 4-1) (Nahrstedt and Butterweck, 1997). This observation agrees with the low level of immunofluorescence found for BPS in the mesophyll cells.

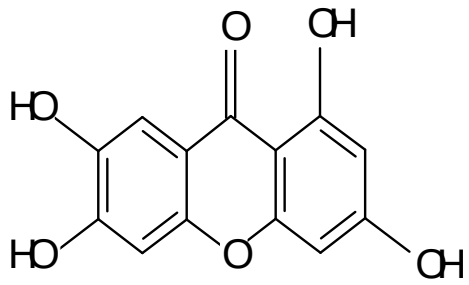

1,3,6,7-tetrahydroxyxanthone
(norathyriol)

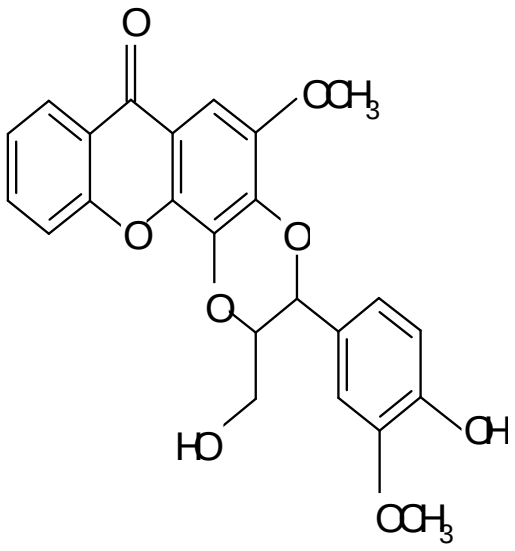

kielcorin

Fig. 4- 1: Chemical structures of xanthones from aerial parts of *H. perforatum*.

In cell suspension cultures of *H. perforatum* treated with the fungus *Colletotrichum gloeosporioides*, a massive accumulation of xanthones was observed (Conceicao *et al.*, 2006). This induced xanthone formation was further increased (at least twelve-fold) when the cultured cells were primed with either methyl jasmonate or salicylic acid. *C. gloeosporioides* is the most devastating pathogen of *H. perforatum*, and jasmonates and salicylate are signalling compounds. A rapid and strong xanthone accumulation was also observed with cell cultures of *H. androsaemum* when treated with methyl jasmonate (Abd El-Mawla and Beerhues, 2002). These findings indicate that xanthones are inducible defense compounds rather than preformed protective agents. Whether intact *H. perforatum* plants form xanthones in response to biotic stress is still open. Depending on the culture conditions, cell cultures and calli of *H. perforatum* were able to produce high amounts of xanthones which were not accumulated in parent plants (Schmidt *et al.*, 2000; Pasqua *et al.*, 2006).

Unlike leaves, roots appear to form xanthones as a preformed chemical barrier against invading pathogens. Pasqua *et al.* (2006) isolated several types of xanthones from roots including paxanthone, 1,3,5,6-tetrahydroxyxanthone, 1,3,6,7-tetrahydroxyxanthone, 1-hydroxy-6,7-dimethoxyxanthone, cadensin G, 1-hydroxy-5,6,7-trimethoxyxanthone and 3-*O*-methylpaxanthone (Fig. 4-2). Kielcorin was found at a concentration of about 0.01% (Nahrstedt and Butterweck, 1997). The concentration of norathyriol was 0.95 mg /100g dry roots (Sparenberg, 1993). According to the immunofluorescence results presented here, the root xanthones are formed in the cortex cells.

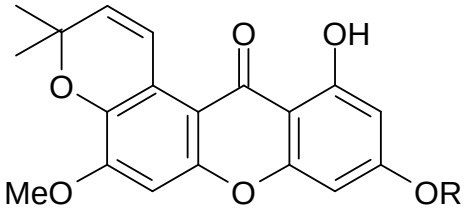

3-*O*-methylpaxanthone: R=Me
Paxanthone: R= H

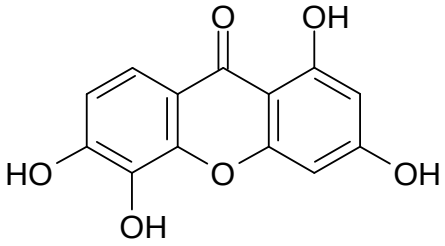

1,3,5,6-tetrahydroxyxanthone

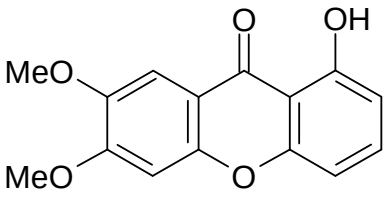

1-hydroxy-6,7-dimethoxyxanthone

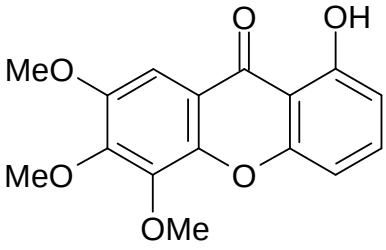

1-hydroxy-5,6,7-trimethoxyxanthone

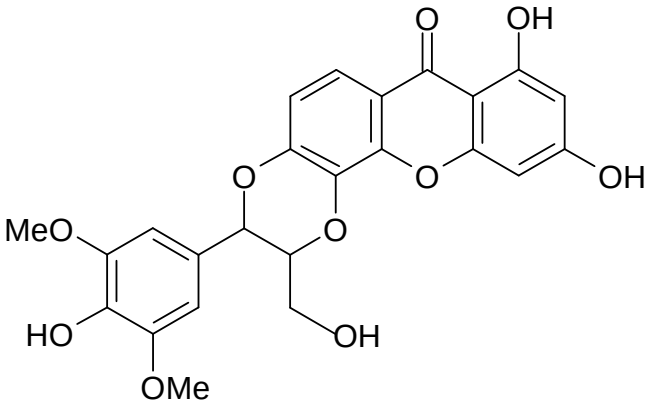

Cadensin G

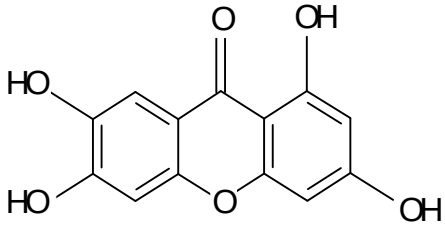

1,3,6,7-tetrahydroxyxanthone
(norathyriol)

Fig. 4- 2: Xanthones isolated from *H. perforatum* roots (Pasqua *et al.* 2006).

Expression of BPS was also observed in seeds of middle-aged fruits. Mature capsules contain about 50-100 small seeds of <1 mm in length and < 0.5 mm in width. The two outermost cell layers of the seed (testa) arise from the outer and inner integument and the layer below the testa is the endosperm (Matzk *et al.*, 2001). The finding that BPS was detected in developing seeds also seems to be related to the protective function of benzophenone derivatives. Sparenberg (1993) reported that the concentration of norathyriol in *H. perforatum* is 1.28 mg /100g dry flower material, followed by 0.95 mg /100g dry roots and 0.22 mg/ 100g dry leaves. It is well known that the mature embryo commonly undergoes a period of dormancy within the protective seed coat (Bowes, 1996). Tisdale and coworkers (1959) reported that *H. perforatum* reproduces through flower and seed production, as well as vagetatively through suckers arising from an underground rhizome. Seeds can remain viable in the soil between 6-10 years. The plant is a perennial reaching maturity in two seasons, with the first-year-growth being mainly directed toward the establishment of the root system (GISD, 2007).

Xanthones and their biogenic precursors, benzophenones, were also detected in species other than *H. perforatum*. Simple benzophenones, prenylated benzophenones, and xanthone derivatives were isolated from the aerial parts and roots of *H. inodorum, H. roeperanum, H. geminiflorum, H. japonicum, H. henryi, H. annulatum, H. scabrum, and H. styphelioides* (Cardona *et al.*, 1992; Rath *et al.*, 1996; Li and Wu, 1997; Wu *et al.*, 1998; Kitanov and Nedialkov, 2001; Nedialkov and Nedialkov, 2002; Tanaka *et al.*, 2004; Gamiotea-Turro *et al.*, 2004; Zheleva-Dimitrova *et al.*, 2007). Xanthones were mainly found in the underground organs. Co-occurrence of simply oxygenated xanthones and more complex prenylated structures has been described, and the 1,3,5,6-oxygenation pattern appears to be the most common one for the alkylated xanthones (Avato, 2005). Roeperanone, a xanthone bearing a terpene alkyl moiety which was identified in the roots of *H. roeperanum*, is the first plant xanthone substituted with a sesquiterpene alkyl group (Avato, 2005). Polyprenylated benzoylphloroglucinol derivatives, named hyperibones, were isolated from aerial parts of *H. scabrum* (Matsuhisa *et al.*, 2002). New complex polyisoprenylated benzophenones, called sampsoninones, were found in aerial parts and roots of *H. sampsonii* (Hu and Sim, 1998, 1999; Xiao *et al.*, 2007).

In addition to *Hypericum* species, xanthones and/or related benzophenones were isolated from all the major and several minor genera of the Clusiaceae (Bennet and Lee, 1989). In this plant family, prenylated compounds are widely distributed. In contrast, simple benzophenones are rare and only few examples have been described in the literature (Avato, 2005). Benzophenone derivatives are present in the fruits, roots, leaves and twigs of Guttiferous plants (Rubio *et al*., 1999). Polyisoprenylated 2,4,6-trihydroxybenzophenones were isolated from several members of the family (Rubio *et al*., 1999). Prenylated xanthones were found in the root bark of *Rheedia benthamiana* (Monache *et al.*, 1983). A polyisoprenylated benzophenone derivative was detected in fruits of *Garcinia perdunculata* (Sahu *et al*., 1989). The bark of *Garcinia myrtifolia* contains three biogenetically related prenylated benzophenones (Spino *et al*, 1995). Benzophenone-xanthone dimers were isolated from the root of *Garcinia dulcis* (Iinuma *et al*., 1996). Six prenylated benzophenone derivatives were found in the fruits of *Clusia plukenetii* (Henry *et al*., 1999). The fruit hulls of *Garcinia mangostana* contain benzophenone glucosides and xanthones (Huang *et al*., 2001). Polyisoprenylated benzophenone derivatives were also isolated from fruits, leaves and seed pericarps of *Garcinia indica* (Kumar and Chattopadhyay, 2007). Polyisoprenylated benzophenones, named semsinones, were detected in the bark of *Garcinia semseii* (Magadula *et al*., 2008). Polyisoprenylated tetracyclic xanthones and polyisoprenylated benzophenones were found in the fruits of *Garcinia cambogia* (Masullo *et al*., 2008).

A second plant family which is well known to contain xanthones is Gentianaceae (Bennett and Lee, 1989). The majority of the natural xanthones have been found in these two families of higher plants, Guttiferae and Gentianaceae. While simple, oxygenated xanthones occur in both families, more highly oxygenated compounds were found in Gentianaceae. Prenylated constituents which are typical for Guttiferae are absent from Gentianaceae (Bennett and Lee, 1989).

The immunofluoresence localization of CHS in *H. perforatum* vegetative parts established that this enzyme is present at a high level in the mesophyll cells of young leaves. In floral organs, as far as studied, CHS is located in the mesophyll of sepals of young buds. To our knowledge, this is the first immunohistochemical localization of CHS in the medicinal plant *H. perforatum*.

CHS is the key enzyme of flavonoids biosynthesis. Flavonoids are probably the most intensively studied secondary metabolites of plants (Koes *et al*., 1994). The biosynthesis of flavonoid compounds and the enzymology of the metabolism have been largely elucidated (Austin and Noel, 2003). Flavonoids exhibit a diverse spectrum of biological functions and play an important role in the interaction between plants and their environment. They not only protect the plant from the harmful effects of UV irradiation but also play a crucial role in plant fertility. A special class of flavonoid polymers, the tannins, plays a structural role in the plant (Koes *et al*, 1994). Flavonoid compounds are produced by most, if not all, higher plants and are synthesized from the phenylalanine derivative *p*-coumaroyl-CoA and three molecules of malonyl-CoA by CHS (Hrazdina *et al*., 1987; Austin and Noel, 2003). During recent years, several publications have dealt with CHS from different types of plants including herbaceous plants and woody plants (Beerhues and Wiermann, 1988 a; Claudot *et al*., 1997). Flavonoid biosynthesis is one of the best systems available for the study of regulation of plant gene expression (Koes *et al*., 1994).

In many plants examined, CHS is located primarily in the epidermal and, to a lesser extent, in the subepidermal tissues. The residual mesophyll is either devoid of CHS or may contain traces of the enzyme (Beerhues *et al*, 1988 b; Lembach *et al*., 1989). A mesophyll-associated CHS was found in a dicotyledonous plant upon fungal infection (Lembach *et al*., 1989). CHS isolated from oat primary leaves shows maximal activity in the differentiating zone of five day old leaves. Activity of CHS was distributed in both the upper and the lower epidermis, but was predominant in the mesophyll layer (Fuisting and Weissenböck, 1980). Flavonids are present in all tissues of oat primary leaves (*Avena sativa*) except for the vascular bundles. However, 80 to 90% of whole-leaf activity of CHS could be measured in the mesophyll at all developmental stages investigated. Based on the discrepancies between CHS expression and flavonoid accumulation patterns in primary leaves of oat, it was postulated that an intercellular

transport of flavonoids may occur (Knogge and Weissenbock, 1986). In leaves of pea (*Pisum sativum*), CHS activity was found only in the epidermis (Hrazdina *et al*., 1982). Cosio and coworkers (1985) have reported that in leaves of soybean, CHS is restricted to the epidermis. Schmelzer *et al*. (1988) have shown that epidermal cells are the site of both synthesis and accumulation of flavonoids in parsley (*Petroselinum crispum*) leaves. The two CHS isoforms in leaves of *Spinacia oleracea* are located in the upper and the lower epidermis and to a minor extent in the subepidermal layers; additionally, traces of the two enzyme forms may be present in the residual mesophyll (Beerhues *et al*., 1988 b). In young stages of needle development in *Larix decidua*, CHS is present in epidermal cells and individual parenchyma cells in the region of the vascular bundles. A later developmental stage exhibits immunofluorescence predominantly in the mesophyll of the needles. CHS is no longer observable at the latest analyzed stages of needle development (Lembach *et al*., 1989).

Most of the flower pigments are flavonoids which act as a visual signal to attract pollinating animals. They belong to the class of red or purple coloured anthocyanins or the yellow coloured aurones and chalcones. It is possible that transport of anthocyanins or their precursors occurs from mesophyl cells to epidermal cells in the corolla of petunia (Koes *et al*., 1990). Alternatively, the expression of CHS in mesophyl cells might be related to the synthesis of colorless flavonols. The transcriptional activity of structural genes, and the rate of anthocyanin biosynthesis, reach a maximum just prior to opening of the flower bud (Koes *et al*., 1994). The expression of *Petunia hybrida* CHS in the tube of the flower occurred mainly, but not strictly, in epidermal cell layers and the mesophyl cells (Koes *et al*, 1990). According to a study of anthers (Sütfeld *et al.* 1978), CHS is present in the ″tapetum fraction″. In-situ localization of CHS has also been performed with tulip anthers using immunofluorescence, and the enzyme was found predominantly in the tapetum cells (Kehrel and Wiermann, 1985).

A phytochemical study of *Hypericum* species demonstrated that the highest yields of flavonoids and proanthocyanidins were detected at the stage of budding of *H. perforatum* and *H. maculatum* (Branther *et al*., 1994). Results obtained by Hannig and coworkers (1995) showed that 46.5% of flavonoids were located in *H. perforatum* leaves, followed by 42.2% in flowers, 7.3% in flower buds and 4% in stems.

The maximum amount of flavonoids in *H. perforatum* flowers was found during the budding stage and the compounds are located mainly in the sepals and petals (Tekel'ová *et al*., 2000).

The histological and anatomical knowledge of *H. perforatum* is still incomplete (Ciccarelli *et al*., 2001). From the morphological and anatomical standpoint of eight entities of the genus *Hypericum*, three kinds of secretory structures have been evidenced: black nodules, translucent glands and secetory canals, which are distributed through various parts of the plant (Maggi *et al*., 2004). The two strikingly different kinds of internal secretory structures are translucent glands and black nodules. Their difference is not just anatomical, but also involves the accumulation of quite different secretory products (Curtis and Lersten, 1990). It has generally been accepted that black nodules are involved in the synthesis and/or the transport of the precursor of hypericin (Fig.1-6) and are finally filled with hypericin (Wen-Zhe *et al*., 2002; Zobayed *et al.*, 2006; Soelberg *et al*., 2007). The black nolules were also found to contain small amounts of hyperforin (Soelberg *et al*., 2007). In contrast, the translucent glands and secetory canals are characterized by the presence of essential oil, but they do not contain napthodianthrones (Ciccarelli *et al*., 2001). Curtis and Lersten (1990) have reported that the protracted period of cell division within the translucent glands is unusual, as is the observation that the amount of oil is not as voluminous as one would expect from the size of mature translucent glands. These translucent glands have been described both as oil-filled and as resinous, but the authors suspect that most of these descriptions are merely assumptions about what such structures could be expected to contain and are not based on any original observations of the actual contents.

Soelberg and coworkers (2007) have reported that the accumulation of hyperforin in the translucent glands supports the proposed hypothesis that hyperforin is in part synthesized by the same biosynthetic machinery as monoterpenes in the chloroplasts of cells delimiting the gland (Fig. 4-3). In this study, BPS was immunolocalized in the internal cell layer of large translucent glands and secretory canals. In contrast, it was not observed in dark nodules. CHS was located in neither secetory structure. Wollenweber and cowerkers (1994) reported the occurrence of a novel xanthone and triterpenes as lipophilic glandular products in leaves and young twigs of

H. balearicum. This was the first time that a xanthone with a 1,2,5-oxygenation pattern was isolated. Furthermore, it was just the second time that the presence of a free xanthone in plant excretion is reported. The other example is *Orphium frutescens* (Gentianaceae), where glandular trichomes on leaves and stems produce tetraoxygenated xanthones (Wollenweber *et al.*, 2004). Curtis and Lersten (1990) already suggested that further anatomical studies of the cavities and nodules in *Hypericum* are necessary. These secretory structures are obviously more important than their current taxonomic value simply as dots or lines of different colours. Their internal variations might help to explain evolutionary pathways in this group.

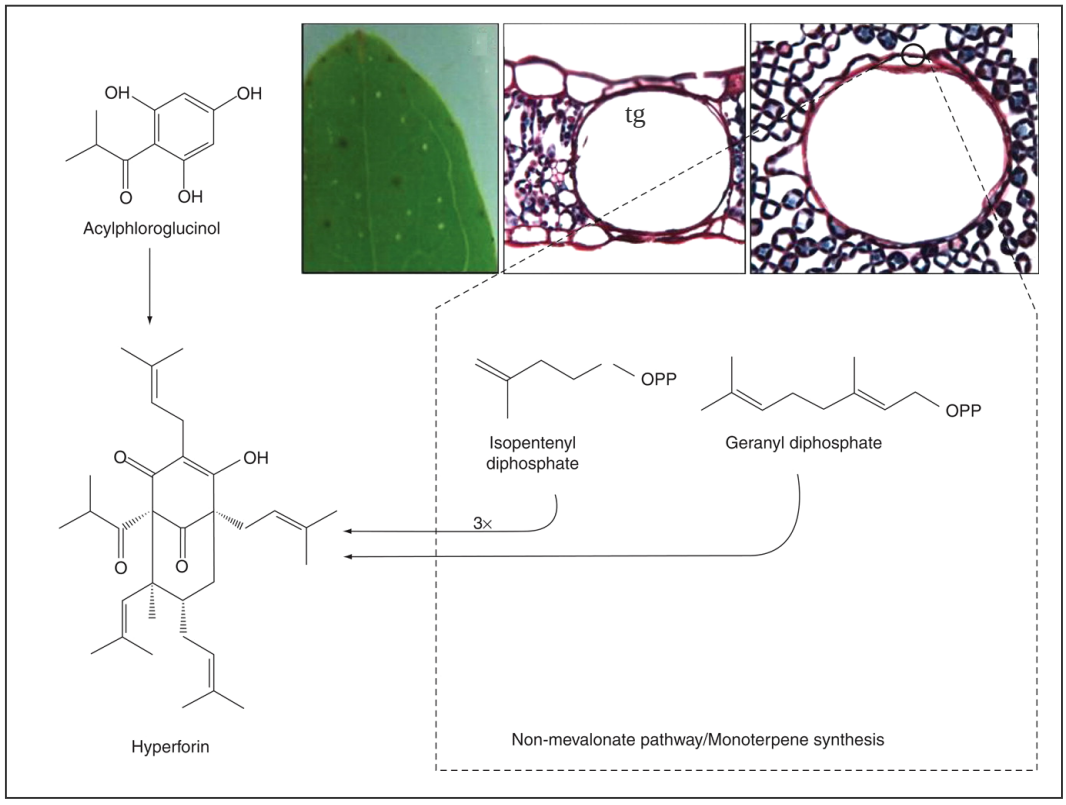

Fig. 4- 3: Hyperforin formation: Intermediates originate from the biosynthesis of monoterpenes, which takes place in the chloroplasts of cells delimiting the translucent gland (tg) (Soelberg *et al.*, 2007).

While hyperforins are polyprenylated acylphloroglucinol derivatives, sampsoniones are polyprenylated benzoylphloroglucinol derivatives and thus BPS products. So far, these compounds have not been detected in *H. perforatum* but they are typical constituents of *H. sampsonii* (Fig. 4-4; Avato, 2005).

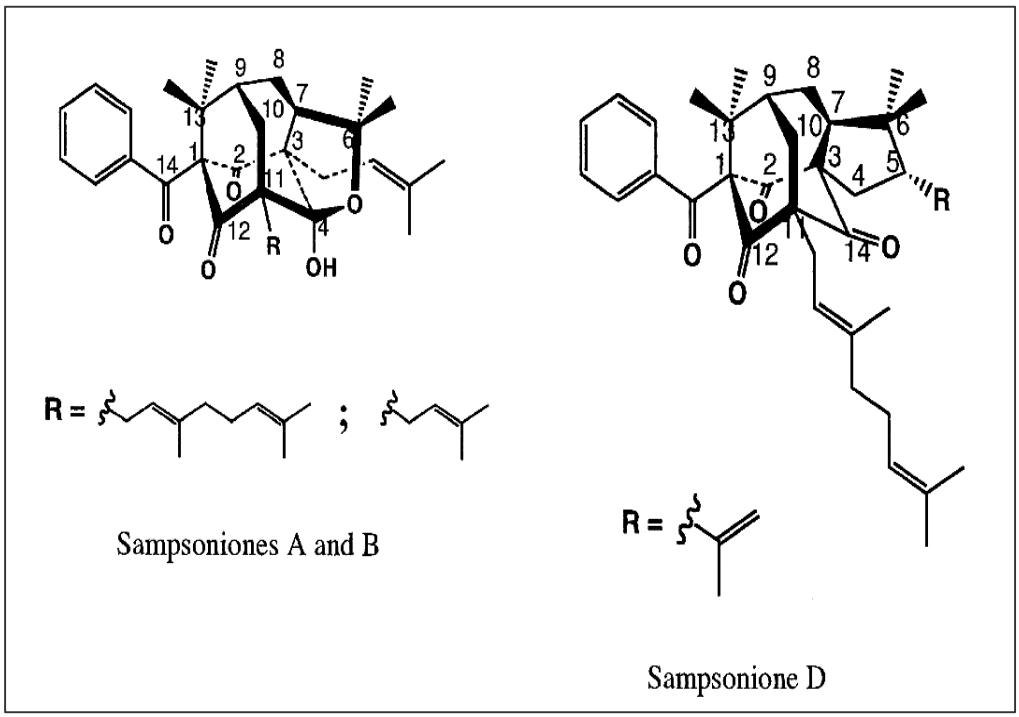

Fig. 4- 4: Chemical structures of sampsoniones from *H. sampsonii*. (Avato, 2005).

Samposoniones A and B are presumably biosynthesized from the biogenetically acceptable precursor 2,4,6-trihydroxybenzophenone and by subsequent alkylation using pyrophosphate compounds (Fig. 4-5; Hu and Sim, 1998). Thus, polyprenylated benzoylphloroglucinol derivatives are synthesized by the same pathway as monoterpens, which are constituents of the essential oil present in the translucent glands and secretory canals.

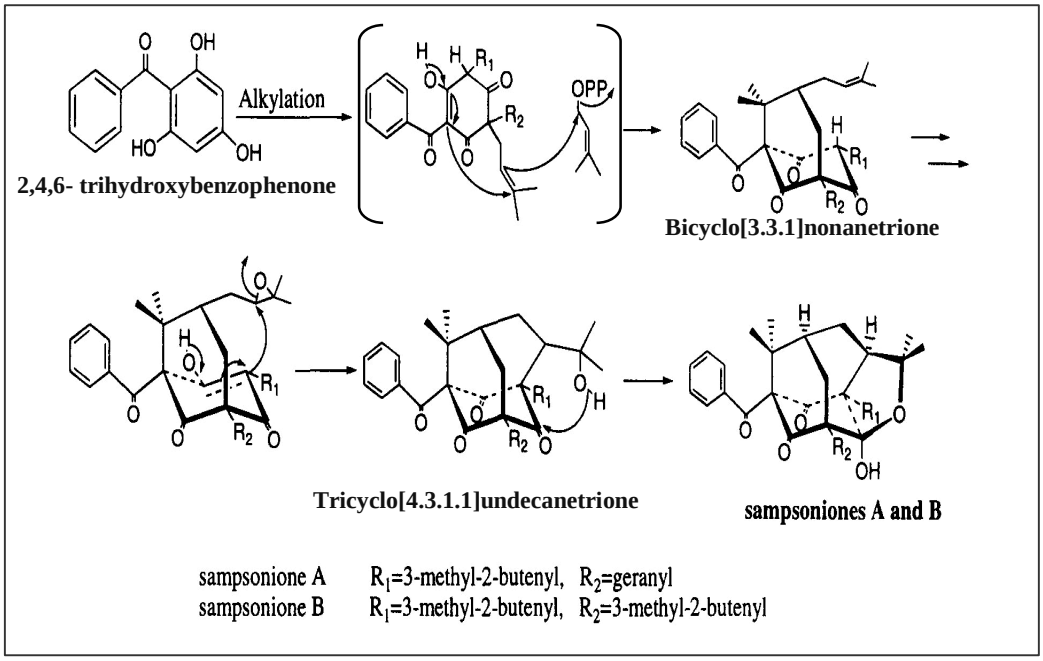

Fig. 4- 5: Possible biosynthesis pathway of sampsoniones A and B (Hu and Sim, 1998).

Further studies are needed to reveal the chemical nature and the distribution among tissues of benzophenone derivatives in *H. perforatum* and related species. So far, it remains largely open if the sites of biosynthesis and accumulation are identical or if transport processes are involved. However, insight into the spatial and temporal regulation of the various polyketide biosynthetic pathways in *Hypericum* species is required to understand the biological functions of the individual PKSs and their biosynthetic products. Finally, these observations, together with biochemical and molecular genetic data, will lay the foundation for metabolic engineering experiments with the medicinal plant *H. perforatum.*

Perspective studies are:

⇒ Follow up the immunofluorescence localization of BPS and CHS in *H. perforatum* floral organs.

⇒ Immunochemical studies of isobutyrophenone synthase (BUS) and subsequent localization of BUS in *H. perforatum* tissues.

⇒ Immunogold labeling of the three PKSs (BPS, BUS, and CHS) at the subcellular level.

⇒ Immunodetection and localization of BPS in *H. perforatum* tissues after elicitation and infection.

⇒ Immunolocalization of PKSs in the related species *H. calycinum* and *H. androsaemum.*

⇒ Immunodetection of PKSs in cell cultures of *Hypericum* species after elicitation.

5 Summary

Ü Extracts from the medicinal plant *Hypericum perforatum* (St. John's wort; Clusiaceae) are widely used as antidepressants. Traditionally, they have been employed as external anti-inflammatory and healing remedies for the treatment of swellings, wounds, and burns.

Ü All pharmacologically active constituents, i.e. hyperforins, hypericins, flavonoids, and xanthones, are derivatives of polyketide metabolism. Thus, *Hypericum* species are interesting systems for studying the biosynthesis of a diversity of aromatic polyketides

Ü Two type III polyketide synthases (PKSs) involved are benzophenone synthase (BPS) and chalcone synthase (CHS). BPS is the key enzyme of benzophenone and xanthone biosynthesis. CHS is the key enzyme of chalcone and flavonoid biosynthesis.

Ü This work describes the tissue-specific localization of BPS and CHS in *H. perforatum* using the immunofluorescence technique and confocal laser scanning microscopy.

Ü BPS and CHS from *H. androsaemum* were heterologously expressed in *E. coli* as both GST-fusion proteins and 6xHis-tagged proteins and purified by affinity chromatographies.

Ü Polyclonal antibodies were raised against the 6xHis-tagged PKSs in rabbits, the IgG fractions were isolated using a protein A sepharose affinity column, and the monospecificity of the IgGs was demonstrated by immunoblotting following SDS- PAGE.

Ü The lack of cross-reactivities between the antibodies and the respective heterologous antigens was confirmed by dot blotting and immunotitration coupled to the measurement of enzyme activities. The absence of immunological relationship between BPS and CHS finally allowed for a separate immunohistochemical localization of the PKSs.

Ü Protein extracts from various *H. perforatum* organs were subjected to SDS-PAGE and immunoblotting. BPS was mainly immunodetected in middle-aged fruits. CHS was found in young leaves and flower buds.

Ü Subsequent immunofluoresence studies of *H. perforatum* vegetative organs showed that BPS was expressed to a low extent in mesophyll cells of young leaves and strongly expressed in the glandular cells of large translucent glands present inside the leaves. In *H. perforatum*, there are different types of secretory tissues including translucent glands, black nodules and secretory canals. In roots, BPS was located in the cortex cells. In floral parts, as far as studied, BPS was found in secretory tissue of sepals of young buds and in middle-aged fruits. In addition, seeds present in the middle-aged fruits contained BPS.

Ü The immunodetection of BPS in middle-aged fruits correlated with the formation of a new, so far unidentified secondary metabolite that was detected by HPLC analysis in methanolic extracts.

Ü CHS was strongly expressed in the mesophyll cells of young leaves and was not present in glands. Nor was the enzyme observed in roots. In floral parts, as far as studied, CHS is located in the mesophyll of sepals of young buds.

6 References

Abd El-Mawla, A. M. A., Beerhues, L. (2002): Benzoic acid biosynthesis in cell cultures of *Hypericum androsaemum*. *Planta,* **214**: 727-733.

Austin, M. B., and Noel, J. P., (2003): The chalcone synthase superfamily of type III polyketide synthases. *Nat. Prod. Rep.*, **20**: 79–110.

Avato, P., (2005): A survey of the *Hypericum* genus: Secondary metabolites and bioactivity. In: Attta-ur-Rahman(ed) Studies in natural products chemistry, *Elsevier B.V.,* **30** : pp 603-634.

Barnes, J. Anderson, L. A., and Phillipson, J. D., (2001): St John's wort (*Hypericum perforatum* L.): a review of its chemistry, pharmacology and clinical properties. *Journal of Pharmacy and Pharmacology*, **53**: 583-600.

Beerhues, L., and Wiermann, R., (1988a): Chalcone synthases from spinach (*Spinacia oleracea* L.): Purification, peptide patterns, and immunological properties of different forms. *Planta,* **173**: 532-543.

Beerhues, L., Robenek, H. and Wiermann R., (1988b): Chalcone synthases from spinach (Spinacia oleracea L.): II. Immunofluorecence and immunogold localization. *Planta* **173**: 544-553.

Beerhues, L., (2006): Molecules of interest-Hyperforin. *Phytochemistry,* **67**: 2201-2207.

Bennet, G. J., and Lee, H. H., (1989): Xanthones from Guttiferae. *Phytochemistry,* **28**: 967-998.

Bisset, N. G. (2001): Herbal drugs and phytopharmaceuticals: a handbook for practice on a scientific basis; [with reference to German Commission E monographs], 2nd, *Medpharm Scientific Publ*., Stuttgart.

Bowes, B. G., and Nicholson, J., (1996): A colour atlas of plant structure. *Manson,* London.

Bradford, M. M., (1976): A rapid and sensitive method for quantitation of microgram quantities of protein utilizing the principle of protein-dye-binding. *Analytical Biochemistry,* **72**: 248-254.

Brantner, A., Kartnig, T., and Quehenberger, F. (1994): Abstract: Comparative phytochemical investigations of *Hypericum perforatum* L. and *Hypericum maculatum* Crantz. *Scientia Pharmaceutica*, **62**: 261-276.

Butterweck, V., (2003): Mechanism of action of St. John's wort in depression. *CNS Drugs*, **17**: 539-562.

Capasso, F., Gaginella, T.S., Grandolini, G., and Izzo, A.A., (2003): Phytotherapy: A quick reference to herbal medicine, *Springer,* Verlag Berlin Heidelberg New York.

Cardona, L., Fernández, I., and Pedro, JosR., (1992): Xanthone constituents of *Hypericum inodorum*. *Heterocycles*, **34**: 479-482.

Ciccarelli, D., Andreucci, A.C. and Pagni, A. A.,(2001): Translucent glands and secretory canals in *Hypericum perforatum* L. (Hypericaceae): Morphological, anatomical and histochemical studies during the course of ontogenesis. *Annals of Botany*, **88**: 637-644.

Claudot, A. C., Ernst, D., Sandermann, H., and Drouet, A., (1997): Chalcone synthase activity and polyphenolic compounds of shoot tissues from adult and rejuvenated walnut trees. *Planta*, **203**: 275-282.

Conceição, L. F. R., Ferreres, F., Tavares, R. M., and Dias, A. C. P., (2006): Induction of phenolic compounds in *Hypericum perforatum* L. cells by *Colletotrichum gloeosporioides* elicitation. *Phytochemistry,* **67**: 149–155.

Coons, A. H., Leduc, E. H., and Connolly, J. M., (1955): Studies on antibody production: I. A method for the histochemical demonstration of specific antibody and its application to a study of the hyperimmune rabbit. *J. Exp. Med.*, **102**: 49-60.

Cosio, E., G., Weissenböck, G., McClure,J. W., (1985): Acifluorfen-induced isoflavonoids and enzymes of therir biosynthesis in mature soybean leaves. *Plant Physiol.*, **78**: 14-19.

Court, W. E., (2003): Hypericin as a potenical antitumour agent. In: Ernst E (ed) *Hypericum-The genus Hypericum*, Taylor & Francis, London, pp 173-178.

Curtis, J. D. and Lersten, N. R., (1990): Internal secretory structures in *Hypericum* (Clusiaceae): *H. perforatum* L. and *H. balearicum* L. *New Phytol*., **114**: 571-580.

Dias, A. C. P., Seabra, R. M., Andrade, P. B., and Fernandes-Ferreira, M., (1999): The development and evaluation of an HPLC-DAD method for the analysis of the phenolic fractions from in vivo and in vitro biomass of *Hypericum* species. *J. LIQ. CHROM. & REL. TECHNOL*., **22**: 215–227.

Dias, A. C. P., Seabra, R. M., Andrade, P. B., Ferreres, F., and Fernandes-Ferreira, M., (2001): Xanthone biosynthesis and accumulation in *calli* and suspended cells of *Hypericum perforatum*. *J. plant Physiol*., **158**: 821-827.

Dias, A. C. P. (2003): The potential of *in vitro* cultures of *Hypericum perforatum* and *Hypericum androsaemum* to produce interesting pharmaceutical compounds, In: Ernst E. (ed) *Hypericum-The genus Hypericum*, *Taylor & Francis*, London, pp 137-154.

Ebermann, R., Alth, G., Kreitner, and M. Kubin, A., (1996): Natural products derived from plants as potential drugs for the photodynamic destruction of tumor cells, *Journal of Photochemistry and photobiology B: Biology*, **36**: 95-97

Fuisting, K., Weissenböck, G., (1980): Flavone synthase in Oat primary leaves: Time course and distribution at the tissue and subcellular level. *Z. Naturforch*. **35c**: 973-977.

Gamiotea-Turro, D., Cuesta-Rubio, O., Prieto-González, S., De Simone, F., Passi, S., and Rastrelli, L., (2004): Antioxidative constituents from the leaves of *Hypericum styphelioides. J. Nat. Prod.*, **67**: 869-871.

GISD (Global Invasive Species database), (2007): online data base *hypericum perforatum.*

Gordon, A. H., (1972): Electrophresis of protein in polyacrylamide and starch gels, Laboratory techniques in biochemistry and molecular biology. 1: *North Holland Publishing Co.*, Amsterdam.

Greeson, J. M., Sanford, B., and Monti, D. A., (2001): St. John's wort (*Hypericum perforatum*): a review of the current pharmacological, toxicological, and clinical literature. *Psychopharmacology*. **153**: 402–414.

Hannig, H. –J., Plescher, A., and Vollrath, G., (1995): Erfahrungen beim großflächigen Anbau von Johanniskraut- Anforderungen an die industrielle Verwertung. *Herba Germanica*, **3**: 96-103.

Hansen, S.H., Jensen, A.G, Cornett, C., Bjørnsdottir, I., Taylor, S. Wright, B. and Wilson, I. D. (1999): High-Performance Liquid Chromatography On-Line Coupled to High-Field NMR and Mass Spectrometry for Structure Elucidation of Constituents of *Hypericum perforatum* L., *Anal. Chem.*, **71**: 5235-5241.

Harlow, E. and Lane D., (1988): Antibodies: A Laboratory manual, *Cold Spring Harbor Laboratory Press.*

Heinrich, M., Barnes, J., Gibbons, S., Williamson, E. M., (2004): Fundamentals of pharmacognosy and phytotherapy, *Churchill Livingstone*, Edinburgh.

Henry, G. E., Jacobs, H., Carrington, C. M. S., McLean, S., and Reynolds, W. F., (1999): Prenylated benzophenone derivatives from Caribbean *Clusia* species (Guttiferae). Plukenetiones B-G and xerophenone A. *Tetrahedron*, **55**: 1581-1596.

Heukeshoven, J. and Dernick, R. (1988): Improved silver staining procedure for fast staining in PhastSystem development unit: Staining of sodium dodecyl sulfate gels. *Electrophoresis*, **9**: 28-32.

Hierck, B. P., Iperen, L. V., Groot, A. C. G.-D., and Poelmann R. E., (1994): Modified indirect immunodetection allows study of murine tissue with mouse monoclonal antibodies. *The Joumal of Histochemistry and Cytochemistry*, **42**: 1499-1502.

Hobbs, C. (1998): St. John's Wort (*Hypericum Perforatum* L.): A Review, online data: Christopher Hobbs.

Hölzl, J. and Petersen, M., (2003): Chemical constituents of *Hypericum* ssp. In: Ernst E. (ed) *Hypericum*-The genus *Hypericum*. *Taylor & Francis*, London, pp 77-93.

Hrazdina, G., Marx, G. A., and Hoch, H. C., (1982): Distribution of secondary slant metabolites and their biosynthetic enzymes in Pea (*Pisum sativum L.*) leaves. *Plant Physiol*, **70**: 745-748.

Hrazdina, G., Zobel, A. M., and Hoch, H. C., (1987): Biochemical, immunological, and immunocytochemical evidence for the association of chalcone synthase with endoplasmic reticulum membranes. *Proc.Natl. Acad. Sci. USA*, **48**: 8966-8970.

Hu, L.-H., and Sim, K.-Y., (1998): Complex caged polyisoprenylated benzophenone derivatives, sampsoninones A and B, from *Hypericum sampsonii*. *Tetrahedron Letters*, **39**: 7999-8002.

Hu, L.-H., and Sim, K.-Y., (1999): Sampsoninones C-H, a unique family of polyprenylated benzophenone derivatives with the novel tetracyclo-[7.3.1.1^{3,11}.0^{3,7}]tetradecane-2,12,14-trione skeleton, from *Hypericum sampsonii* (Guttiferae). *Tetrahedron Letters*, **40**: 759-762.

Huang, Y. L., Chen, C. C., Chen, Y. J., Huang, R. L. and Shieh, B. J., (2001): Three xanthones and a benzophenone from *Garcinia mangostana*. *J. Nat. Prod.*, **64**: 903-906.

Hutzler, P., Fischbach, R., Heller, W., Jungblut, T. P., Reuber S., Schmitz, R., Veit, M., Weissenböck, G. and Schnitzler, J. P., (1998): Tissue localization of phenolic compounds in plants by confocal laser scanning microscopy. *Journal of Experimental Botany*, **49**: 953-965.

Iinuma, M., Tosa, H., Ito, T., Tanaka, T., and Riswan, S., (1996): Three new benzophenone-xanthone dimers from the root of *Garcinia dulcis*. *Chemical and Pharmaceutical Bulletin,* **44:** 1744-1747.

Jez, J. M, Ferrer, J.-L., Bowman, M. E., Austin, M. B., Schröder, J., Dixon, R. A., and Noel, J. P., (2001): Structure and mechanism of chalcone synthase-like polyketide synthases. *Journal of Industrial Microbiology & Biotechnology*, **27**: 393–398.

Kehrel, B., and Wiermann, R., **(1985):** Immunochemical localization of phenylalanine ammonia-lyase and chalcone synthase in anthers. *Planta*, **163**:183-190.

Kitanov, G. M., and Blinova, K. F., (1987): Modern state of the chemical study of species of the genus *Hypericum*. *Chemistry of natural compounds*, **23**: 151-166.

Kitanov, G.M., and Nedialkov, P.T., (1998): Mangiferin and isomangiferin in some *Hypericum* species. *Biochem. Syst. Ecol.,* **26**: 647-653.

Kitanov, G. M., and Nedialkov, P. T., (2001): Benzophenone *O*-glucoside, a biogenic precursor of 1,3,7-trioxygenated xanthones in *Hypericum annulatum*. *Phytochemistry*, **57**: 1237-1243.

Knogge, W., and Weissenböck, G., (1986): Tissue-distribution of secondary phenolic biosynthesis in developing primary leaves of *Avena sativa* L., *Planta*, **167**: 196-205.

Koes, R. E., Blokland, R., Quattrocchio, F., Tunen A. J., and Mol, J. N. M., (1990): Chalcone synthase promoters in Petunia are active in pigmented and unpigmented cell types. *The Plant Cell*, **2**: 379-392.

Koes, R. E., Quattrocchio, F., and Mol, J. N. M., (1994): The flavonoid biosynthetic pathway in plants: Function and evolution. *BioEssays*, **16**: 123- 132.

Kumar, S., and Chattopadhyay, S. K., (2007): High-performance liquid chromatography and LC-ESI-MS method for the identification and quantification of two biologically active polyisoprenylated benzophenones xanthochymol and isoxanthochymol in different parts of *Garcinia indica. Biomed. Chromatogr*., **21**: 139-163.

Laemmli, U. K., (1970): Cleavage of structural proteins during the assembly of the head of bacteriophage T4. *Nature*, **227**: 680-685.

Lembach, A., Beerhues, L., and wiermann, R., (1989): In situ localization of chalcone synthase in Larix needles by indirect immunofluorescence. *Protoplasma*, **153**: 58-61.

Li, W.-S., and Wu, S.-L., (1997): Xanthones and triterpenoids from *Hypericum* geminiflorum. *Chinese Pharmaceutical Journal*, **49**: 145-156.

Liu, B., Paul, H. F., Schmidt, W. and Beerhues, L., (2003): Benzophenone synthase and chalcone synthase from *Hypericum androsaemum* cell cultures: cDNA cloning, functional expression, and site-directed mutagenesis of two polyketide synthases. *The Plant Journal*, **34**: 847-855.

Magadul, J., J., Kapingu, M.C., Bezabih, M., and Abegaz, B. M., (2008): polyisoprenylated benzophenones from *Garcinia semseii*. *Phytochemistry Letters*, **1**: 215-218.

Maggi, F., Ferretti, G., Pocceschi, N., Menghini, L. and Ricciutelli, M., (2004): Morphological, histochemical and phytochemical investigation of the genus *Hypericum* of the Central Italy. *Fitoterapia*, **75**: 702-711.

Maisenbacher, P. and Kovar, K.-A., (1992): Adhyperforin: A Homologue of hyperforin from *Hypericum perforatum*. *Planta.Med*., **58**: 291-293.

Masullo, M., Bassarello, C., Suzuki, H., Pizza, C., and Piacente, S., (2008): Polyisoprenylated benzophenones and unusual polyisoprenylated tetracyclic xanthone from the fruits of *Garcinia scambogia*. *J. Agric. Food Chem.*, **56**: 5205-5210.

Matsuhisa, M., Shikishima, Y., Takaishi, Y., Honda, G., Ito, M., Takeda, Y., Shibata, H., Higuti, T., Kodzhimatov, O. K., and Ashurmetov, O., (2002): Benzophloroglucinol derivatives from *Hypericum scabrum*. *J. Nat. Prod*., **65**: 290-294.

Matzk, F., Meister, A., Brutovská, R. ,and Schubert, I., (2001): Reconstruction of reproductive diversity in *hypericum perforatum* L. opens novel strategies to manage apomixes. *The plant journal*, **26**: 275-282.

McCutcheon, A. R., (2000): St. John`s wort. In: Chandler, F. (ed) Herbs: everyday reference for health professionals, *Canadian Pharmacists Association*, Ottawa, pp 196-205.

Monache, G. D., Monache, F. D., and Bettolo, G. B. M., (1983): Chemical investigation of the genus *Rheedia*. II. Prenylated xanthones from *Rheedia gardneriana*. *J. Nat. Prod.*, **46**: 655-659.

Murashige, T., Skoog, F., (1962): A revised medium for rapid growth and bio assays with tobacco tissue cultures. *Physiol*. *Plant*., **15**: 473-497.

Muruganandam, A.V., Ghosal, S., Bhattacharya, S.K., (2000): The role of xanthones in the antidepressant activity of *Hypericum perforatum* involving dopaminergic and serotoninergic systems. *Biog. Amines.*,**15**: 553-567.

Müller, W. E., (2003): Current St. John's wort research from mode of action to clinical efficacy. *Pharmacol. Res*., **47**: 101-109.

Nedialkov, P. T., and Kitanov, G. M., (2002): Two benzophenone *O*-arabinosides and a chromone from *Hypericum annulatum*. *Phytochemistry*, **59**: 867-871.

Nohrstedt, A. and Butterweck, V., (1997): Supplement: Biologically active and other chemical constituents of the herb of *Hypericum perforaturn* L. *Pharmacopsychiat*, **30**: 129 – 134.

Pasqua, G., Avato, P., and Mulinacci, N., (2006): High-value metabolites from *Hypericum perforatum*: a comparison between the plant *and in vitro* systems. In: Floriculture, *ornamental and plant biotechnology volume II- global science books*, UK, pp 507-513.

Rath, G., Potterat, O., Mavi, S., and Hostettmann, K., (1996): Xanthones from *Hypericum roeperanum. Phytochemistry*, **43**: 513-520.

Renshaw, S., (2007): Immunohistochemistry. (methods expresee), Bloxham: Scion. UK.

Rhodes, M. J. C., (1994): Physiological roles for secondary metabolites in plants: Some progress, many outstanding problems. *Plant Molecular Biology*, **24**: 1-20.

Robson, N. K. B., (2003): *Hypericum* botany. In: Ernst E. (ed) *Hypericum*-The genus *Hypericum*. *Taylor & Francis*, London, pp 1-22.

Rubio, O. C., Cuellar, A. C., Rojas, N., Castro, H. V., Rastrelli, L., and Aquino R., (1999): A polyisoprenylated benzophenone from Cuban propolis. *J. Nat. Prod.*, **62**: 1013-1015.

Sahu, A., Das, B., and Chatterjee, A., (1989): Polyisoprenylated benzophenones from *Garcinia perdunculata*. *Phytochemistry*, **28**: 1233-1235.

Sambrook, J., Fritsch, E. F. und Maniatis, T., (1989): Molecular cloning: a laboratory manual, 2^{ed}, *Cold Spring Harbor Laboratory Press*.

Schmelzer, E., Jahnen, W., and Hahlbrock, K., (1988): In situ localization of light-induced chalcone synthase mRNA, chalcone synthase, and flavonoid end products in epidermal cells of parsley leaves. *Proc. Nati. Acad. Sci. USA (Botany)*, **85**: 2989-2993.

Schmidt, W., Abd El-Mawla, A. M. A., Wolfender, J.L., Hostettmann, K., Beerhues, L., (2000): Xanthones in cell cultures of *Hypericum androsaemum*. *Planta Med.*, **66**: 380-381.

Seidler-Łożykowska, k., (2003): Secondary metabolites content of *Hypericum* sp. in different stages and plant parts. In: Ernst E. (ed) *Hypericum*-The genus *Hypericum*. *Taylor & Francis*, London, pp 100-105.

Soelberg, J., JØrgensen, L. B., and Jäger, A. K., (2007): hyperforin accumulates in the translucent glands of *Hypericum perforatum*. *Annals of Botany*, **99**: 1097-1100.

Sparenberg, B., (1993): MAO-inhibitierende Eigenschaften von Hypericum-inhaltsstoffen und Untersuchungen zur Analytik und Isolierung von Xanthonen aus *Hypericum perforatum* L. *Thesis*, University of Marburg, Germany.

Spino, C., Lal, J., Sotheeswaran, S., and Aalbersberg, W., (1995): Three prenylated phenolic benyophenones from *Garcinia myrtifolia*. *Phytochemistry*, **38**: 233-236.

Stueber, K., (2003): *Hypericum perforatum*, Johanniskraut, Tafel 407. online data: Biolib. de. A collection of historic and modern biology books.

Sütfeld, R., Kehrel, B., Wiermann, R. (1978): Characterization, development and localization of flavonone synthase in tulip anthers. *Z. Naturforsch*., **33c**: 841-846.

Tanaka, N., Takaishi, Y., Shikishima, Y., Nakanishi, Y., Bastow, K., Lee, K. Honda, G., Ito, M., Takeda, Y., Kodzhimatov, O. K., and Ashurmetov, O., (2004): Prenylated benzophenones and xanthones from *Hypericum scabrum*. *J. Nat. Prod*., **67**: 1870-1875.

Tekel'ová, D., Repčák, M., Zemková, E., and Tóth, J., (2000): Quantitative changes of dianthrones, hyperforin and flavonoids content in the flower ontogenesis of *Hypericum perforatum*. *Planta Med.* **66**: 788-780.

Tisdale, E. W., Hironaka, M., and Pringle, W. L., (1959): Observations on the Autecology of *Hypericum perforatum*. *Ecology,* **40**: 54-62.

Tsai, S.-C. (2004): Preview, a fine balancing act of type III polyketide synthase. *Chemistry & Biology,* **11**: 1177–1178.

Upton, R., (1997): St. John's wort (*Hypericum perforatum*): Qualtity control, analytical and therapeutic monograph. *American herbal pharmacopoeia and therapeutic compendium.*

Walker, J. M., (1996): Nondenaturing polyacrylamide gel electrophoresis of protein. In: Walker, J. M. (ed) The protein protocols handbook. *Humana Press Inc.*, Totowa, NJ., pp 51-54.

Wen-Zhe, L., Hong-Fei, L. and Yheng-Hai, H., (2002): Ultrastructure of the multicellular nodules in *Hypericum perforatum* leaves. *Acta Botanica Sinica* **44**: 649- 656.

Wollenweber, E., Dorr, M., Roitman, J. N., and Arriaga-Giner, F. J., (1994): Triterpenes and a novel natural xanthone as lipophilic glandular products in *Hypericum balearicum.* Z. *Naturforsch.*, **49c**: 393-394.

Wu, Q.-L, Wang, S.-P., Du, L.-J., Yang, J.-S, and Xiao, P.-G., (1998): Abstract: Xanthones from *Hypericum japonicum, H. henryi*. *Phytochemistry*, **49**: 1395-1402.

Xiao, Z. Y., Mu, Q., Shiu, W. K. P., Zeng, Y. H., and Gibbones, S., (2007): Polyisoprenylated benzoylphlotoglucinol derivatives from *Hypericum sampsonii*. *J. Nat. Prod.*, **70**: 1779-1782.

Yang, J., Huang, J., Gu, H., Zhong, Y., and Yang, Z., (2002): Duplication and adaptive evolution of the chalcone synthase genes of Dendranthema (Asteraceae). *Mol. Biol. Evol.*, **19**: 1752-1759.

Zheleva-Dimitrova, D., Gevrenova, R., Nedialkov, P., and Kitanov, G., (2007): Simultaneous determination of benzophenones and gentisein in *Hypericum annulatum* moris by high performance liquid chromatography. *Phtochem. Anal.*, **18**: 1-6.

Zobayed, S. M. A., Afreen, F., and Kozai, T., (2005): Temperature stress can alter the photosynthetic efficiency and secondary metabolite concentrations in St. John's wort. *Plant Physiology and Biochemistry*, **43**: 977-984.

Zobayed, S. M. A., Afreen, F., Goto, E., and Kozai, T., (2006): Plant-environment interactions: Accumulation of hypericin in dark glands of *Hypericum perforatum*. *Annals of Botany*, **98**: 793-804.